

Aus dem Institut für Molekular- und Zellbiologie der Hochschule Mannheim

Direktor: Prof. Dr. rer. nat. Mathias Hafner

Development of a quick, robust and chemically-defined differentiation  
protocol from human induced pluripotent stem cells towards cortical  
neurons to phenotype Alzheimer's Disease

Inauguraldissertation  
zur Erlangung des Doctor scientiarum humanarum (Dr. sc. hum.) der  
Medizinischen Fakultät Mannheim  
der Ruprecht-Karls-Universität  
zu  
Heidelberg

vorgelegt von  
Alexandra Kowalski

aus  
Saarbrücken

2019

Dekan: Prof. Dr. med. Sergij Goerd  
Referent: Prof. Dr. rer. nat. Mathias Hafner

# TABLE OF CONTENTS

Page

LIST OF ABBREVIATIONS.....	1
<b>1 INTRODUCTION.....</b>	<b>4</b>
1.1 Neurodegenerative diseases will rise in prevalence.....	4
1.1.1 Alzheimer's Disease.....	5
1.1.2 Genetic risk factors and mutations involved in AD.....	9
1.1.3 Drugs used in AD cannot influence the disease, but they can ameliorate symptoms.....	11
1.2 Pluripotent stem cells: a new promise for drug discovery.....	12
1.3 Cell culture conditions of PSCs and the importance of xeno-free and chemically-defined culture conditions.....	13
1.3.1 Matrigel.....	14
1.3.2 Bovine serum albumin.....	15
1.4 Deriving cortical neurons from hiPSCs.....	16
<b>2 MATERIALS AND METHODS.....</b>	<b>21</b>
2.1 Instruments.....	21
2.2 Cell culture.....	21
2.2.1 Dishes and flasks.....	21
2.2.2 Cell lines.....	21
2.2.3 Cell culture media ingredients, coatings and buffers.....	22
2.2.4 Small molecules and organic molecules.....	23
2.2.5 Proteins.....	25
2.2.6 Preparation of media.....	26
2.2.7 Coating of dishes and flasks.....	27
2.3 Cell culture procedures.....	29
2.3.1 Culturing & passaging of cells.....	29
2.3.2 Freezing of cells.....	29
2.3.3 Thawing of cells.....	29
2.3.4 Differentiation of cells.....	30

2.4	A $\beta$ -ELISA.....	32
2.4.1	A $\beta$ MSD ELISA materials.....	32
2.4.2	Collection of supernatants for A $\beta$ -ELISA .....	32
2.4.3	Performing of A $\beta$ -ELISA by A $\beta$ Peptide Panel 1 (6E10) V-PLEX Kit .	32
2.5	Multielectrode array (MEA) analysis .....	34
2.5.1	MEA materials .....	34
2.5.2	Coating of MEA-plates with PLO and LN521 .....	34
2.5.3	Seeding of cells into MEA plate .....	34
2.5.4	MEA measurement.....	34
2.6	Immunofluorescence staining .....	35
2.6.1	Immunofluorescence staining materials.....	35
2.6.2	Buffers .....	35
2.6.3	Primary antibodies .....	36
2.6.4	Secondary antibodies and other stains.....	39
2.6.5	Immunofluorescence staining of cells .....	41
2.7	RNA purification, reverse transcription and qPCR.....	43
2.7.1	RNA purification and PCR reagents .....	43
2.7.2	TaqMan probe assays .....	43
2.7.3	RNA isolation from cell culture samples .....	44
2.7.4	DNA digestion with RapidOut DNA Removal Kit with subsequent cDNA transcription by Transcriptor First Strand cDNA Synthesis.....	45
2.7.5	cDNA Synthesis with Transcriptor First Strand cDNA Synthesis Kit..	46
2.7.6	DNA digestion with ezDNAse Enzyme with subsequent cDNA transcription by with SuperScript IV VILO MasterMix .....	46
2.7.7	cDNA preparation and qPCR by Biomark HD.....	48
2.7.8	Data analysis of qPCR results .....	50
2.7.9	Statistical analysis for qPCR.....	50
<b>3</b>	<b>RESULTS.....</b>	<b>52</b>
3.1	Implementation of xeno-free hiPSC-culture conditions.....	52
3.1.1	The xeno-free coating agent LN521 is suitable for hiPSC-culture .....	52
3.1.2	A gradual change from E6 medium towards Basal Medium containing xeno-free B27 supplement is suitable for neural induction .....	54
3.2	Optimization of a xeno-free and chemically defined differentiation protocol	58
3.2.1	MEK inhibition accelerates neural induction in hiPSCs.....	58
3.2.2	hiPSC lines may be susceptible towards neural crest differentiation .	60

3.2.3	Inhibition of canonical WNT signaling is not sufficient to block neural crest formation.....	66
3.2.4	Induction conditions are reproducible in various hiPSC lines .....	72
3.2.5	SHH inhibition does not affect neural induction and could be used in case of ventralization of the culture .....	75
3.2.6	Various expansion conditions after neural induction lead to neuronal outcome in cells.....	77
3.2.7	A non-neuronal cell type overgrows the neuronal culture .....	83
3.2.8	A freezable neural progenitor cell type is acquired in the established differentiation protocol .....	88
3.2.9	hiPSC-derived neurons become electrophysiologically active in a time-dependent manner .....	90
3.2.10	A $\beta$ phenotype can be recapitulated <i>in vitro</i> by the use of the established differentiation protocol .....	92
4	DISCUSSION .....	94
4.1	Implementation of xeno-free and chemically-defined cell culture conditions	94
4.2	Development of a robust differentiation protocol to generate hiPSC-derived cortical neurons .....	95
4.3	Establishment of a quick differentiation protocol from hiPSC towards cortical neurons .....	98
4.4	Alzheimer's Disease modeling with hiPSC-derived neurons .....	99
4.5	General conclusion.....	100
5	SUMMARY .....	102
6	ZUSAMMENFASSUNG.....	103
7	REFERENCES .....	104
8	APPENDIX .....	115
8.1	Publications .....	115
8.2	Presentations and poster contributions .....	115

9 LEBENSLAUF ..... 116

10 ACKNOWLEDGEMENTS..... 117

## LIST OF ABBREVIATIONS

<b>Term</b>	<b>Abbreviation</b>
°C	degrees Celsius
µg	microgram
µM	micromolar
Aβ	amyloid β
AICD	APP intracellular domain
AD	Alzheimer's Disease
APP	amyloid precursor protein
APPs	APP soluble
ApoE	Apolipoprotein E
B2M	β-2 microglobulin
BF1	brain factor 1 (gene: FOXP1)
BM	basal medium
BMP	bone morphogenic protein
BDNF	brain-derived neurotrophic factor
BSA	bovine serum albumin
Ca <sup>2+</sup>	calcium ion
cDNA	complementary DNA
Cl	clone
CTF	carboxy-terminal fragment
Cyclo	Cyclopamine
D	day
(db)cAMP	N6,2'-O-Dibutyryl adenosine 3',5'-cyclic monophosphate sodium salt (dibutyryl cyclic AMP)
DM	dorsomorphin dihydrochlorate
DMSO	dimethyl sulfoxide
DPBS	Dulbecco's phosphate buffered saline
E6	Essential 6
E8	Essential 8
FA	formaldehyde
fAD	familial AD

<b>Term</b>	<b>Abbreviation</b>
FCS	fetal calf serum
FGF	fibroblast growth factor
FOXP1	forkhead box protein G1
FTD	frontotemporal dementia
GABA	$\gamma$ -aminobutyric acid
GAD1 (GAD67)	glutamate decarboxylase 1
GAPDH	glyceraldehyde-3-phosphate dehydrogenase
GDNF	glial-derived neurotrophic factor
GWAS	genome-wide association studies
hiPSC	human induced pluripotent stem cell
hPSC	human pluripotent stem cell
LDL	low density lipoprotein
LDN	LDN 193189
Ig	immunoglobulin
LMX1A	LIM homebox transcription factor 1 $\alpha$
LN521	laminin-521
MAP2	microtubule-associated protein 2
MAPT	microtubule-associated protein tau
MCI	mild cognitive impairment
MEA	multi electrode array
MEF	mouse embryonic fibroblasts
Mg <sup>2+</sup>	magnesium ion
min	minutes
mL	milliliter
MM	maturation medium
mM	millimolar
Na-azide	sodium azide
NANOG	homebox protein NANOG
NFT	neurofibrillary tangle
ng	nanogram
nM	nanomolar
NPC	neural progenitor
OCT4 (POU5F1)	octamer binding protein 4

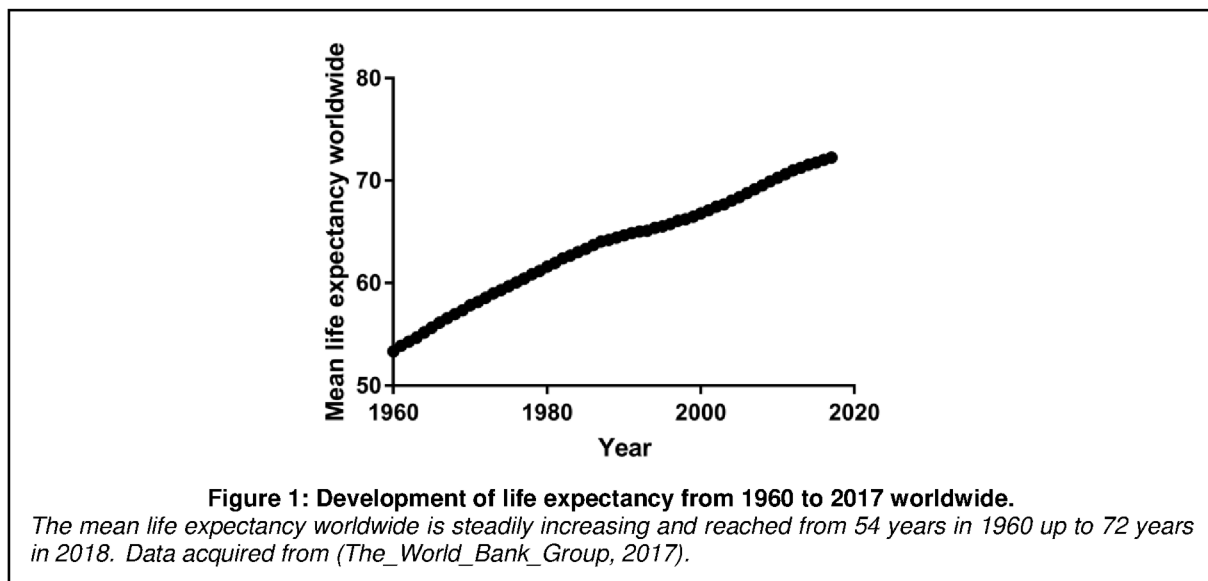


<b>Term</b>	<b>Abbreviation</b>
OSKM	OCT4, SOX2, Klf4, c-Myc, reprogramming factors to derive hiPSCs
OTX2	homeobox protein OTX2
PAX6	paired box protein Pax-6
PD	PD0325901
Pen/Strep	Penicillin/Streptomycin
PLO	poly-L-ornithine
POU5F1 (OCT4)	POU-domain class 5 transcription factor 1
PSC	pluripotent stem cell
PSEN	Presenilin
qPCR	quantitative polymerase chain reaction
RPL13	ribosomal protein L13
rh	recombinant human
SATB2	special AT-rich sequence-binding protein 2
SD	standard deviation
sec	seconds
SEM	standard error of mean
SLC17A6 (vGLUT2)	gene name of vGLUT2
SLC32A1 (vGAT1)	gene name of vGAT1
SOX1	transcription factor SOX1
SOX2	transcription factor SOX2
SOX10	transcription factor SOX10
TBR1	T-box brain protein 1
TBR2	T-box brain protein 2
UBC	poly-ubiquitin-C
vGAT1 (SLC32A1)	vesicular GABA transporter
vGLUT2	vesicular glutamate transporter 2
w	with
WNT	Wingless int-1
w/o	without
w/v	weight per volume

# 1 INTRODUCTION

## 1.1 Neurodegenerative diseases will rise in prevalence

Thanks to an increasing supply of nutrition and especially advances in health care, humans are living longer today than probably ever before in history (Figure 1) (The\_World\_Bank\_Group, 2017). Nevertheless, in a steadily older-growing world population, age-related diseases gain more and more in importance for society.



Neurodegenerative diseases may be considered as age-related diseases: their incidence appears mostly in elderly people. As nowadays, life expectancy is greater than in the years before, the risk of acquiring a neurodegenerative disease is growing as well and will continue to do so in the future (Figure 2)(Drew and Ashour, 2018).

Neurodegenerative diseases are diseases that lead to the degeneration of neurons in specific parts of the brain. Several of these exist, affecting different parts of the brain, some earlier or more severely than others, such as Alzheimer's Disease, Parkinson's Disease, Huntington's Disease, Amyotrophic Lateral Sclerosis, to name a few.

Alzheimer's Disease (AD) leads to dementia in the elderly with progressive loss of memory (dementia), but also mood disorders and changes in behavior. Patients are not able to live alone and handle daily tasks anymore, need care and therefore, social and health care costs were massively increasing over the last years to handle the disease (Alzforum, 2018).

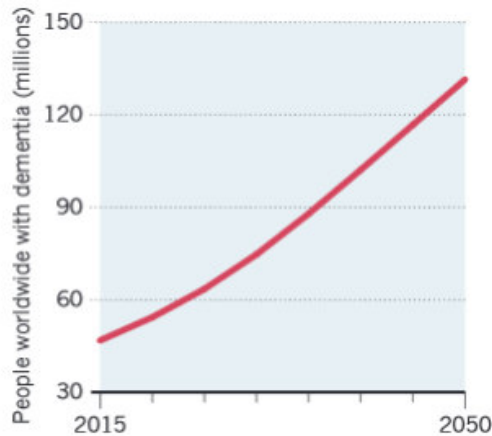


**Figure 2: Estimated prevalence of dementia from 2015 until 2050.**

Due to the older growing world population it is estimated that dementia cases will rise as well. In 2015 approximately 50 million people suffered from dementia, it is expected that the number will rise up to 130 million cases in 2050. Figure from (Drew and Ashour, 2018).

Here, we focus on Alzheimer's Disease, a neurodegenerative disease with an impact on the cortex, which is by far the most known of tauopathies, diseases that involve pathology around the tau protein.

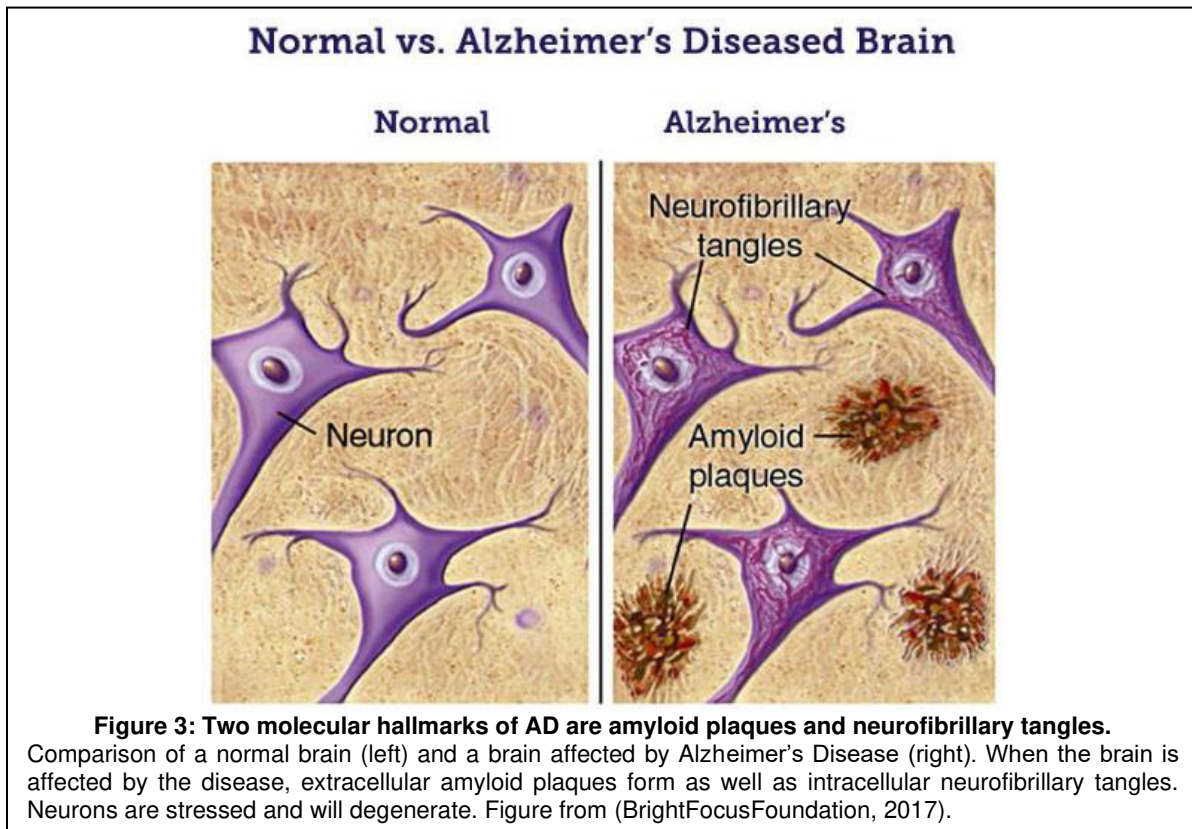
### 1.1.1 Alzheimer's Disease

In 2015 AD affected already 24 million people worldwide with a tendency to increase 2-fold every 20 years (Mayeux & Stern 2012). Alzheimer's Disease is with 60-70% the most frequent cause of dementia in patients (WHO, 2019). It comes along with several symptoms which show declined cognitive functions, such as reduction in thinking, feeling, behaving and perception, leading to impaired judging and finally to fully established dementia (Alzforum, 2018).

Alzheimer's Disease was discovered and defined by the psychiatrist Alois Alzheimer in 1906 and published in the monograph "*Eine seltsame Erkrankung der Hirnrinde*" in 1907 (Alzheimer, 1907). He observed symptoms like rapid memory loss, disorientation in familiar places and hallucinations in his patient Auguste Deter, who was at the age of 51 when the first symptoms appeared in 1906. After her death by the age of 56, Alois Alzheimer examined her brain and found degeneration of the brain and the deposition of A $\beta$ -plaques. When performing silver staining on brain slices, he could identify neurofibrillary tangles (NFTs) inside of neurons as well as remaining tangles after neuron death (Alzheimer, 1907). These neurofibrillary tangles consist mainly of tau proteins, as nowadays known (Kosik et al., 1986). Alois Alzheimer has observed such symptoms already before in other patients. As these patients were already at the age of 70 or older, he did not pay attention as he considered these symptoms as age-

related until he discovered the symptoms in Auguste Deter. These observations already pointed to the fact that AD can be divided into early-onset familial AD (fAD), which is being inherited in a genetic manner, and to late-onset sporadic AD, which appears in aged individuals.

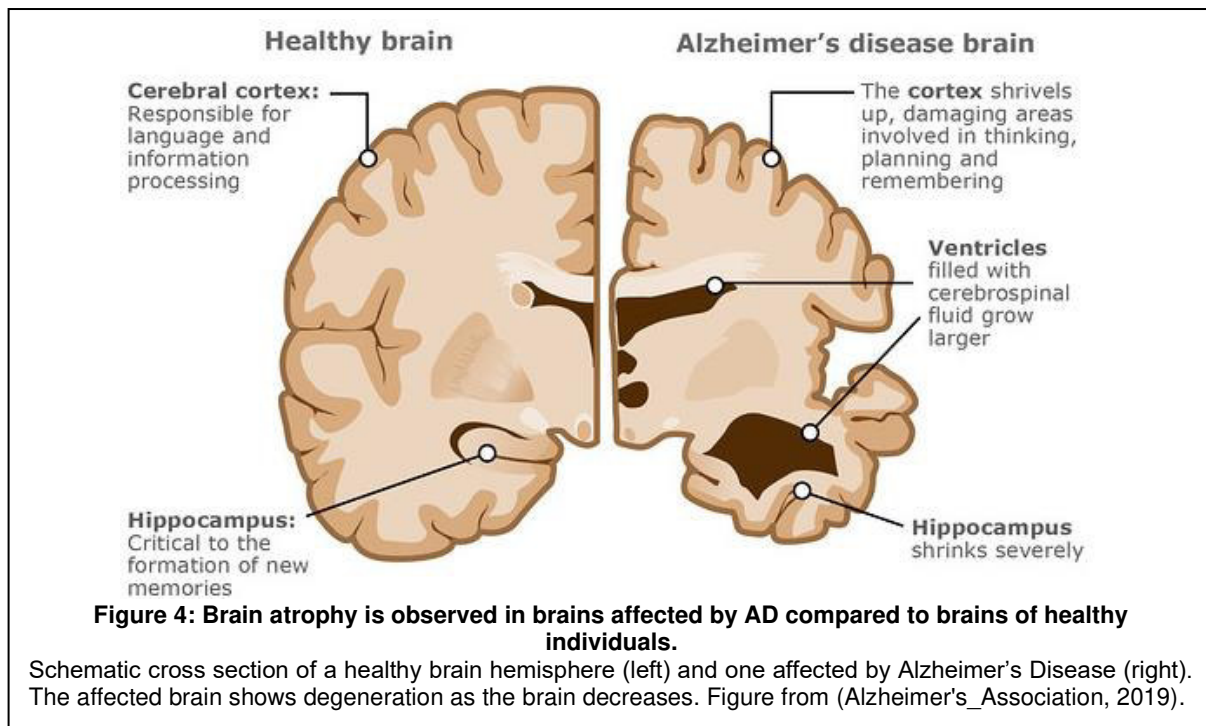
Phenotypic hallmarks of AD are the extracellular A $\beta$ -plaques, also called amyloid- $\beta$  plaques, and NFTs (Figure 3).



Amyloid is a term for a protein-polysaccharide complex which is prone for forming fibrillary structures with  $\beta$ -sheet structure. Amyloid  $\beta$ , as the name already implicates, is also considered as an amyloid protein. A $\beta$ -plaques mainly consist of aggregated A $\beta$  proteins, which are either formed in a too high amount or consist of a too high ratio of a more aggregation-prone variant. Usually, neurons in the brain process the amyloid precursor protein (APP) by proteolytic cleavage into A $\beta$ 40, typically a 40 amino acid long fragment and to a lesser extent the more aggregation prone A $\beta$ 42 (roughly 10% of A $\beta$ 40) (Janelidze et al., 2016). In AD, a higher amount of A $\beta$ 42 compared to A $\beta$ 40 is formed, which is more prone to form aggregates and deposits in the brain. Certain genetic fAD-causing mutations appear in the proteins that are involved in the proteolytic processing of APP (Alzforum, 2018).

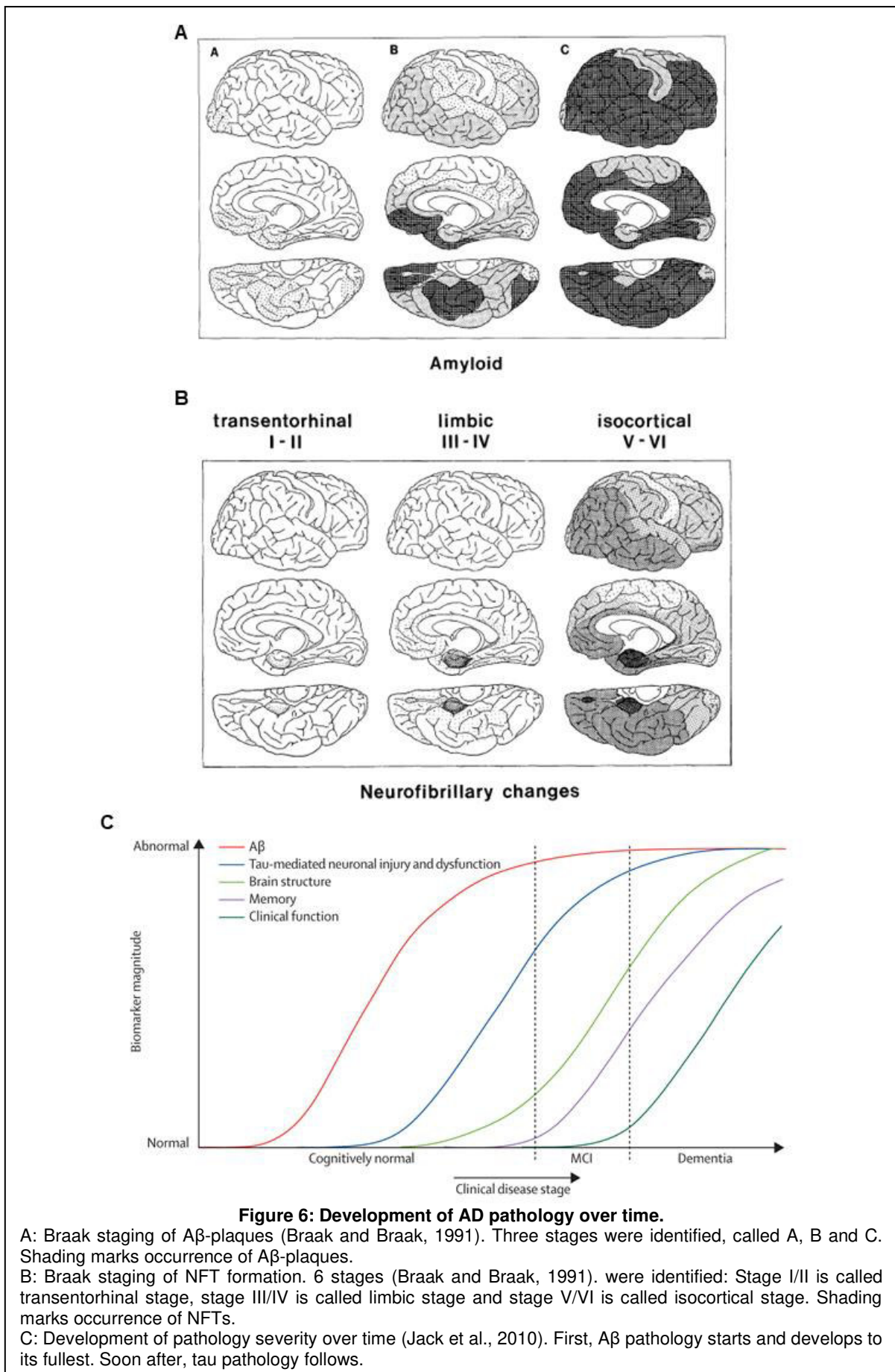
NFTs are usually intracellular helical deposits which mainly consist of the microtubule-associated protein tau (Kosik et al., 1986). Tau is a protein that normally binds to

microtubules in the axons of neurons and leads to their assembly and stabilization (Iqbal et al., 2005). Tau processing and microtubule dynamics, that is affected by tau, are very balanced processes that lead to a constant turnover of microtubules and proteins. This fine-tuned behavior seems to be in disbalance in disease. Due to enhanced post-translational modifications, mostly hyperphosphorylations, tau is detaching from microtubules, which are being destabilized, and they lose integrity (Alonso et al., 1994). Hyperphosphorylated tau is able to capture physiological tau and forms NFTs, making the physiological tau unavailable for microtubules (Alonso et al., 1994). It is believed that microtubules degrade and the affected neurons degenerate. Caused by enhanced neuronal cell death, brain mass shrinks compared to brains of healthy individuals which is even visible at a gross pathology level in later stages of the disease (Figure 4).



Development of brain pathology can also be described by different subsequent stages, so called Braak stages (Braak and Braak, 1991): Braak and Braak investigated *post mortem* brains of healthy individuals and patients with AD symptoms. They could find a timely expansion of A $\beta$ -plaques and NFTs in the brain (Figure 5A and B). Braak and Braak divided the staging for A $\beta$ -plaque distribution into 3 successive stages, called stage A, B and C (Figure 5A). Braak staging of NFT pathology was divided into 6 successive Braak stages, namely I to VI. These stages are further characterized as

the transentorhinal stage (stages I and II), the limbic stage (stages III and IV) and the



isocortical stage (stages V and VI), according to their distribution pattern (Figure 5B). How A $\beta$ -plaques and tau pathology spread in the brain, is not yet clear. However, it is hypothesized that distribution of pathology is similar to prion-like behavior (Jucker and Walker, 2013).

Interestingly, A $\beta$ -plaque progression does not correlate with any AD symptoms but starts sometimes decades before first symptoms of AD are detected. Therefore, A $\beta$ -plaque pathology is a very early indicator or biomarker for AD (Arriagada et al., 1992). Mild cognitive impairment (MCI) is diagnosed in patients with AD at later stages of disease pathology (Figure 5C). During this time point, A $\beta$  pathology is already fully developed and tau pathology has strongly progressed. With increasing staging, symptoms worsen, leading to dementia (Figure 5C).

Diseases which show neurofibrillary tangle formation are named tauopathies and AD is by far the most prominent, known and prevalent tauopathy (Goedert and Jakes, 2005). Unlike for other tauopathies, in which mutations are found in the MAPT gene, this is not the case in AD although tau plays a crucial role in the pathogenesis of AD (Alzforum, 2018). Nevertheless, in AD molecular mechanisms of the disease and the interaction between plaques and NFTs still remain to be elucidated.

Nowadays, genetic risk factors for AD are known as well as mutations leading to fAD.

### 1.1.2 Genetic risk factors and mutations involved in AD

In several genome-wide association studies (GWAS) for AD, the Apolipoprotein E (ApoE) locus was determined as risk factor for both sporadic and familial AD (Bertram et al., 2010). ApoE is a protein that is responsible for the transport of lipids and other proteins and binds to low density lipoprotein (LDL) receptors.

Three major isoforms of ApoE exist: ApoE2, ApoE3 and ApoE4. The normal variant of ApoE is ApoE3, which is also the most common variant in the population (Raber et al., 2004). Risk factor for AD is the isoform ApoE4 (Corder et al., 1993). Carrying one allele increases the likelihood to develop AD by approximately 4-fold, two alleles up to 13-fold. Further, the ApoE4 allele leads to an earlier onset of disease in a dose-dependent manner (Raber et al., 2004). ApoE2 is much less common, the function is also not fully understood, but it seems to reduce the risk for developing AD while increasing the risk for developing a cardiovascular disease (Serrano-Pozo et al., 2011). Further, it was found out that ApoE4 is able to influence A $\beta$  (Huang et al., 2017; Lin et al., 2018).

Mainly mutations that affect the amyloid precursor protein (APP) or components of its processing pathway, such as mutations in *Presenilin (PSEN) 1* or *2* are found in fAD. APP, which is a membrane-spanning protein in neurons, is being processed in the amyloidogenic pathway by a  $\beta$ -secretase, which releases APPs $\beta$ -protein into the extracellular matrix (Figure 6). Subsequently, the  $\gamma$ -secretase, which is a catalytic protease complex, is cleaving the APP further, releasing A $\beta$  into the extracellular space (Figure 6). The catalytic subunits of the  $\gamma$ -secretase are encoded by *PSEN1* and *2* (Kimberly et al., 2000).

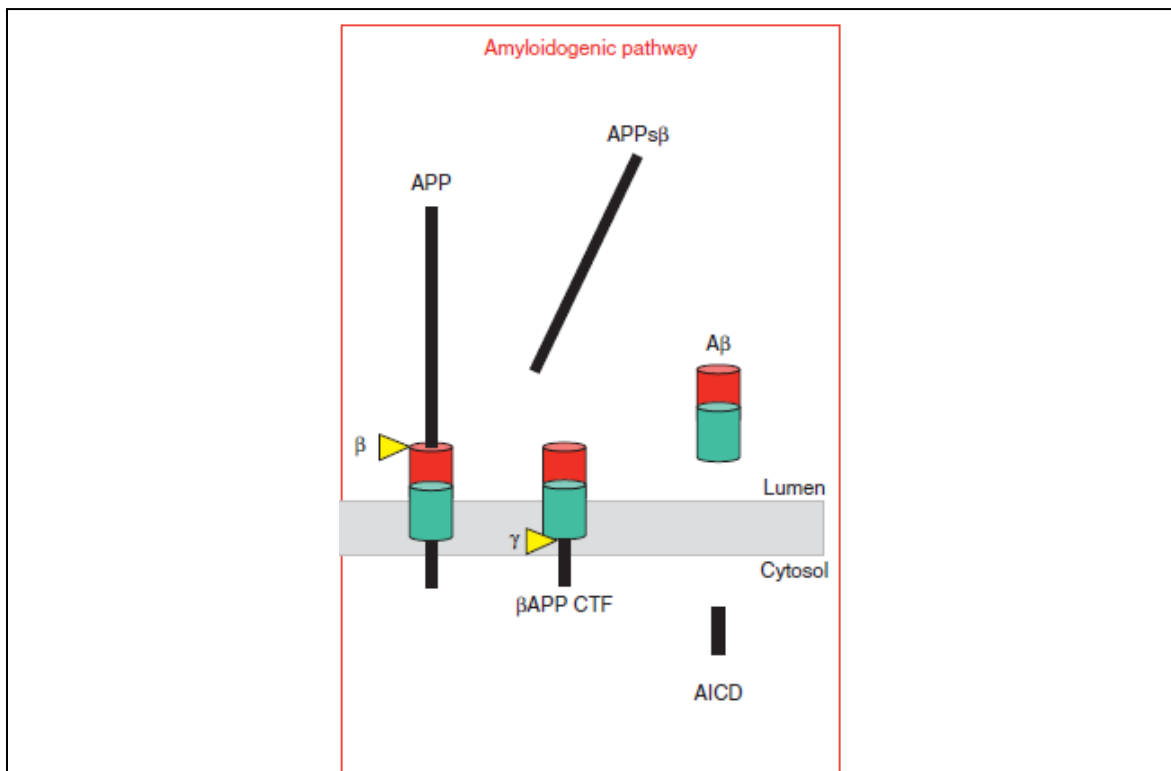


**Figure 8: The amyloidogenic processing pathway of the amyloid precursor protein.**

The amyloid precursor protein (APP), which is a transmembrane protein in neurons, is cleaved by the  $\beta$ -secretase, which releases the APPs $\beta$ -part into the extracellular matrix. Subsequently, the  $\gamma$ -secretase is cleaving a further part of APP into A $\beta$  into the extracellular matrix. APP: amyloid precursor protein,  $\beta$ :  $\beta$  secretase,  $\gamma$ :  $\gamma$ -secretase, APPs: APP soluble, CTF: carboxy-terminal fragment, AICD: APP intracellular domain. Figure adapted from (Haass et al., 2012).

An all-embracing overview of all discovered mutations for fAD so far can be found on <https://www.alzforum.org/mutations>.

Although NFTs can be found in brains of AD patients, no mutations in the MAPT gene were found in AD but are associated with closely related tauopathies such as frontotemporal dementia (FTD). Therefore, it is of great interest to understand the molecular mechanisms of AD pathology and the involvement of NFTs, as well as what discriminates the different tauopathies in their disease pathology.



Another important aspect in AD is neuroinflammation: the immune system in the brain becomes activated and may lead to damage in the brain. Alternatively, a dysfunctional immune system could fail in the normal cleaning and renewing processes in the brain, as well. In this regard, mutations in microglia, the resident immune cells of the brain, which are similar to macrophages, were identified that play a role in AD, such as mutations in TREM2 and CD33 (Alzforum, 2018; Bertram et al., 2010; Sirkis et al., 2016). These mutations seem to be associated with a reduced microglia function and an increased risk of developing AD.

Processes in pathology however remain not completely understood, especially in their interplay, or what process and pathology starts earlier and what are subsequent events that build on each other. Here, novel models for better understanding disease at an earlier stage can be of great advantage.

### 1.1.3 Drugs used in AD cannot influence the disease, but they can ameliorate symptoms

Only two types of drugs for AD and other tauopathies were brought to market until now: the two drug classes are acetylcholine esterase inhibitors and antagonists of NMDA-type glutamate receptor (Orr et al., 2017). However, these treatments do not cure AD and other tauopathies, they rather ameliorate some cognitive symptoms and bring benefits for only a few months.

Drug discovery efforts could not lead to new treatment paradigms in the last 16 years. Although various AD mouse models exist, they cannot reflect all parts of AD pathology. In AD animal models a lot of treatment approaches work to diminish A $\beta$ -plaques and improve cognition, nevertheless translatability to humans is not working well (Franco and Cedazo-Minguez, 2014).

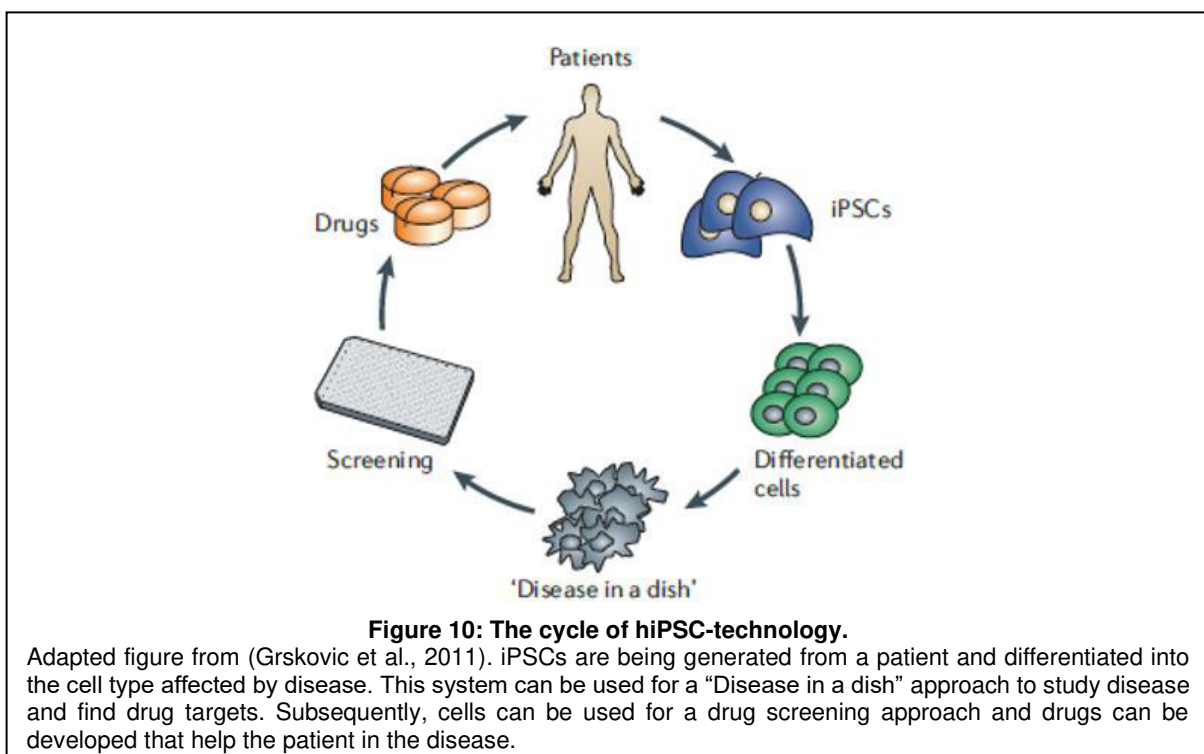
Therefore, other disease models which are more authentic are necessary. One approach is the use of patient-specific human induced pluripotent stem cells (hiPSCs) (Sterneckert et al., 2014). By the help of this technology, neuronal cell types affected in AD, for instance cortical neurons, could be generated and disease modeling could be performed with a cell culture model that could not be closer related to the patient. Further, the hiPSC-technology could be used for drug discovery and drug screening approaches, therefore, it will be highlighted in more detail.

## 1.2 Pluripotent stem cells: a new promise for drug discovery

In 1998 Thomson and his lab were able to isolate embryonic stem cells from human embryos and culture them *in vitro* (Thomson et al., 1998). It was possible to expand these cells indefinitely and in theory, these cells bear the potential to be able to differentiate into any cell type of the human body. With this success, hopes arised that these human embryonic stem cells (hESCs) could be used for developmental studies, as well as for drug discovery and regenerative medicine.

Unfortunately, the use of hESCs comes along with ethical concerns as the ESCs bear the potential to create a human being when implanted into a blastocyst and more importantly, a human embryo is typically destroyed in the process of deriving these stem cells (Lo and Parham, 2009). Therefore, research on and with hESCs is not allowed in all countries and also tightly regulated in those that allow their use (Lo and Parham, 2009).

Contrary accounts for induced pluripotent stem cells: these can be derived by reprogramming of somatic (fully matured) cells from the body of any individual (Takahashi et al., 2007). The simple overexpression of a set of few (typically four – OCT4, SOX2, KLF4, c-MYC) pluripotency – associated transcription factors is enough to “reprogram” a mature cell into a pluripotent state. These cells are fully pluripotent and can not only be eternally propagated, but also differentiated into all three germ layers (Takahashi et al., 2007). When first published by Yamanaka and colleagues, it



was quickly regarded as a promising alternative source of embryonic stem cells. This is also highlighted by the fact that Professor Yamanaka was awarded the Nobel Prize for Medicine and Physiology already in 2012, only five years after the discovery. When derived from patients with a specific disease, such as AD, these cells are a great tool to derive patient-specific cells suitable for disease modeling. Such a cellular system can further be used for drug discovery in later stages, such as drug screening and drug development (Figure 7). The hiPSC-technology was already successfully used for disease modeling of a wide range of diseases, including, among others, cardiac, neurological and neurodegenerative diseases such as Huntington's or Parkinson's Disease (Ebert et al., 2009; Ho et al., 2016; Moretti et al., 2010; Reinhardt et al., 2013; Ren et al., 2015). Also for AD, such cell culture systems were already used for disease modeling and even drug screening approaches (Brownjohn et al., 2017; Choi et al., 2014; Duan et al., 2014; Huang et al., 2017; Kondo et al., 2013; Kondo et al., 2017; Woodruff et al., 2016).

Therefore, with the growing need of adequate cell culture systems for drug discovery, the hiPSC technology bears a new promise for drug discovery in the future.

### 1.3 Cell culture conditions of PSCs and the importance of xeno-free and chemically-defined culture conditions

In 1959 Russel and Burch invented the "3R-concept": It postulates that the use of animals and products derived out of them in research should be reduced, replaced and refined (reprinted in 1992 (Russel and Burch, 1992)). In the case of cell culture, especially also in PSC culture, a lot of animal-derived ingredients are used, for instance in cell culture media, or coating proteins and growth factors.

In this attempt, it is an elegant idea to replace animal-derived factors by recombinant proteins of the same species of the culture to derive a xeno-free (free of foreign species) culture.

When Thomson isolated human embryonic stem cells from blastocysts in 1998, he and his colleagues grew the cells on a feeder layer which were irradiated mouse embryonic fibroblasts (MEFs) in fetal calf serum (FCS)- components containing medium (Thomson et al., 1998). In his paper he mentioned that when growing ES cells in the absence of MEFs, the ES cells started to differentiate, indicating the importance of

MEFs in maintaining the pluripotency of hESCs, but it was unknown which trophic factors the MEFs provide.

Nevertheless, the growth of hESCs on MEFs and in the conditioned media the MEFs produce, the cell culture system was very variable and not well defined. Development away from feeder layers and conditioned medium towards Matrigel (which is purified extracellular matrix) coating and more defined cell culture media gained in importance (Xu et al., 2001). In the next years, members of the Thomson lab started to optimize ESC culture medium and developed the chemically defined “TeSR” medium which allowed the culturing of hESCs in a feeder-free way (Ludwig et al., 2006). Further optimization finally led to the identification of the only eight absolutely necessary components of PSC-medium and the medium, called Essential 8 (E8) medium, is since then the state of the art for culturing both hESCs and hiPSCs under fully defined conditions (Chen et al., 2011).

Other components from animal origin used in many, even more defined cell culture systems are Matrigel and bovine serum albumin (BSA), which can be found in cell culture media as well as a carrier protein in soluble protein preparations.

### 1.3.1 Matrigel

When culturing hiPSCs and derived neural precursors and neurons, Matrigel is one of the major coating agents used. Matrigel is an extracellular matrix extracted from Engelbreth-Holm-Swarm mouse sarcoma. For this purpose, the tumor needs to be propagated in mice (Kibbey, 1994). As an extract, it may contain growth factors and extracellular proteins, which may vary from batch to batch and interfere when growing hiPSCs: Cells might spontaneously start differentiating.

Xeno-free alternatives for Matrigel coating are recombinant proteins of the extracellular matrix, such as vitronectins, collagens, fibronectins and laminins, some of which are used when culturing hPSCs (Chen et al., 2011; Lam and Longaker, 2012; Yasuda et al., 2018). It was found that hiPSCs produce  $\alpha$ -laminins to build their extracellular matrix for attachment but not the other proteins (Laperle et al., 2015). When knock-out cells were cultivated, they could survive using coating of recombinant laminin-521 (Laperle et al., 2015).

### 1.3.2 Bovine serum albumin

Another factor, that is ubiquitously used in cell culture media or supplements is bovine serum albumin (BSA). BSA is the main protein component of bovine serum and it bears several beneficial effects *in vivo* and for *in vitro* cell culture: It acts as an antioxidant, it binds several components such as various molecules, fatty acids, hormones, ect. That is the reason, why BSA was still kept as a medium component when serum was removed from cell culture conditions.

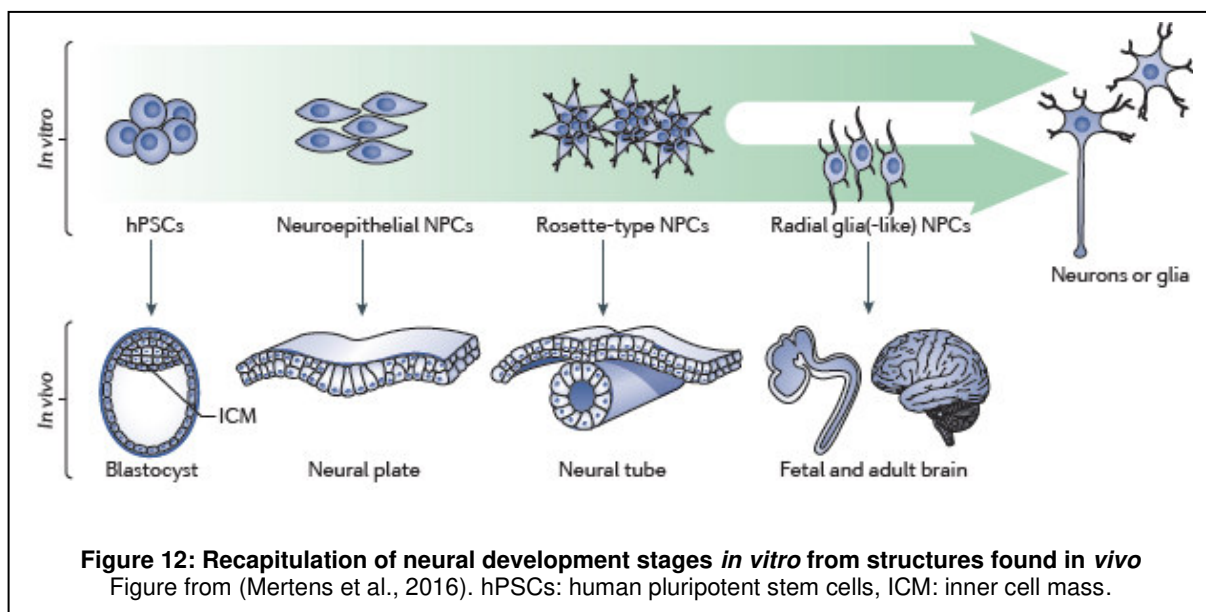
Besides the mentioned use, BSA can act as a carrier protein when preparing soluble protein solutions to block unspecific binding sites for proteins in cell culture ware.

When working with human cell culture, BSA can be replaced by human serum albumin (HSA) to derive a xeno-free cell culture condition. Unfortunately, HSA, which is extracted from blood donations, is more expensive.

BSA is also component of the B27 supplement, which is widely used in media when culturing neurons or differentiating PSCs towards neurons to replace serum. Fortunately, a xeno-free B27 supplement consists which uses HSA instead. Further, B27 supplement might either include traces of vitamin A or may be free of vitamin A. Both supplements are being used in case of neural induction, although it was shown by Li and colleagues, that it might have an adverse effect on neural induction (Espuny-Camacho et al., 2013; Kirkeby et al., 2012; Kirwan et al., 2015; Li et al., 2009; Shi et al., 2012a; Shi et al., 2012b).

## 1.4 Deriving cortical neurons from hiPSCs

Pluripotent stem cells have the potential to theoretically differentiate into any cell type of interest. In the case of AD and other tauopathies, the affected cell types are cortical neurons. In this regard, it is of interest to derive cortical neurons from hiPSCs. A way to derive the right cell type is to differentiate hiPSCs towards the desired cell type by mimicking differentiation *in vivo* and to transfer findings into *in vitro* (Figure 8) (Mertens et al. 2016). Findings *in vivo* usually derived from experiments performed in *Xenopus*, chick embryos, mice or other species. It is thought that early development is a conserved process among a variety of species and therefore, most findings should be applicable also to human. Nevertheless, not all details could already be clarified in humans. An advantage of hESCs and hiPSCs is that unknown facts of development can also be analysed in this system. Therefore, some findings are also attributed to the use of hPSCs.



During gastrulation in *Xenopus*, it was found out that a part of the ectoderm forms the neuroectoderm. This happens as some signaling molecules from underlying organizer regions influence the formation of neuroectoderm by secreting components that influence pathways. In this regard, the bone morphogenic protein (BMP) inhibitor Noggin was identified: It is secreted by the Spemann organizer and leads to formation of neuroectoderm together with other signaling clues (Lamb et al., 1993). BMP activity induces epidermis formation in that part of ectoderm which does not form neuroectoderm (Wilson and Hemmati-Brivanlou, 1995). In later stages other secreted

proteins were identified, which were for instance follistatin, an antagonist of Activin signaling in the TGF- $\beta$  pathway (Hemmati-Brivanlou and Melton, 1994).

Various differentiation protocols from PSCs towards cortical neurons exist, but all protocols differ in some small details. In general, such differentiation protocols were divided into three different phases:

- 1) neural induction
- 2) expansion
- 3) final maturation

During neural induction, hiPSCs are forced out of the pluripotency state into the direction of the neuroectoderm to obtain neuroepithelial cells, which represent neural progenitors. During expansion, neural progenitors are expanded to generate a larger pool of cells and the neural progenitor cell (NPC) type is being manifested. The final maturation should lead to a final differentiation of NPCs into functional neurons.

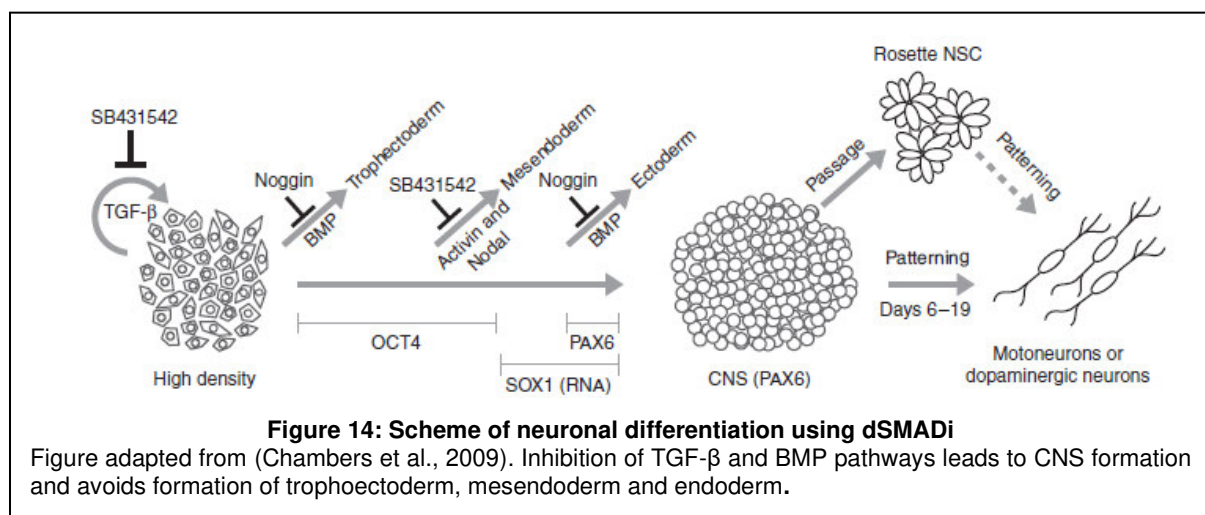
Two major signaling pathways are important for maintaining a pluripotent stem cell state in hiPSCs: FGF (typically basic FGF, also known as FGF2) signaling, which signals through the MAPK/MEK pathway, and TGF/Activin signaling, which signals through the SMAD2/3 pathway. These are also the only growth factors needed in the abovementioned E8 medium (Chen et al., 2011; Greber et al., 2011; Vallier et al., 2005).

Different approaches exist for neural induction of hPSCs: they can be grown as aggregates forming embryoid bodies or as adherent culture.

When the embryoid body approach was used, it was found that no extrinsic signals were needed when aiming for neuroectoderm formation and postulated to be the default pathway when no other clues are used (Zhang et al., 2001). Nevertheless, this strategy greatly depends on “clean” media components and no unwanted tendencies of the PSCs to more efficiently differentiate into other than the neuroectodermal lineages. At later stages, inhibitors of BMP or TGF- $\beta$  were applied which derived from findings of *Xenopus* described above (Elkabetz et al., 2008; Smith et al., 2008) The key for neural induction in an adherent system was to apply the so called double SMAD inhibition (dSMADi) which included the inhibition of both BMP and TGF- $\beta$  pathways by

SB431542 and Noggin/Dorsomorphin which inhibit ALK4/5/7 (Activin/Nodal/TGF- $\beta$  receptors) and ALK2/3/6 (BMP type I receptors) respectively, which signal through SMAD proteins (Figure 9) (Chambers et al., 2009). Inhibition of the TGF- $\beta$  pathway antagonizes the pluripotency state of hiPSCs and prevents formation of mesendoderm, while the inhibition of the BMP pathway prevents formation of the trophoectoderm and the non-neural ectoderm (Chambers et al., 2009; D'Amour et al., 2005; Tchieu et al., 2017; Xu et al., 2002). Thus, dSMADi seems to be beneficial for neuroectoderm formation.

Most protocols which followed still involved dSMADi, but addressed further pathways to enhance the induction towards dorsal forebrain, such as the WNT or MEK pathways (Greber et al., 2011; Moya et al., 2014; Qi et al., 2017; Shi et al., 2012a; Shi et al., 2012b).



WNT signaling is known to be involved on one hand in anterior-posterior patterning (Kirkeby et al., 2012; Moya et al., 2014), on the other hand in dorso-ventral patterning together with the antagonizing SHH signaling, which is responsible for ventral development (Li et al., 2009; Maroof et al., 2013). Further, it was found that WNT signaling might also contribute to neural crest formation (Chambers et al., 2012; Mica et al., 2013; Tchieu et al., 2017): neural crest progenitors form neurons of the peripheral nervous system and other cell types from the periphery.

Further, it was described that WNT signaling is a factor of variability among hPSC lines (Blauwkamp et al., 2012; Moya et al., 2014; Ortmann and Vallier, 2017): it might be differentially activated in various PSC lines, but also change dynamically over time.



The differential activity of WNT might contribute to different differentiation potentials or propensities (Blauwkamp et al., 2012; Moya et al., 2014; Ortmann and Vallier, 2017). Therefore, WNT inhibition might be beneficial for avoiding neural crest formation. Nevertheless, the differentiation from hiPSCs towards mature and functional neurons is a lengthy process needing up to several months to derive functional neurons (Kirwan et al., 2015).

The role of FGF2 during neural induction has been quite controversial: Some groups claim its activation is necessary for neural induction (LaVaute et al., 2009), others describe more advantageous effects when FGF signaling is inhibited (Greber et al., 2011; Yao et al., 2006).

A way to accelerate neural induction and thus neuronal differentiation was described by Greber and colleagues (Greber et al., 2011): He described that when inhibiting MEK1/2, a downstream signaling pathway of FGF2, neural induction could be accelerated and sensory neurons could be generated within 8 days (Chambers et al., 2009). Part of the confusion could stem from the fact that when transferring procedures from mouse PSCs: There, FGF signaling is crucial and blockage is detrimental for neural induction. It should be noted that mouse PSCs exist in a “naïve” state that appears to be developmentally slightly upstream of the “primed” pluripotent state of hiPSCs. In order to differentiate into neuroectoderm, mouse PSCs therefore have to transition through the primed state, which is, like hiPSCs, dependent on FGF signaling (Greber et al., 2011).

On the other hand, FGF signaling plays an important role after neural induction during the expansion phase, in which NPCs can be expanded and stabilized (Elkabetz et al., 2008; Falk et al., 2012; Shi et al., 2012a; Yao et al., 2006; Zhang et al., 2001).

In 2017, a very fast differentiation protocol was published by Qi et al.: In their protocol, morphologically mature cortical neurons could be derived within 16 days of differentiation by the use of the accelerating effect by, among others, inhibiting the FGF2 pathway (Qi et al., 2017).

The drawback of this protocol is that no progenitor exists as no expansion step is included in this protocol (Qi et al., 2017). Such an NPC type could be used for genetic manipulation or freezing in between so that the initial step of differentiation could be

skipped. Further, a colleague tried to reproduce the protocol. Morphologically, only 2 out of 5 differentiation attempts were successful (data not shown).

Differentiation of hPSCs into neurons can be performed, as described earlier, in 3D or in 2D culture, both approaches bear their advantages and disadvantages: 3D recapitulates the situation *in vivo* more physiologically. The drawback is, that several cell types are formed and that it is impossible to derive a single cell type of interest (Lancaster and Knoblich, 2014). Therefore, differentiation in 2D has the advantage that single cell types can be formed more accurately with less foreign cell type contamination and better control over cell morphology and signaling can be maintained.

Therefore, here, the aim was to develop a robust, and quick 2D differentiation protocol which is xeno-free and chemically-defined and can ideally be applied to any available hiPSC line.

## 2 MATERIALS AND METHODS

### 2.1 Instruments

<b>Instruments</b>	<b>Company</b>
ArrayScan	Thermo Fisher
Maestro Pro	Axion Biosystems
NanoDrop	Thermo Fisher
QiaCube	Qiagen
QuantStudio 7 Flex Real Time PCR System	Thermo Fisher
Biomark HD	Fluidigm
Juno	Fluidigm

### 2.2 Cell culture

#### 2.2.1 Dishes and flasks

<b>Plate format/flask format</b>	<b>Company</b>	<b>Order number</b>	<b>Growth Area</b>
<b>6-well plate</b>	Nunc	140675	9.5cm <sup>2</sup>
<b>12-well plate</b>	Nunc	150628	3.5cm <sup>2</sup>
<b>96-well plate µclear</b>	Greiner	655950	0.34cm <sup>2</sup>
<b>T75 flask</b>	Greiner	658175	75cm <sup>2</sup>
<b>T175 flask</b>	Greiner	660175	175cm <sup>2</sup>

#### 2.2.2 Cell lines

<b>hiPSC line</b>	<b>Referred to as</b>	<b>Source</b>	<b>Phenotype</b>	<b>Sex</b>	<b>Age</b>	<b>Reprogram- ming method</b>	<b>Reprogram- ming factors</b>
SBAD3 Cl1	hiPSC_1	StemBANCC	healthy control line	female	31 years	Sendai virus	OSKM
SFC840 Cl3	hiPSC_2	StemBANCC	healthy control line	female	n/a	Sendai virus	OSKM

SFC086 Cl1	hiPSC_3	StemBANCC	healthy control line	female	n/a	Sendai virus	OSKM
SFC808 Cl4	hiPSC_PSEN1	StemBANCC	PSEN-1 intron 4 deletion	female	n/a	Sendai virus	OSKM
MAPT WT CIF9 (IPSC0028)	hiPSC_4	Sigma	healthy control line	female	24 years	retroviral	OSKM
MAPT WT FsRed clone 1E11	hiPSC_5	engineered from IPSC0028	healthy control line, fusion red tag at MAPT locus	female	24 years	retroviral	OSKM
MAPT Pbi Ebi FsRed clone 1D9	hiPSC_MAPT	engineered from IPSC0028	Biallelic P201S biallelic E10-16	female	24 years	retroviral	OSKM

### 2.2.3 Cell culture media ingredients, coatings and buffers

Product	Company	Order number
<b>Media ingredients</b>		
Accutase in DPBS	Life Technologies	A11105-01
Advanced DMEM/F12	Life Technologies	12634-028
B27 supplement w/o vitamin A (50x), serum-free	Life Technologies	12587-010
CTS-B27 (50x), serum-free	Life Technologies	A1486701
DMEM/F12	Life Technologies	31330-095
Dimethyl sulphoxide (DMSO)	Serva	20385.01
Essential 6 Medium	Life Technologies	A1516501
Essential 8 Flex Kit	Life Technologies	A-11105-01
L-Glutamine, 200mM	Life Technologies	25030-024
Neurobasal medium	Life Technologies	21103-049
N2 supplement (100x), serum-free	Life Technologies	17502-48
Penicillin/Streptomycin (Pen/Strep) (100x)	Life Technologies	15140-122
<b>Coatings reagents</b>		
Matrigel, hESC-qualified	Corning	354277

<b>Product</b>	<b>Company</b>	<b>Order number</b>
recombinant human (rh) Laminin-521 (LN521)	BioLamina	LN521-03
poly-L-ornithine solution, 0.01%	Sigma-Aldrich	P4957
rh Vitronectin (VTN-N)	Thermo Fisher Scientific	A14700
<b>Buffers and liquids</b>		
distilled water	Life Technologies	15230-071
Dulbecco's phosphate buffered saline (DPBS) with Mg <sup>2+</sup> & Ca <sup>2+</sup>	Life Technologies	14040-091
DPBS w/o Mg <sup>2+</sup> & Ca <sup>2+</sup>	Life Technologies	14190-169

#### 2.2.4 Small molecules and organic molecules

<b>Small molecule</b>	<b>Company</b>	<b>Catalog number</b>	<b>CAS number</b>	<b>Mode of action</b>
ascorbic acid	Sigma-Aldrich	A4544	50-81-7	Vitamin C, reducing agent, antioxidant
CHIR99021	AbbVie internal compound	-	252917-06-9	Inhibitor of Glycogen Synthase 3 (GSK3)
Cyclopamine	Tocris	1623	4449-51-8	Sonic hedgehog (SHH) inhibitor
DAPT	Sigma-Aldrich	D5942	208255-80-5	$\gamma$ -secretase inhibitor
dbcAMP	Sigma-Aldrich	D0627-1G	16980-89-5	cAMP analogue, penetrates cell membrane
Dorsomorphin dihydrochloride	Tocris	3093	1219168-18-9	AMPK inhibitor, BMP type I receptor inhibitor
IWP2	Tocris	3533	686770-61-6	PORCN inhibitor, inhibits processing and

Small molecule	Company	Catalog number	CAS number	Mode of action
				secretion of WNT molecules
LDN193189	Sigma-Aldrich	SML0559-5MG	1062368-24-4	ALK2 and 3 inhibitor
PD0325901	Tocris	4192	391210-10-9	MEK1/2 inhibitor
SB431542	Tocris	1614	301836-41-9	Inhibitor of TGF- $\beta$ type I receptor/ALK5, ALK4, ALK7 inhibitor
XAV939	Tocris	3748	284028-89-3	Tankyrase inhibitor
Y-27632	Calbiochem	688000-10MG	146986-50-7	P160 ROCK inhibitor

#### 2.2.4.1 Preparation of small molecules and organic molecules

Powder of small molecules and organic molecules was diluted according to the manufacturer's protocol, aliquoted in tubes and stored at  $-20^{\circ}\text{C}$ . Aliquots were used within 6 months and then prepared freshly. Thawed aliquots were stored in the fridge and used within several days.

Small molecule	Stock concentration	Working concentration	Preparation
Ascorbic Acid	200 $\mu\text{M}$	200nM	solved in sterile, distilled water, sterile-filtered
CHIR99021	10mM	0.5 $\mu\text{M}$ – 3 $\mu\text{M}$	solved in DMSO
Cyclophamide	5mM	5 $\mu\text{M}$	solved in DMSO
DAPT	10mM	10 $\mu\text{M}$	solved in DMSO
dcAMP	100mM	500 $\mu\text{M}$	solved in sterile, distilled water, sterile-filtered

<b>Small molecule</b>	<b>Stock concentration</b>	<b>Working concentration</b>	<b>Preparation</b>
Dorsomorphin dihydrochloride	10mM	1 $\mu$ M	solved in DMSO
IWP2	5mM	1 $\mu$ M	solved in DMSO
LDN193189 hydrochloride	0.5mM	0.5 $\mu$ M	solved in DMSO
PD0325901	10mM	1 $\mu$ M	solved in DMSO
SB431542	10mM	10 $\mu$ M	solved in DMSO
XAV939	10mM	2 $\mu$ M	solved in DMSO
Y-27632	5mM	10 $\mu$ M	solved in sterile, distilled water

## 2.2.5 Proteins

<b>Protein</b>	<b>Company</b>	<b>Order Number</b>
Brain-derived neurotrophic factor (BDNF), animal-free	Peprtech	AF-450-02
Human Serum Albumin(HSA), non-denatured	Merck	126654
Fibroblast growth factor (FGF)- basic, animal-free	R&D Systems	AF-100-18B
Glial-derived neurotrophic factor (GDNF), animal-free	Peprtech	AF-450-10
WNT-3a	R&D Systems	5036-WN

### 2.2.5.1 Preparation of proteins

Lyophilized proteins were diluted according to the manufacturers protocol: Proteins were diluted to 100 $\mu$ g/mL in sterile water. Then, further dilution was prepared in DPBS containing Mg<sup>2+</sup> and Ca<sup>2+</sup> with 0.1% of HSA as a carrier protein. Solutions were aliquoted in tubes and stored at -20°C.

<b>Protein</b>	<b>Stock concentration</b>	<b>Working concentration</b>	<b>Preparation</b>
FGF-basic (FGF)	10µg/mL	10ng/mL	first in water, then in DPBS with carrier protein
BDNF	10µg/mL	10ng/mL	first in water, then in DPBS with carrier protein
GDNF	10µg/mL	10ng/mL	first in water, then in DPBS with carrier protein

## 2.2.6 Preparation of media

### 2.2.6.1 E8flex Medium

E8flex medium was prepared as recommended by the supplier: From the basal E8 medium, 10mL of medium were removed and 10mL of the E8 flex supplement were added. Medium was stored at 4°C and used no longer than for 4 weeks.

### 2.2.6.2 Basal Medium (BM)

<b>Ingredient</b>	<b>Stock concentration</b>	<b>Dilution</b>	<b>Final concentration</b>
<b>DMEM/F12</b>	1x	1:2	0.5x
<b>Neurobasal</b>	1x	1:2	0.5x
<b>N2 supplement</b>	100x	1:200	0.5x
<b>B27 supplement</b>	50x	1:100	0.5x
<b>Pen/Strep</b>	100x	1:100	1x
<b>Glutamine</b>	200mM	1:200	1mM

After preparation, medium was sterile-filtered and stored at 4°C until use, but no longer than for 4 weeks.



### 2.2.6.3 Maturation Medium (MM)

<b>Ingredient</b>	<b>Stock concentration</b>	<b>Dilution</b>	<b>Final concentration</b>
BM	1x	-	1x
dbcAMP	100mM	1:200	500µM
ascorbic acid	200µM	1:1000	200nM
LN521	100µg/mL	1:100	1µg/mL
BDNF	10µg/mL	1:1000	10ng/mL
GDNF	10µg/mL	1:1000	10ng/mL

Medium was stored at 4°C until use, but no longer than for 2 weeks. Within the first days of maturation, medium was supplemented by DAPT and PD.

### 2.2.7 Coating of dishes and flasks

Following amount of coating solution was administered to the flasks/wells of a cell culture plate:

<b>Well/Flask</b>	<b>Coating volume</b>
<b>T175</b>	17.5mL
<b>T75</b>	7.5mL
<b>6-well</b>	1mL
<b>12-well</b>	0.5mL
<b>96-well</b>	60µL

#### 2.2.7.1 Preparation of Matrigel aliquots

Matrigel was thawed slowly on ice in the fridge overnight. Then, aliquots were prepared according to the manufacturer's dilution factor provided: The aliquots should have the amount necessary to dissolve in 25mL of DMEM/F12 medium.

After aliquoting, which was performed on ice, aliquots were stored at -20°C

### *2.2.7.2 Coating with Matrigel*

Frozen Matrigel aliquots were dissolved in 25mL of cold DMEM/F12, mixed and flasks or wells were quickly coated. Coated plastic were was stored in an incubator at 37°C for 2 to 4 hours. In case of long-term storage, plastic ware was sealed with parafilm and stored in the fridge until use, but not for longer than 2 weeks.

### *2.2.7.3 Coating with LN521*

Cell culture dishes were coated with 5µg/mL LN521 by diluting the stock in DPBS with Mg<sup>2+</sup> and Ca<sup>2+</sup>. Coating solution was simply added to the flasks or wells of the cell culture plate, the dishes were sealed with parafilm to prevent drying and stored at 4°C on a shaker for at least 2 hours, but not longer than 3 weeks. After a week in fridge, coating solution needed to be supplemented with DPBS with Mg<sup>2+</sup> & Ca<sup>2+</sup> to prevent drying from long term storage.

### *2.2.7.4 Coating with VTN-N*

VTN-N was solved 1:200 in DPBS with Mg<sup>2+</sup> and Ca<sup>2+</sup> to derive a 2.5µg/mL coating solution. Plastic ware was coated and stored in the incubator for 2 hours until use. In case of long-term storage, plastic ware was sealed with parafilm and stored in the fridge until use, but not for longer than 2 weeks.

### *2.2.7.5 Double-coating with poly-L-ornithine (PLO) and LN521*

Cell culture dishes were first coated with poly-L-ornithine (PLO) by diluting the stock-solution to 0.001% of PLO with DPBS with Mg<sup>2+</sup> and Ca<sup>2+</sup>. Dishes were sealed with parafilm and stored at 4°C on a shaker for at least 4hrs or overnight. Then, coating was aspirated, dishes were washed once with DPBS with Mg<sup>2+</sup> and Ca<sup>2+</sup> and then, coated with LN521 as described before.

## 2.3 Cell culture procedures

### 2.3.1 Culturing & passaging of cells

hiPSCs were grown on plastic dishes or well plates coated with 5µg/mL of recombinant human LN521.

Cells were grown until 70-100% of confluency and were passaged then. For passaging, cells were washed with DPBS w/o Mg<sup>2+</sup> & Ca<sup>2+</sup>, detached and singularized by incubation with Accutase for 5-8min at 37°C, transferred to medium and centrifuged at 300xg for 5min and replated on a new dish in E8flex medium supplemented with 10µM of Y-27632. The next day or a few hours later, medium was changed to E8flex only to get rid of Y-27632. E8flex medium was changed every day or every other day, depending on medium consumption. In case of weekends medium change was performed every 2.5 days. The splitting ratio or seeding density was adjusted to the needs. Cells were split between a ratio of 1:6 to 1:12 or seeded as 10 000 to 35 000cells/cm<sup>2</sup> depending on how quick they proliferated and when the cells were needed for a differentiation round.

### 2.3.2 Freezing of cells

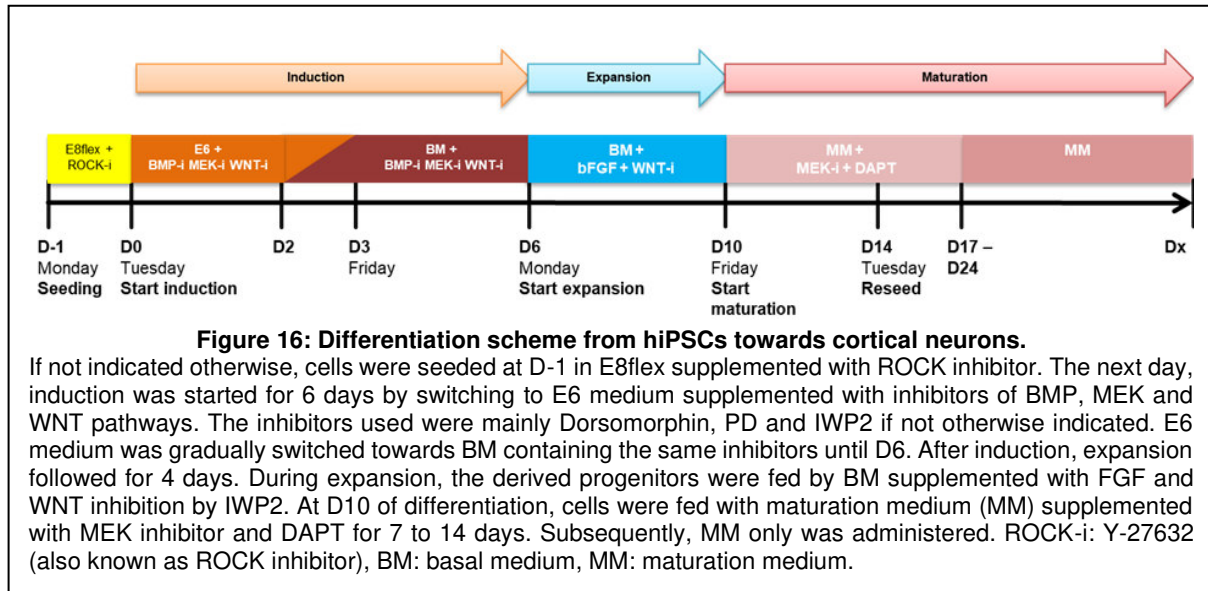
Cells were passaged as described before. After the centrifugation step, cells were resuspended in freeze medium consisting of the culturing media supplemented with 10% DMSO and 10µM Y-27632 in a cryo vial. The vial was quickly placed into a controlled rate freezing container and transferred to -80°C for a few days. Then, cells were transferred to liquid nitrogen until use.

### 2.3.3 Thawing of cells

Cryo tubes with frozen cells were quickly thawed in a 37°C-water bath and transferred into culture medium. Then, cells were centrifuged as described, resuspended carefully in culture medium supplemented with 10µM Y-27632 and plated on a coated dish. A minimum of 4 hours later or the next day, cell medium was replaced by medium without Y-27632.

### 2.3.4 Differentiation of cells

If not otherwise indicated, cells were induced for 6 days, expanded for 4 days and finally matured until use (Figure 10)



#### 2.3.4.1 Induction

For induction, cells were seeded between 200 000 – 500 000 cells/cm<sup>2</sup> in E8flex supplemented with 10 μM Y-27632 onto LN521-coated dishes, if not indicated otherwise. As soon as the cells formed a fully confluent layer, preferable the day after seeding, induction was started with E6 medium supplemented with small molecules as indicated. On day 2, a 50%-mixture of E6 medium and basal medium (BM) was prepared and supplemented with small molecules as indicated. On day 3, medium was replaced by BM supplemented with the small molecules as indicated. Medium change was performed every day except on weekends, when medium was changed every 2.5 days. If not indicated otherwise, RNA samples were collected at D0, D3 and D6. The same days, 96-well plates were fixed for immunofluorescence analysis if needed.

#### 2.3.4.2 Expansion

If not indicated otherwise, a part of the cells from induction were expanded from day 6 onwards. For expansion, medium was changed to expansion medium which consists of BM supplemented with pathway modulators as indicated. Usually, FGF only, FGF and IWP2 or FGF together with IWP2 and Cyclopamine (Cyclo) were used.

#### *2.3.4.3 Maturation*

After 4 days of expansion, cells were fed with maturation medium supplemented with PD and DAPT. After 4 days, cells were reseeded onto PLO/ LN521 coated plates in MM supplemented with PD, DM and 10 $\mu$ M Y-27632. The next day, medium was changed to get rid of the Y-27632. From then on, medium was changed twice a week, every 3-4 days. As soon as all cells revealed a neuronal morphology, MM only was added without any supplements. This was the case after 1-2 weeks.

## 2.4 A $\beta$ -ELISA

### 2.4.1 A $\beta$ MSD ELISA materials

Reagents/Kits	Company	Order number
V-PLEX Kit A $\beta$ -ELISA by A $\beta$ Peptide Panel 1 (6E10)	Meso Scale Discovery	K15200G

### 2.4.2 Collection of supernatants for A $\beta$ -ELISA

Supernatant of cells was collected into falcon tubes or Eppendorf tubes and centrifuged at 300xg for 3min to get rid of cells or cell debris. Supernatant from centrifugation was frozen at -80°C until use.

### 2.4.3 Performing of A $\beta$ -ELISA by A $\beta$ Peptide Panel 1 (6E10) V-PLEX Kit

The A $\beta$ -ELISA was performed according to the supplier's protocol:

#### 2.4.3.1.1 Blocking

First, the wells of the MSD-ELISA plates were blocked with 150 $\mu$ L of Diluent 35. Plates were sealed and incubated with shaking at room temperature for 1 hour.

#### 2.4.3.1.2 Washing and sample addition

Wells were washed 3 times with 150 $\mu$ L of 1x MSD Wash Buffer. Then, 25 $\mu$ L of 1x detection antibody solution was added into the wells with subsequent adding of 25 $\mu$ L of 7 calibrator solutions and 1 zero-calibrator were prepared. The calibrator stock solution was prepared by adding the three A $\beta$ -peptides A $\beta$ 38, A $\beta$ 40 and A $\beta$ 42 into Diluent 35. This A $\beta$  calibrator stock was diluted 1:4 in Diluent 35 to obtain 7 calibrator solutions. As the zero calibrator, Diluent 35 only is used. Further, 25 $\mu$ L of the undiluted supernatant samples were added as triplicates onto the plates. The plate was sealed and incubated on a shaker for 2 hours.

#### 2.4.3.1.3 Detection

After incubation, plate was washed again with 150 $\mu$ L/well of 1x MSD Wash Buffer. Then, 150 $\mu$ L/well of Read Buffer T was added and the plate was directly analyzed on an MSD instrument.

#### 2.4.3.1.4 Data analysis and statistics

The measured data were analyzed by MSD Discovery Workbench Software. Concentrations of the three different A $\beta$ -peptides A $\beta$ 38, A $\beta$ 40 and A $\beta$ 42 in the samples could be determined by the calibrator dilutions. The concentrations of A $\beta$ 40 and A $\beta$ 42 in the samples were used to calculate the A $\beta$ 42 to A $\beta$ 40 ratio.

This ratio was used for statistical analysis to determine whether it changes over time in an hiPSC line or if it changes between a healthy control hiPSC line and a PSEN1-disease line which is known to produce more of the A $\beta$ 42 peptide. Statistical analysis was performed with GraphPad Prism 7 on the technical triplicates of the samples. First, the samples were tested for normal distribution by Shapiro-Wilk test. In case of equal variances, an unpaired t-test was used. In case of unequal variances, the Welch's t-test was used to determine significant differences between the samples.

## 2.5 Multielectrode array (MEA) analysis

### 2.5.1 MEA materials

Product	Company	Order number
CytoView MEA 48 plate, black	Axion Biosystems	M768-tMEA-48B

### 2.5.2 Coating of MEA-plates with PLO and LN521

MEA plates were coated according to the manufacturer with some modifications: Wells were coated with PLO-solution overnight at room temperature, then washed with DPBS with  $Mg^{2+}$  and  $Ca^{2+}$ . Then, 5 $\mu$ g/mL LN521 coating was prepared in MM with all ingredients supplemented, means supplemented with Y-27632, PD and DAPT. A 5 $\mu$ L-drop was placed into the middle of the dry well and incubated in a cell culture incubator for 1hr. After incubation, cells were plated directly.

### 2.5.3 Seeding of cells into MEA plate

After 1hr of LN521 coating incubation a 5 $\mu$ L cell suspension drop containing 75 000 cells were pipetted into the coating drop. Cells were incubated for 1hr in the drop. Afterwards, 300 $\mu$ L of cell culture medium was filled carefully into the wells.

### 2.5.4 MEA measurement

For assessing the functional activity of neurons, the MEA plate with attached neurons could be measured in the Maestro Pro MEA device and recordings were recorded by the AxIS Navigator Software.

Before recording, the electrode plate was placed into the Maestro Pro MEA device for 30min. Then, 3 recordings were programmed, each recording took 10min and recordings were started every 30min. For analysis, the third of the 3 recordings was analyzed and compared to other time points of measurement. Data were analyzed by the AxIS Metric Plotting tool.



## 2.6 Immunofluorescence staining

### 2.6.1 Immunofluorescence staining materials

<b>Solution/buffers</b>	<b>Company</b>	<b>Order number</b>
Dulbecco's phosphate buffered saline (DPBS) with Mg <sup>2+</sup> & Ca <sup>2+</sup>	Life Technologies	14040-091
Bovine serum albumin (BSA)	Sigma Aldrich	A9647-50G
Fetal calf serum (FCS)	Sigma Aldrich	C8056
Sodium azide	Sigma Aldrich	S2002-25G
Triton X-100	Sigma Aldrich	X100

### 2.6.2 Buffers

#### 4% (w/v) formaldehyde (FA)

in DPBS with Mg<sup>2+</sup> & Ca<sup>2+</sup>

#### Block/perm solution

10% FCS

1% BSA

0.2% Triton X-100

in DPBS with Mg<sup>2+</sup> & Ca<sup>2+</sup>

#### Antibody solution

0.1% BSA

in DPBS with Mg<sup>2+</sup> & Ca<sup>2+</sup>

#### 0.1% (w/v) sodium azide

in DPBS with Mg<sup>2+</sup> & Ca<sup>2+</sup>

## 2.6.3 Primary antibodies

Antigen	Antibody Name	Species and Isotype	Clone	Clonality	Company	Order number	Stock concentration	Working dilution	Working concentration
AP2 $\alpha$	AP-2 alpha supernatant 1mL	mouse IgG1 ( $\kappa$ -light chain)	n.a.	monoclonal	Developmental Studies Hybridoma Bank	5-E 4	28 $\mu$ g/ml	1:200	0.14 $\mu$ g/mL
Cytokeratin 18	Anti-Cytokeratin 18 antibody ab52948	rabbit IgG	-	polyclonal	Abcam	ab52948	1mg/mL	1:300	3.3 $\mu$ g/mL
FOXG1	Anti FOXG1 antibody - ChIP Grade ab18259	rabbit IgG	-	polyclonal	Abcam	ab18259	0.7 - 1mg/mL	1:150 - 1:300	4.6 $\mu$ g/mL - 2.3 $\mu$ g/mL
MAP2	Monoclonal Anti-MAP2 (2a + 2b) Clone AP-20	mouse IgG1	AP-20	monoclonal	Sigma-Aldrich	M1406-.2ML	n/a	1:200	n/a
MAP2	Anti-MAP2 antibody ab5392	chicken IgY		polyclonal	Abcam	ab5392	19mg/mL	1:10 000	1.9 $\mu$ g/mL
Oct-4A	Oct-4A (C30A3) Rabbit mAb	rabbit IgG	C30A3	monoclonal	Cell Signaling	2840	n/a	1:200	n/a

Antigen	Antibody Name	Species and Isotype	Clone	Clonality	Company	Order number	Stock concentration	Working dilution	Working concentration
Otx2	Human Otx2 Antibody	goat IgG	-	polyclonal	R&D Systems	AF1979	0.2mg/mL	1:250	0.8µg/mL
PAX6	Purified anti-Pax6 Antibody	rabbit IgG	Poly19013	polyclonal	BioLegend	901301	2mg/mL	1:150 – 1:300	13µg/mL – 6.6µg/mL
PAX6	Pax6, bioreactor supernatant, 0.1mL	mouse IgG, kappa light chain	n.a.	monoclonal	Developmental Studies Hybridoma Bank	AB 528427	500µg/L	1:60-1:80	8.3µg/mL – 6.25µg/mL
SATB2	Anti-SATB2 antibody [SATBA4B10] ab51502	mouse IgG1	SATBA4B10	monoclonal	Abcam	ab51502	0.1mg/mL	1:100	1µg/mL
SOX1	Human/Mouse/Rat SOX1 Antibody	goat IgG	-	polyclonal	R&D Systems	AF3369	0.2mg/mL	1:200	2µg/mL
SOX2	Sox2 (D6D9) XP(R) Rabbit mAb	rabbit IgG	D6D9	monoclonal	Cell Signaling	3579S	n/a	1:200 - 1:400	n/a
SOX10	Human SOX10 Antibody	goat IgG	-	polyclonal	R&D	AF2864	0.2mg/mL	1:100	2µg/mL
3R Tau	Anti-TAU (3-repeat isoform)	Mouse IgG	clone 8E6/C11	monoclonal	Millipore	05-803	n/a	1:2000	n/a

Antigen	Antibody Name	Species and Isotype	Clone	Clonality	Company	Order number	Stock concentration	Working dilution	Working concentration
	RD3) clone 8E6/C11								
Tau	Anti-Tau antibody (ab64193)	rabbit	-	polyclonal	Abcam	Ab64193	0.2mg/mL	1:500	0.4µg/mL
TBR1	Anti-TBR1 antibody (ab31940)	rabbit IgG	-	polyclonal	Abcam	ab31940	1mg/mL	1:300	3.3µg/mL
Tubulin β3 (TUBB3)	Purified anti- Tubulin β3 (TUBB3) Antibody	mouse IgG2a	TUJ1	monoclonal	Biolegend	801202	1mg/mL	1:1000	1µg/mL
vGAT1 (SLC32A1)	VGAT Rabbit polyclonal antibody	rabbit IgG	-	polyclonal	Proteintech	14471-1- AP	0.15mg/mL	1:300	0.5µg/mL
vGLUT2	VGLUT2 (D7D2H) Rabbit mAb	rabbit IgG	D7D2H	monoclonal	Cell Signaling	71555	n/a	1:100	n/a

All antibodies were prepared as recommended in the datasheet prior to dilution for staining.

## 2.6.4 Secondary antibodies and other stains

<b>Antibody</b>	<b>Company</b>	<b>Order number</b>	<b>Stock concentration</b>	<b>Working dilution</b>	<b>Working concentration</b>
Alexa Fluor488-conjugated AffiniPure Donkey Anti Rabbit IgG (H+L)	Jackson-ImmunoResearch Laboratories	711-545-152	1.5mg/mL	1:500	3µg/mL
Cy3-conjugated AffiniPure Donkey Anti Goat IgG (H+L)	Jackson-ImmunoResearch Laboratories	705-165-147	1.5mg/mL	1:500	3µg/mL
Cy <sup>TM</sup> 5 AffiniPure Donkey anti mouse Cy5	Jackson-ImmunoResearch Laboratories	715-175-151	1.5mg/mL	1:500	3µg/mL
Alexa Fluor 647 conjugated AffiniPure Donkey anti mouse IgG (H+L)	Jackson-ImmunoResearch Laboratories	715-605-150	1.5mg/mL	1:500	3µg/mL
Hoechst 33342 trihydrochloride trihydrate	Invitrogen	H3570	10mg/mL	1:2000	5µg/mL
Donkey anti-Mouse IgG (H+L) secondary Antibody, Alexa Fluor 488	Invitrogen	A21202	2mg/mL	1:1000	2µg/mL
Donkey anti-Rabbit IgG (H+L) secondary Antibody, Alexa Fluor 488	Invitrogen	A1206	2mg/mL	1:1000	2µg/mL

<b>Antibody</b>	<b>Company</b>	<b>Order number</b>	<b>Stock concentration</b>	<b>Working dilution</b>	<b>Working concentration</b>
Donkey anti-Goat IgG (H+L) secondary Antibody, Alexa Fluor 555	Invitrogen	A21432	2mg/mL	1:1000	2 $\mu$ g/mL
Donkey anti-Chicken IgY (H+L) secondary Antibody, Alexa Fluor 555	Invitrogen	A21437	2mg/mL	1:1000	2 $\mu$ g/mL
Donkey anti-Rabbit IgG (H+L) secondary Antibody, Alexa Fluor 647	Invitrogen	A31573	2mg/mL	1:1000	2 $\mu$ g/mL

#### *2.6.4.1 Reconstitution of secondary antibodies from Jackson ImmunoResearch Laboratories*

Antibodies were rehydrated in 400 $\mu$ L of water and 400 $\mu$ L of glycerol, aliquoted & stored at -20°C until use.

## 2.6.5 Immunofluorescence staining of cells

### 2.6.5.1 Fixation of cells

Depending on the cell type to be fixed, cells were washed with DPBS containing  $Mg^{2+}$  and  $Ca^{2+}$  and fixed with 4% formaldehyde in DPBS for 15min. In case of neurons to prevent neurite detachment, cells were not washed and fixed for 15min with 4% formaldehyde in DPBS by adding equal volume of 8% formaldehyde to cells in their medium. After incubation, cells were washed with DPBS with  $Mg^{2+}$  and  $Ca^{2+}$  and stored in 0.1% Na-azide solution in the fridge until further processing.

### 2.6.5.2 Blocking and permeabilization of cells

Fixed cells were washed with DPBS containing  $Mg^{2+}$  and  $Ca^{2+}$  and incubated with block/perm solution for 30-60min.

### 2.6.5.3 Incubation of cells with primary antibody

After blocking and permeabilization, cells were washed with DPBS containing  $Mg^{2+}$  and  $Ca^{2+}$ . Then, cells were incubated with antibody solution that contained the primary antibodies for labeling the desired antigen overnight at 4°C. In case of control wells, cells were incubated with antibody solution only.

### 2.6.5.4 Incubation of cells with secondary antibody

After incubation of cells with primary antibody, cells were washed with DPBS containing  $Mg^{2+}$  and  $Ca^{2+}$  for three times and then incubated with secondary antibody that bind to the corresponding primary antibodies. Cells were incubated for 1hr. Then, cells were washed for 3 times and stored in 0.1% Na-azide until imaging.

### 2.6.5.5 Image acquisition by ArrayScan

For image acquisition by the ArrayScan, the HCS-software was used. Settings were adjusted for the different stainings, such as plate format and form factor that was stored already by the ArrayScan software, magnification, that was usually set to 20x, and exposure time that was adjusted manually or by the help of the auto-exposure algorithm.

In case of nuclear staining, exposure percentage was set to 25, in case of neurite staining, it was set to 45. This percentage was used to adjust exposure time.

After exposure time was adjusted, settings were saved and plates with the different stainings were acquired in an automated way by the help of the Momentum software. Image adjustment was also performed by the HCS-software. For the input settings of brightness and contrast, the negative controls were used.



## 2.7 RNA purification, reverse transcription and qPCR

### 2.7.1 RNA purification and PCR reagents

<b>Kits or ingredients</b>	<b>Supplier</b>	<b>Order Number</b>
RNeasy Plus Mini Kit	Qiagen	74106
QIAshredder	Qiagen	79656
SuperScript IV VILO MasterMix with edDNase Enzyme	Thermo Fisher Scientific	11766500
TaqMan Fast Universal PCR Master Mix (2x), no AmpErase UNG	Thermo Fisher Scientific	4352042
RapidOut DNA Removal Kit	Thermo Fisher Scientific	K2981
Transcriptor First Strand cDNA Synthesis Kit	Roche	04 896 866 001
MicroAmp EnduraPlate Optical 96-Well Clear Reaction Plates with Barcode	Thermo Fisher Scientific	4483354
TaqMan Fast Advanced Master Mix	Thermo Fisher Scientific	4444557
Sample loading reagent 20x	Fluidigm	100-7610
Assay loading reagent 2x	Fluidigm	100-7611

### 2.7.2 TaqMan probe assays

<b>Gene</b>	<b>Company</b>	<b>Assay ID</b>	<b>Assay ID used at FNC</b>
ACTB	Thermo Fisher	Hs99999903_m1	-
B2M	Thermo Fisher	Hs00984230_m1	-
<i>EMX2</i>	Thermo Fisher	-	Hs00244574_m1
<i>FOXP1</i>	Thermo Fisher	Hs01850784_s1	Hs01850784_s1
<i>GAPDH</i>	Thermo Fisher	Hs99999905_m1	Hs02786624_g1
<i>LMX1A</i>	Thermo Fisher	Hs00892663_m1	Hs00898455_m1
<i>NANOG</i>	Thermo Fisher	Hs02387400_g1	Hs02387400_g1
<i>OTX2</i>	Thermo Fisher	Hs00222238_m1	Hs00222238_m1
<i>PAX6</i>	Thermo Fisher	Hs00240871_m1	Hs01088114_m1
<i>POU5F1 (OCT4)</i>	Thermo Fisher	Hs04260367_gH	Hs04260367_gH

<i>RPL13</i>	Thermo Fisher	-	Hs00744303_s1
<i>SOX10</i>	Thermo Fisher	Hs00366918_m1	Hs00366918_m1
<i>UBC</i>	Thermo Fisher	-	Hs01871556_s1
<i>WNT1</i>	Thermo Fisher	Hs00180529_m1	-
<i>WNT3</i>	Thermo Fisher	Hs00902257_m1	-
<i>WNT3A</i>	Thermo Fisher	Hs00263977_m1	-

### 2.7.3 RNA isolation from cell culture samples

RNA isolation and purification were performed by the help of the RNeasy Plus Mini Kit and the QIAshredder Kit from Qiagen.

RNA was usually collected from cells grown in 12- or 6-wells of a plate. Wells were washed with DPBS without Mg<sup>2+</sup> and Ca<sup>2+</sup>. Then, cells were lysed with RLT-Plus buffer included in the RNeasy Plus Mini Kit. Lysed cells in RLT-Plus buffer were collected into Eppendorf tubes and stored at -20°C for short term storage, at -80°C for long term storage until use.

Frozen samples were thawed on ice and homogenized by using the QIAshredder Kit: 350µL of the lysed samples were transferred into a QIAshredder homogenizer which was placed into a collection tube and centrifuged at full speed for 2min. The homogenized lysate was then further processed in the QiaCube which performed the following steps in an automated way:

The homogenized lysate was transferred to a gDNA Eliminator spin column. The column was centrifuged at 8000xg for 30sec. The flow-through was further used and same volume of 70% EtOH was added and mixed. The solution was pipetted into an RNeasy mini column and centrifuged at 8000xg for 15sec. The RNA sample was bound to the column, flow-through was discarded.

700µL of RW1 buffer was added to the RNeasy mini column, everything was centrifuged at 8000xg for 15sec and flow-through was discarded.

Then, column was washed twice with 500µL of RPE buffer by centrifugation at 8000xg for 2min.

Then, RNeasy mini column was transferred to a fresh collection tube, 30µL of water was pipetted, column was centrifuged for 1min at 8000xg and eluate containing the mRNA was used for further processing.

The mRNA prepared by the QiaCube was measured on the NanoDrop to determine the RNA content.

The next step was digestion of genomic DNA. This step is performed depending on the cDNA synthesis procedure used.

DNA digestion with RapidOut DNA Removal Kit was used together with Transcriptor First Strand cDNA Synthesis Kit.

DNA digestion with ezDNAse Enzyme was used together with SuperScript IV VILO MasterMix, as they come together in one kit.

#### 2.7.4 DNA digestion with RapidOut DNA Removal Kit with subsequent cDNA transcription by Transcriptor First Strand cDNA Synthesis

For DNA digestion, the RapidOut DNA Removal Kit was used which contains DNase I and DNase Removal Reagent to get rid of the DNase.

DNA removal is necessary to avoid amplification of genomic DNA and therefore leading to false results in the qPCR process.

For DNA removal, DNase I was added to RNA samples, 0.5 $\mu$ L of DNase I was needed per 10 $\mu$ L reaction volume:

<b>Component</b>	<b>Amount/volume</b>
RNA sample	Up to 8.5 $\mu$ L (1 $\mu$ g)
10x DNase buffer with MgCl <sub>2</sub>	1x
DNase I	0.5 $\mu$ L (0.05U/ $\mu$ L)
water	up to 10 $\mu$ L
Total volume	10 $\mu$ L

The mixture was incubated at 37°C for 30min. After incubation, sample was cooled down on ice.

To remove the DNase, DNase Removal Reagent (DRR) was added to the sample and incubated for 2min at room temperature so that the DRR bound the DNase I. Occasionally, the mixture was mixed. Then, DRR was pelleted by centrifugation at 800xg for 1min to remove DNase I.

The supernatant that contained the RNA was carefully collected into a fresh RNase-free tube.

Afterwards, cDNA synthesis was performed by the Transcriptor First Strand cDNA Synthesis

### 2.7.5 cDNA Synthesis with Transcriptor First Strand cDNA Synthesis Kit

The cDNA synthesis was performed by the help of the Transcriptor First Strand cDNA Synthesis Kit.

#### 2.7.5.1 Denaturation

cDNA, dT15 primer and water were mixed, samples were placed into a PCR-Cycler and heated up to 65°C for 10min. Afterwards, samples were cooled on ice.

#### 2.7.5.2 Synthesis

For cDNA synthesis, a master mix of following ingredients was prepared:

<b>Component</b>	<b>Final amount</b>
5x Transcriptor Reverse Transcriptase Reaction Buffer	1x
Protector RNase Inhibitor (40U/μL)	1U/μL
Deoxynucleotide Mix	1mM
Transcriptor Reverse Transcriptase	0.5U/μL
DTT	5mM
Total volume	<b>40-60μL</b>

The master mix was added to the denatured mixture. Everything was mixed and placed into a PCR Cycler. Samples were heated up to 50°C for 1hr and then heated up to 85°C for 5min. Afterwards, samples were cooled on ice or stored at -20°C until further use.

### 2.7.6 DNA digestion with ezDNase Enzyme with subsequent cDNA transcription by with SuperScript IV VILO MasterMix

Samples were mixed with 1x ezDNase Buffer and ezDNase enzyme:

<b>Component</b>	<b>Final amount</b>
10x ezDNase Buffer	1μL
ezDNase enzyme	1μL

RNA sample	up to 8 $\mu$ L (1pg – 2.5 $\mu$ g total RNA)
nuclease-free water	to 10 $\mu$ L
Total volume	<b>10<math>\mu</math>L</b>

Mixture was incubated for 2min at 37°C and incubated on ice until further use.

Afterwards, cDNA synthesis was performed by using the SuperScript IV VILO MasterMix

#### 2.7.6.1 cDNA Synthesis with SuperScript IV VILO MasterMix

SuperScript IV VILO MasterMix was mixed with nuclease-free water. The master mix was added to the denatured mixture. Additionally, a negative control was needed.

Component	RT reaction	no RT reaction
RNA sample from previous step	10 $\mu$ L	10 $\mu$ L
SuperScript IV VILO Master Mix	4 $\mu$ L	-
SuperScript IV VILO No RT Control	-	4 $\mu$ L
Nuclease-free water	6 $\mu$ L	6 $\mu$ L
Total volume	<b>20<math>\mu</math>L</b>	<b>20<math>\mu</math>L</b>

Everything was mixed and placed into a PCR Cycler and following heating incubations were performed:

Temperature	Time
<b>25°C</b>	10min
<b>50°C</b>	10min
<b>85°C</b>	5min

Afterwards, samples were cooled on ice or stored at -20°C until further use.

#### 2.7.6.2 qPCR by QuantStudio 7 Flex Real Time PCR System

After genomic DNA digestion and cDNA synthesis, the TaqMan qPCR mixture was prepared:

<b>Components</b>	<b>qPCR reaction</b>	<b>Negative control</b>
cDNA	5 $\mu$ L	-
nuclease-free water	4 $\mu$ L	9 $\mu$ L
TaqMan Fast Universal PCR Master Mix (NoAmpErase UNG)	10 $\mu$ L	10 $\mu$ L
Assay Probe	1 $\mu$ L	1 $\mu$ L
<b>Total volume</b>	<b>20<math>\mu</math>L</b>	<b>20<math>\mu</math>L</b>

Each qPCR reaction was pipetted into 2-3 wells of a 96-well MicroAmp EnduraPlate to have technical duplicates or triplicates. The plate was placed into the QuantStudio 7 Flex Real Time PCR System and run under fast conditions. The following program was run:

<b>Steps</b>	<b>Temperature</b>	<b>Time</b>
Initial step	95°C	20sec
40 cycles:		
Denaturation	95°C	1sec
Annealing and extension	60°C	20sec

### 2.7.7 cDNA preparation and qPCR by Biomark HD

The following steps were performed by Joseph Tamm, Foundational Neuroscience Center, AbbVie.

#### 2.7.7.1 Quantification of RNA samples

cDNA was prepared as already described in chapter 2.8.4 “DNA digestion with RapidOut DNA Removal Kit with subsequent cDNA transcription by Transcriptor First Strand cDNA Synthesis”. cDNA samples were incubated at 65°C to degrade any present RNA and subsequently, RNA concentration was measured using the Quant-iT OliGreen ssDNA Kit:

Samples were mixed with the aqueous working solution, incubated 2-5min at room temperature and fluorescence was measured. By the help of a standard curve, the RNA concentration was determined. Samples were diluted to 20ng/ $\mu$ L.

Subsequently, a preamplification step is performed.

### 2.7.7.2 Preamplification step

Samples were preamplified by using the TaqMan PreAmp Master Mix:

Component	Volume per reaction	Final concentration
TaqMan PreAmp Master Mix (2x)	2.5 $\mu$ L	1x
Pooled assay mix (0.2x, each assay)	1.25 $\mu$ L	0.05x (each assay)
cDNA sample	1.25 $\mu$ L	0.02-5ng/ $\mu$ L
Total volume	5 $\mu$ L	-

The pooled assay mix consists of all primer pairs needed for later qPCR and is already premixed by the supplier.

Preamplification is performed by the following schedule:

Step	Temperature	Time	Cycles
Enzyme activation	95°C	10min	Hold
Denature	95°C	15sec	13 cycles
Anneal/Extend	60°C	4min	
Enzyme inactivation	99°C	10min	Hold
Final	4°C	$\infty$	Hold

After preamplification, the 5 $\mu$ L sample is diluted in 50 $\mu$ L of water and a small part is used for qPCR sample preparation.

### 2.7.7.3 qPCR sample preparation

For qPCR, sample premix master mix was prepared:

Component	Volume
TaqMan Fast Advanced Master mix 2x	444 $\mu$ L
Sample loading reagent 20x	44.4 $\mu$ L

Then, qPCR reactions were prepared.

<b>Component</b>	<b>Volume for 1 reaction</b>
Sample premix	4 $\mu$ L
Preamplified cDNA products diluted 1:10	3.27 $\mu$ L
Total PCR reaction mix volume	<b>7.27<math>\mu</math>L</b>

The Fluidigm 96.96 IFC was placed into the Juno for priming for 21min. Afterwards, 5 $\mu$ L of each TaqMan assay was pipetted into the assay inlets of the Fluidigm 96.96 IFC, which consists of TaqMan 20x qPCR assays and 2x assay loading reagent.

Samples were loaded into the Fluidigm 96.96 IFC sample inlets. Juno mixed the assays with the samples and the plate was placed into Biomark HD, where qPCR takes place. Cycling times were performed as shown in the table:

<b>Steps</b>	<b>Temperature</b>	<b>Time</b>
Thermal mixing	70°C	40min
Initial step	60°C	30sec
Denaturation	98°C	60sec
35 cycles:		
Denaturation	97°C	5sec
Annealing and extension	60°C	20sec

### 2.7.8 Data analysis of qPCR results

For relative quantification, CT values of RNA samples were analyzed by the  $2^{-(\Delta\Delta-CT)}$ -method: CT-values of the samples were normalized to the CT values of 2-3 housekeeping genes of the same sample as indicated, and then normalized to D0 samples. Afterwards, fold change was calculated.

In case that CT-values were undetected, they were set to the max of cycle number, means CT=40 or in case of the Biomark HD qPCR, they were set to 28. If enough replicates were present, statistical analysis could be performed.

### 2.7.9 Statistical analysis for qPCR

For statistical analysis, GraphPad Prism Version 7 was used.



### *2.7.9.1 One-way ANOVA with multiple comparisons*

In the case that various conditions needed to be compared for a time point, one-way ANOVA was used if the data were normally distributed.

To compare the means among the different conditions, multiple comparisons analysis was used. In that regard, Tukeys correction was applied which takes into consideration the scattering of the data, leading to a more precise result.

### *2.7.9.2 Unpaired t-test and Welch's t-test*

When two conditions were compared with each other, the samples were tested for normal distribution by Shapiro-Wilk test.

In case of equal variances, an unpaired t-test was performed. If variances were different, a Welch's t-test was performed.

## 3 RESULTS

### 3.1 Implementation of xeno-free hiPSC-culture conditions

#### 3.1.1 The xeno-free coating agent LN521 is suitable for hiPSC-culture

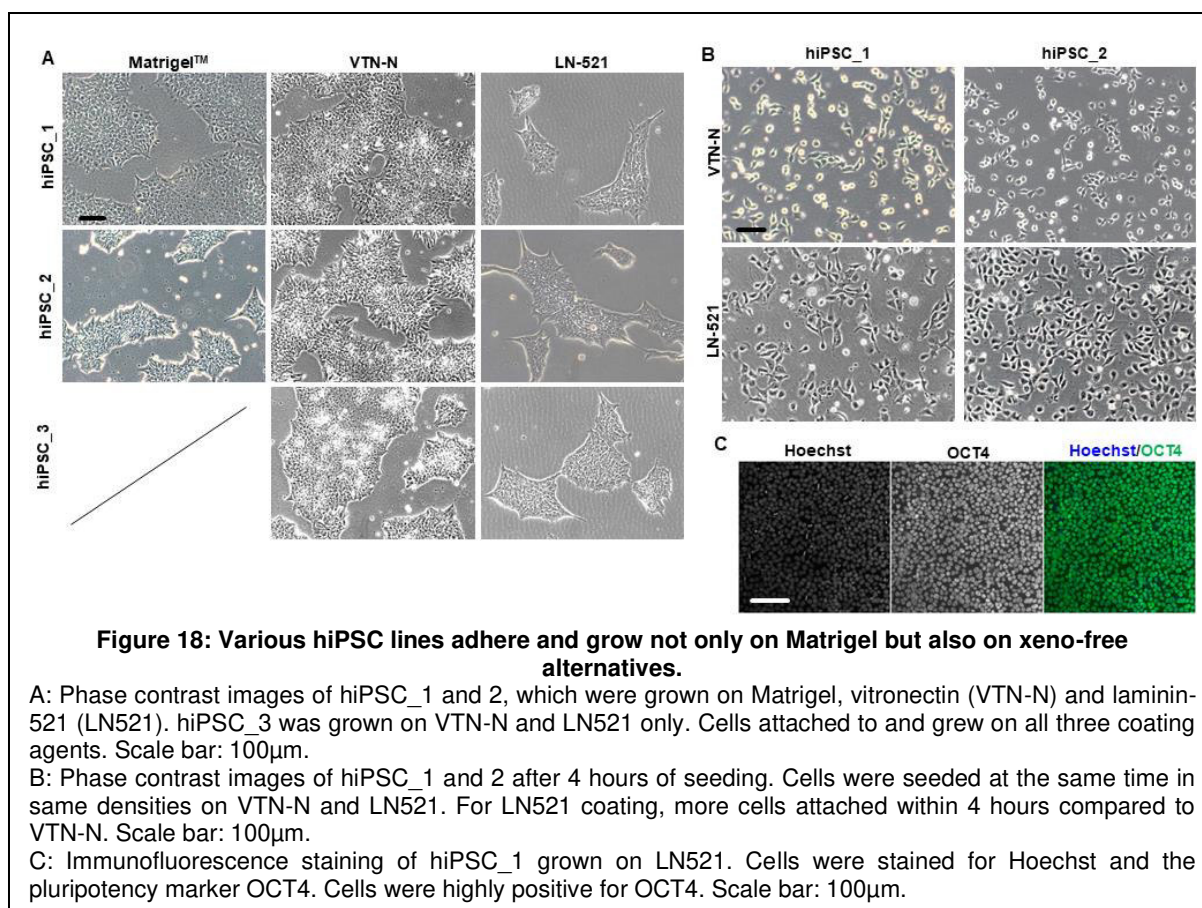
To establish a xeno-free cell culture system, the conventional culture conditions were examined thoroughly and ingredients deriving of animal-origin were identified and replaced by xeno-free versions.

In hiPSC-culture, various culture media can be used, such as mTeSR, StemFlex and E8 medium. In order to start with a xeno-free hiPSC-culture, E8flex medium was used which is already a xeno-free medium (Chen et al., 2011). This medium consists of only 8 necessary ingredients for hiPSC culture, described by Chen et al. (Chen et al., 2011). During neural induction conventional culture conditions use a combination of media and supplements. Frequently, a mixture of Neurobasal medium supplemented with B27 supplement (without vitamin A) and DMEM/F12 medium with N2 supplement, is used (Shi et al., 2012a). During induction, several pathway modulators are used to influence the cells towards differentiation into the neuroectoderm. These modulators are either small molecules or recombinant proteins. In this regard, rather small molecules were used for better stability and robustness of differentiation.

In later stages, cells need to be expanded. In this regard, the same basal medium can be used, but different pathway modulators are needed, for instance the growth factor basic fibroblast growth factor (FGF) (Elkabetz et al., 2008; Falk et al., 2012; Shi et al., 2012a; Yao et al., 2006; Zhang et al., 2001).

After expansion, cells need to be finally matured into neurons. Here again, different pathway modulators are beneficial for success, for instance brain-derived neurotrophic factor (BDNF) and glial-derived neurotrophic factor (GDNF), which are neurotrophic factors that promote neuron maturation and survival (Love et al., 2005; Vicario-Abejon et al., 1998).

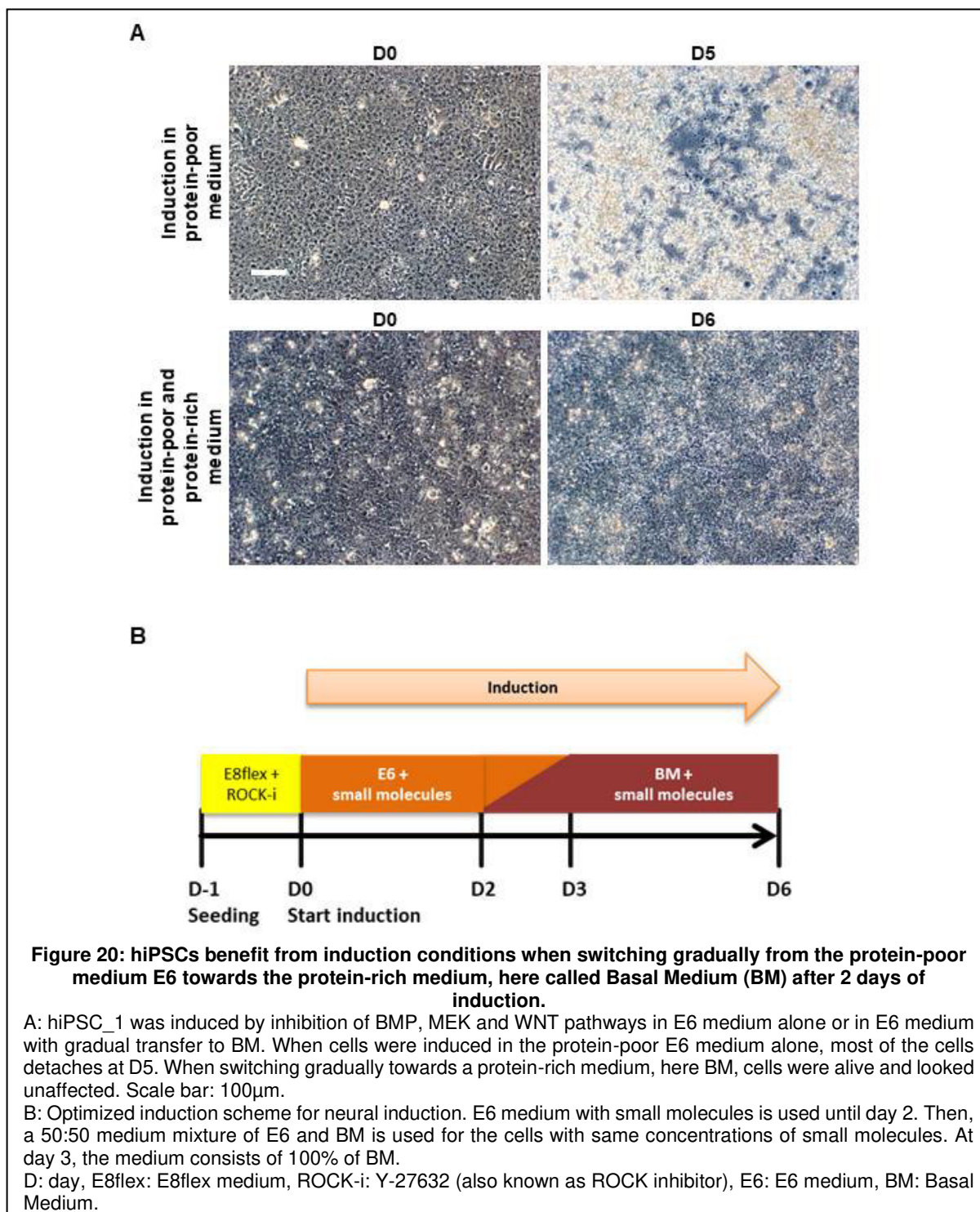
In this regard, the proteins needed during differentiation, were switched to recombinant proteins manufactured in an animal-free manner. In this setting, these proteins were FGF, BDNF and GDNF. Further, the carrier protein needed for preparation of these proteins was switched from bovine serum albumin (BSA) to human serum albumin (HSA).



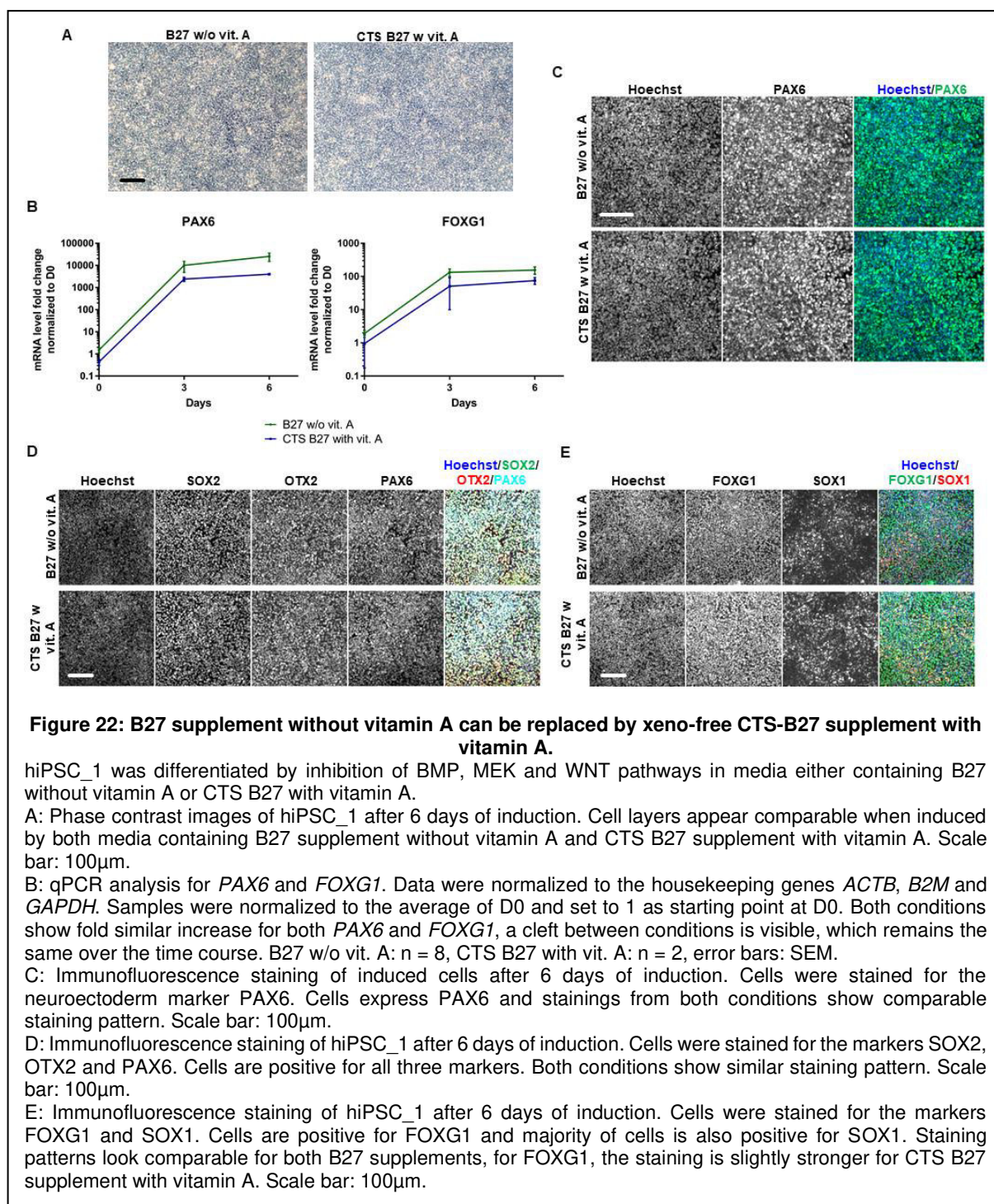
Two other main ingredients of animal origin found in culture media and components were the coating agent Matrigel and BSA, which is found in cell culture media as well as in protein solutions as carrier proteins as mentioned before. Matrigel is an extracellular matrix isolated from Engelbreth-Holm-Swarm mouse sarcoma (Kibbey, 1994). A xeno-free alternative for Matrigel represent human recombinant extracellular matrix proteins, such as vitronectin (VTN) or laminins (Badenes et al., 2016; Laperle et al., 2015; Yasuda et al., 2018). Here, VTN-N and laminin-521 (LN521) coatings were tested with three hiPSC lines (hiPSC\_1-3). For both coatings, cells could attach to the cell culture dish (Figure 11A). In the end, LN521 was picked as the general coating component. Majority of cells seeded onto LN521-coated dishes could already attach within 4 hours compared to VTN-N-coated dishes, in which only a part of the cells was visibly attached at that moment (Figure 11B). When checking hiPSC\_1 on LN521 coating, the pluripotency marker OCT4 was still expressed homogeneously on protein level after 5 passages, indicating that LN521 does not have negative effects on pluripotency (Figure 11C). The findings led to the conclusion that LN521 is a xeno-free alternative for Matrigel as hiPSCs adhere very quickly to LN521 compared to VTN-N and LN521 does not affect pluripotency of hiPSCs.

### 3.1.2 A gradual change from E6 medium towards Basal Medium containing xeno-free B27 supplement is suitable for neural induction

In a next step, Basal Medium (BM), which is usually used in the course of differentiation, was switched initially to the fully defined E6 medium. This medium is the direct equivalent of E8 medium, but without the pluripotency-supporting growth factors FGF and TGF- $\beta$  (Chen et al., 2011). Due to a low protein content of E6 medium, cells did not survive when E6 medium supplemented with several pathway inhibitors



was used for a longer treatment than for 4 days (Figure 12). As E6 medium is a very “poor” medium compared to BM, which contains high concentrations of BSA/HSA, the small molecules supplemented in the E6, needed for pathway modulation, possibly reached a higher efficient concentration as they cannot be masked by the missing serum albumin in the medium. This higher effective concentration of small molecules probably reached a threshold that was toxic for the cells. Qi and colleagues also observed this phenomenon and therefore suggested to alternatively titrate the concentrations of small molecules (Qi et al., 2017). In this regard it was found that



gradual switch from E6 medium to BM eliminated the need to titrate all the small molecules (Figure 12A and B).

For neural inductions, B27 supplement without vitamin A (without retinoids) was replaced by CTS-B27 with vitamin A. CTS is a product line which stands for cell therapy systems. Products are manufactured with very high certified standards and can therefore be even used for therapeutic approaches. At the time of experiments, no CTS-B27 without vitamin A was available. This could have been used for more consistency with regards to vitamin A. Opposite opinions exist on the effect of vitamin A during neural induction for forebrain progenitors: Some groups claim it has adverse effects on neural induction and therefore, do not use it (Kirkeby et al., 2012; Li et al., 2009), other groups use it and still derive cortical neurons (Espuny-Camacho et al., 2013; Kirwan et al., 2015; Shi et al., 2012b).

When comparing B27 w/o vitamin A to CTS-B27 with vitamin A, there was no obvious morphological difference between the cells (Figure 13A). Therefore, it was concluded that B27 supplement without vitamin A can be replaced by the xeno-free version CTS-B27 containing vitamin A and that vitamin A does not appear to have an effect in this differentiation setting. This might be due to two reasons:

On one hand, vitamin A simply does not have an effect during neural induction. Or vitamin A is not exposed long enough or in high enough concentrations during the whole induction: B27 supplement is included in BM only and not in the E6 medium. Therefore, vitamin A is present from day onwards in lower concentrations and it is only present fully from day 3 onwards. Further, vitamin A is only present in traces in the B27 supplements. Immunofluorescence stainings for several markers also showed great similarity between both B27 supplements (Figures 13C-E). For FOXG1 staining, the cells showed potentially stronger signal when using CTS-B27 supplement (Figure 13E).

On RNA level, both B27 supplements led to a similar increase for the neuroectoderm marker *PAX6* at D3 and D6 respectively (Figure 13B). However, CT values for the experiments with the different B27 supplements already varied at D0, which might contribute to the cleft at subsequent time points (Figure 13B).

To summarize, gradual switch from E6 medium towards BM was suitable for neural induction, especially when titrating small molecules wants to be avoided. Further, the CTS-B27 supplement represents a xeno-free alternative for the conventionally used

B27 supplement: There is no obvious effect of the vitamin A on neural induction in this setting and the xeno-free version of the supplement also did not have an adverse effect.

## 3.2 Optimization of a xeno-free and chemically defined differentiation protocol

### 3.2.1 MEK inhibition accelerates neural induction in hiPSCs

In previous protocols, neural induction in hiPSCs takes around 12 days (Kirwan et al., 2015; Shi et al., 2012a). Therefore, the aim was to identify manipulations of the protocol to accelerate the process of neural induction. In their publication Greber and colleagues described that inhibition of the MEK pathway, which is responsible for FGF signal integration, could accelerate neural induction and within two weeks, they could even generate sensory neurons derived from hiPSCs (Greber et al. 2012).

To test the accelerating effect of MEK inhibition for neural induction, inhibitors of BMP and TGF- $\beta$ , commonly called double SMAD inhibition (termed here as “dSMADi”) were compared with dSMADi containing additionally a MEK inhibitor. Immunofluorescence stainings indicated that after 6 days of induction cells expressed strong nuclear PAX6 protein in the condition with MEK inhibition compared to dSMADi, in which PAX6 expression was still very weak (Figure 14 A). Interestingly, when leaving out the TGF- $\beta$  inhibitor, stainings looked comparable, indicating that TGF- $\beta$  inhibitor was not necessary in our induction setting (Figure 14A).

On mRNA level, all three induction conditions led to a 100 to 1000-fold decrease of the pluripotency marker *OCT4* during differentiation (Figure 14B). MEK inhibition led to an increase of *PAX6* expression, which reached a plateau at D5 with an approximate 6500-fold upregulation compared to D0 (Figure 14B). In comparison, dSMADi showed only an approximately 650-fold upregulation from D4 onwards, indicating an approximately 10-fold lower increase in expression on mRNA level compared to the other two conditions containing MEK inhibition (Figure 14B).

For *FOXP1*, the upregulation was the slowest for dSMADi reaching the same level of the other two conditions at D6, whereas the other conditions had a stronger upregulation from day 2 onwards and reached a plateau already at day 3 or 4 during induction (Figure 14B).

For *PAX6* a significant difference between the dSMADi condition compared to the other two conditions was seen from days 2 to 6. P-values were ranging between 0.0017 at day 6 and 0.0483 at day 4 for comparisons of dSMADi to the double inhibition of BMP and MEK pathways. The two other conditions, inhibitions of BMP, TGF- $\beta$  and MEK pathways and inhibitions of BMP and MEK pathways only, did not show any differences, indicating both conditions worked comparably. Significant differences



between dSMADi and the triple inhibition BMP, TGF- $\beta$  and MEK pathways were detected for all days except for day 5.

Statistical analysis for *FOXG1* did not show any differences between the conditions except at D4 a significant difference between dSMADi and the condition in which BMP and MEK pathways were inhibited was detected. However, a trend was observed, similar to *PAX6*, that dSMADi was slower upregulating *FOXG1* (Figure 14B). It is possible that with larger sample size, a statistically significant difference might be detected.

In this setting it was found out that when leaving out the TGF- $\beta$  inhibitor (inhibiting BMP and MEK pathways only), neural induction took place in the same speed as in the condition with additional inhibition of the TGF- $\beta$  pathway, indicating no beneficial effect of the TGF- $\beta$  inhibitor in this experimental setting (Figure 14B).

In conclusion, the experiments confirmed that MEK inhibition accelerated neural induction and that at least BMP inhibition was needed for neural induction.

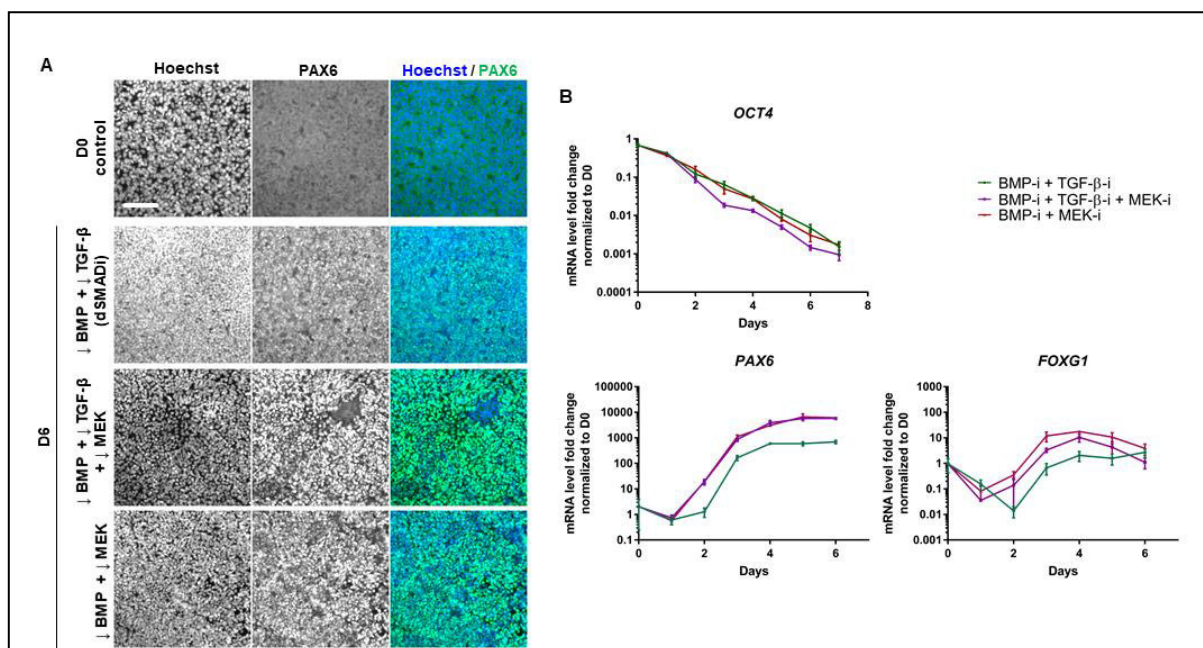


**Figure 24: MEK inhibition accelerates neural induction.**

Cells were induced by either inhibition of TGF- $\beta$  and BMP pathways (dSMADi), or by inhibition of TGF- $\beta$ , BMP and MEK pathways, or by inhibition of BMP and MEK pathways alone.

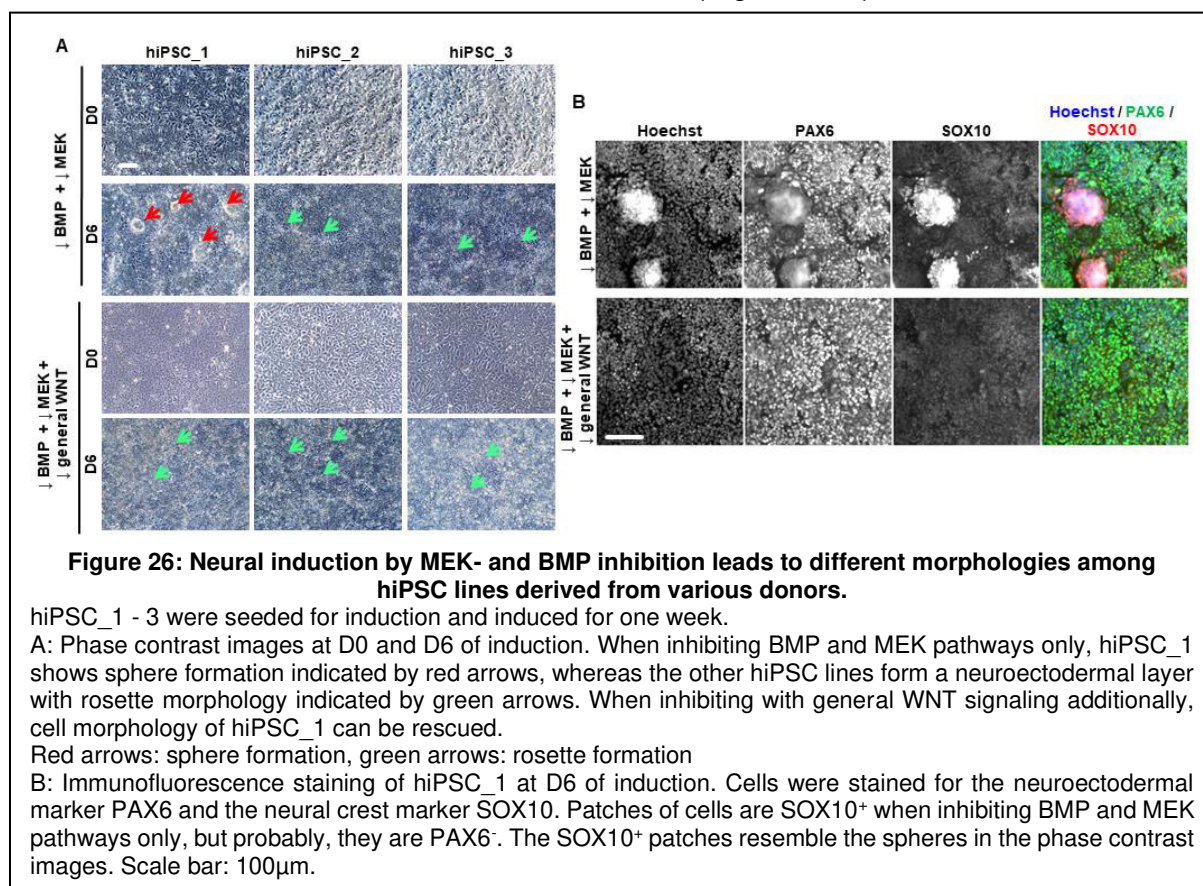
A: Immunofluorescence stainings of the cells at D0 and D6 of induction. Cells were stained for the neuroectodermal marker PAX6. Cells induced by conditions containing MEK inhibition showed greater PAX6 staining compared to dSMADi. Scale bar: 100 $\mu$ m.

B: qPCR analysis of the pluripotency gene *OCT4*, the neuroectodermal marker *PAX6* and the forebrain marker *FOXG1*. Data were normalized to housekeeping genes *GAPDH*, *RPL13* and *UBC* and then to D0. Samples of each time point were tested for normal distribution by Shapiro-Wilk-test. Except at D1 for *PAX6*, data were normally distributed. For these samples, a one-way ANOVA test was performed with Tukey's multiple comparison. Conditions containing MEK inhibitor quicker upregulated *PAX6* and *FOXG1* mRNA. For *PAX6* mRNA, dSMADi was significantly different from the other two conditions, except at D5: Here, only dSMADi differed from inhibition of BMP and MEK pathways. Conditions containing MEK inhibition were not significantly different from each other. For *FOXG1* no significant difference was found among the conditions, except at D4, dSMADi was significantly different from inhibition of BMP and MEK pathways. n=3, error bars: SEM. qPCR was performed by Joseph Tamm, FNC.

### 3.2.2 hiPSC lines may be susceptible towards neural crest differentiation

To see whether BMP and MEK inhibition alone were robust and reproducible, three hiPSC lines from healthy but different donors (named here “hiPSC\_1, 2, 3”, respectively) were induced by this condition.

From D6 onwards, first differences on morphological level could be observed for hiPSC\_1 compared to the other two lines (Figure 15A): hiPSC\_2 and 3 formed neural rosettes within 6 days of induction, whereas some cells of hiPSC\_1 started to form spheroid structures on top of the homogeneous cell layer (Figure 15A, red arrows: sphere formation, green arrows: examples for rosette structures). As a possible explanation, it was assumed that these spheres might be cells of neural crest origin as it was described that they form separately of CNS progeny (Munst et al., 2018). In neural development, formation of neural crest is mainly dependent on WNT signaling (Blauwkamp et al., 2012; Moya et al., 2014; Tchieu et al., 2017). Therefore, in a next experiment, cells were treated by inhibition of BMP, MEK and an inhibitor of general WNT signaling (termed here as “WNTi”), IWP2. IWP2 inhibits WNT secretion in cells, thus blocking both canonical and non-canonical WNT signaling that is endogenously produced by the cells (Chen et al., 2009). After 6 days, hiPSC\_1 culture morphology looked the same as the other two hiPSC lines (Figure 15A). To further validate this



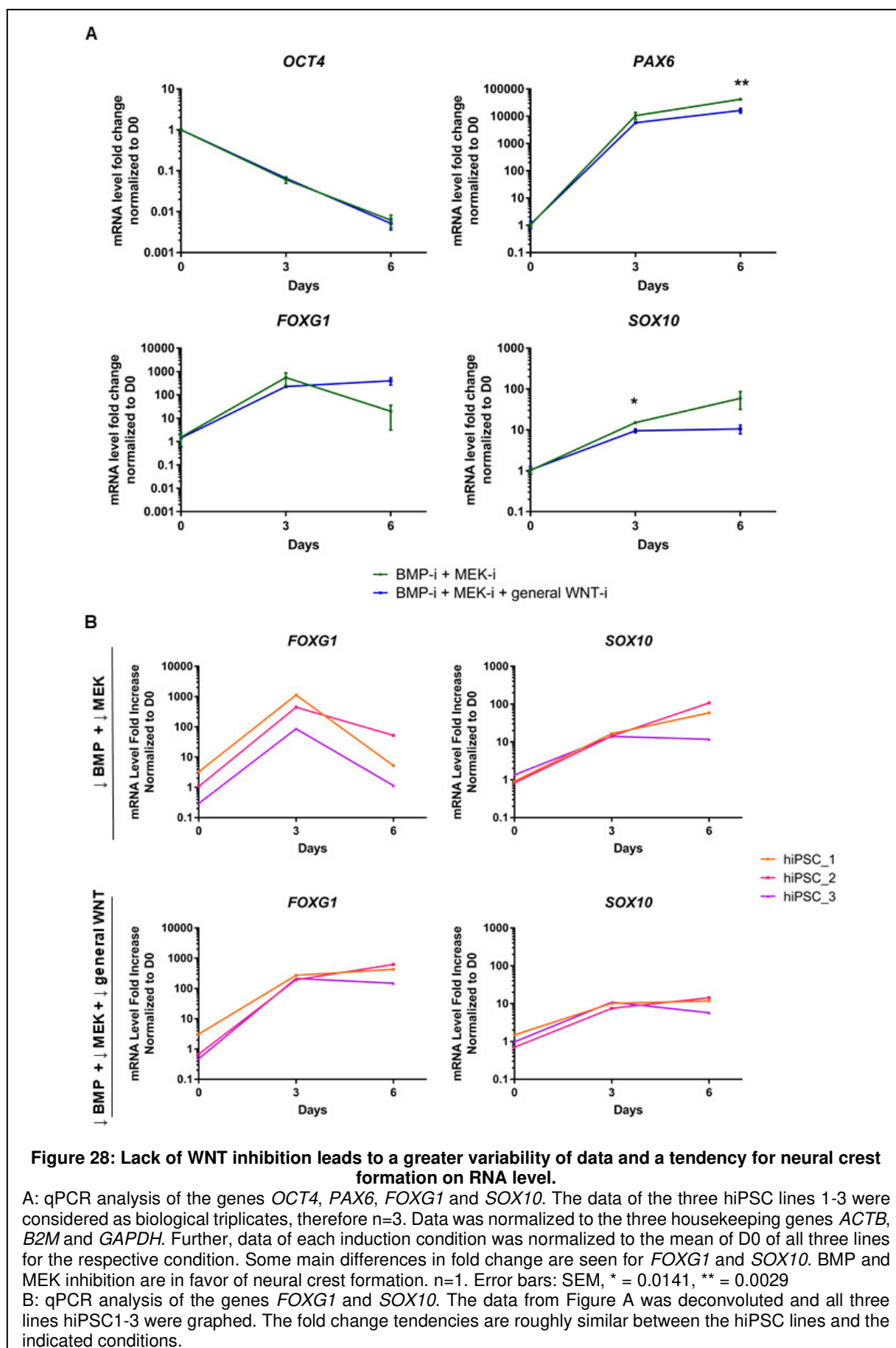
hypothesis, immunofluorescence analysis was used. When comparing both conditions by immunofluorescence staining, the spheroid structures stained positive for the neural crest marker *SOX10*, but weakly for the CNS marker *PAX6*. When cells were treated with the additional general WNT inhibitor, no *SOX10*<sup>+</sup> cells could be detected by immunofluorescence staining anymore (Figure 15B).

For mRNA analysis all three lines were considered as biological replicates (Figure 16A).

Both conditions led to a similar fold decrease for *OCT4*, indicating the exit of the cells from the pluripotent state (Figure 16A). Both conditions led to a strong increase in expression of the neuroectoderm marker *PAX6* by several orders of magnitude (Figure 16A). It appeared that BMP and MEK inhibition alone could lead to an even higher increase of *PAX6* mRNA. Some further differences could be observed for the forebrain marker *FOXC1* and the neural crest marker *SOX10* (Figure 16A): When inhibiting BMP and MEK pathways in the cells, *FOXC1* fold change increased up to 550-fold until day 3, and then subsequently fold increase dropped to 20 compared to inhibition of BMP, MEK and general WNT pathways, in which *FOXC1* fold change was increasing up to 230-fold at day 3 and 400-fold through day 6 (Figure 16A). When comparing *SOX10* fold change, both conditions led to a 15 or 10-fold increase until day 3, but then for inhibition of BMP and MEK pathways, the fold change increased further up to 60, whereas for inhibition of BMP, MEK and general WNT pathways, a plateau was reached (Figure 16A).

When regarding all lines individually for *FOXC1* and *SOX10*, the behavior of the cells during time and condition was mostly similar. Differences could be seen among the different conditions which reflect the differences in Figure 6A: Inhibition of BMP and MEK pathways led to a decrease of *FOXC1* from D3 onwards and rather a progressive increase of *SOX10*, whereas for the condition with additional WNT inhibition, *FOXC1* and *SOX10* increased until D3 reaching a plateau (Figure 16B).

In summary, it was found out that some hiPSC lines seem to be prone for neural crest

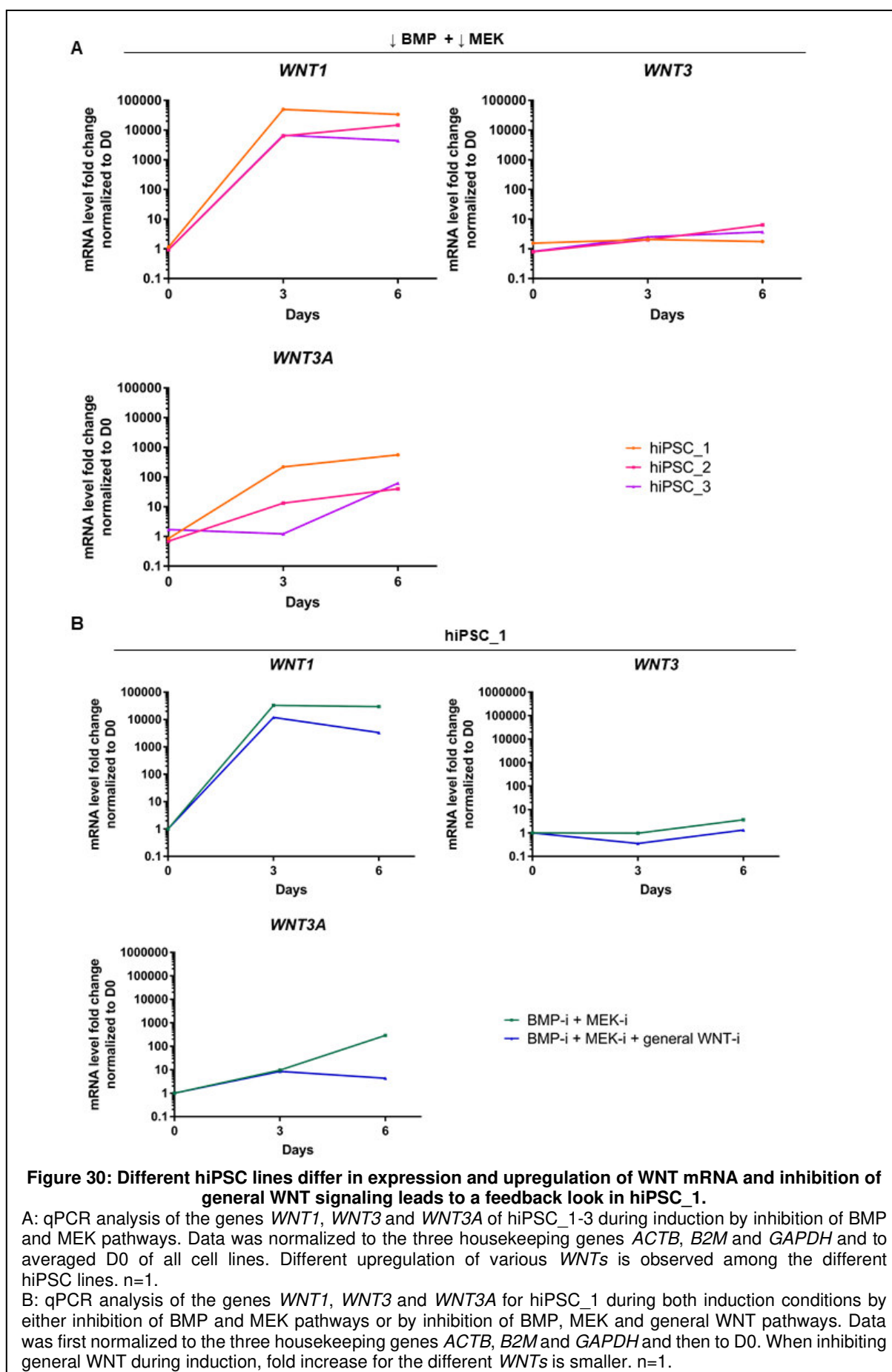


formation during neural induction. Here, hiPSC\_1 was forming SOX10<sup>+</sup> spheres when no general WNT inhibitor was applied. This condition also led to an upregulation of *SOX10* mRNA in the cells and faster downregulation of the forebrain marker *FOXP1*. Further, when inhibiting BMP and MEK pathways only, a greater variability of the data was seen when compared to the condition with additional general WNT inhibition.

The reason for all the differences can be attributed to endogenous WNT signaling in the cells. This is consistent with descriptions in a review of Ortmann and Vallier (Ortmann and Vallier, 2017). They described that WNT signaling might vary among pluripotent stem cell lines and that WNT signaling can also be dynamic, concluding that WNT activity and expression might change from time to time. The expression of the three different WNT molecules WNT1, WNT3 and WNT3A was analyzed in the context of inhibition of BMP and MEK inhibition in the three hiPSC lines hiPSC\_1-3. The expression between the three hiPSC lines for each of the WNTs at D0 was comparable. However, the fold increase during differentiation varied among the WNTs and among hiPSC lines: hiPSC\_1, which also showed the strongest propensity to form neural crest, showed the highest upregulation of *WNT1* (50 000 fold at D3, 34 000 at D6) and *WNT3A* (200 to 560-fold) compared to the two other lines, which showed a lower upregulation. This might be the reason why hiPSC\_1 forms neural crest spheres when inhibited by BMP and MEK inhibitors only.

As hiPSC\_1 was the only cell line showing neural crest development, *WNT* fold changes were observed in this cell line under inhibition of BMP and MEK pathways and under inhibition of BMP, MEK and additional general WNT pathways. Not much difference was observed for *WNT3* compared to the other *WNTs*. Expression of *WNT3* was already low throughout induction, but a 3-fold higher upregulation was observed in the case BMP and MEK inhibition was used compared to the condition with additional WNT inhibition (Figure 7B). Further, the highest upregulation was observed for *WNT1*: Approximately a 30 000-fold upregulation was observed when inhibiting BMP and MEK pathways only. When using additionally general WNT inhibition, an upregulation of only 12 000-fold was observed on mRNA level, with a tendency to

decrease in further time course (Figure 17B). The difference lied between 3 to 10-fold



differences between the two conditions on mRNA level.

For *WNT3A*, the fold change increased to roughly 10-fold at day 3, and further increased up to 300-fold when no WNT inhibitor was used during neural induction (Figure 17B). When WNT inhibitor was applied, the fold increase only reached 9 to 4-fold at days 3 and 6 respectively (Figure 17B).

The data indicated that WNT transcription on RNA level seemed to be reduced when general WNT signaling was inhibited, indicating a possible feedback-loop in the cultures (Figure 17B). *WNT1* and *WNT3A* seemed to have a greater influence than *WNT3* as greater fold increases were observed (Figure 17A and B).

In conclusion, the application of a general WNT inhibitor could avoid neural crest formation in this setting by inducing a feedback-loop on *WNT1* and *WNT3A* on RNA level. The application of general WNT inhibition led to a more robust condition as the variable endogenous WNT signaling was shut down in the cells, leading to a more comparable differentiation behavior in different pluripotent stem cell lines.

### 3.2.3 Inhibition of canonical WNT signaling is not sufficient to block neural crest formation

As WNT signaling was identified as driver for neural crest differentiation, two pathways could be responsible: Non-canonical and/or canonical WNT signaling.

To assess these possibilities, differentiation in hiPSC\_1 was induced by inhibition of BMP-, MEK- and general WNT pathways by IWP2, or by inhibition of BMP-, MEK- and canonical WNT pathways only by XAV939 (XAV). XAV is a tankyrase inhibitor and therefore, induces degradation of  $\beta$ -catenin, leading to inhibition of the canonical WNT pathway. To further clarify the role of WNT signaling, differentiation in hiPSCs was also induced by inhibition of BMP-, MEK- and general WNT pathways with additional canonical WNT activation by 0.5 $\mu$ M of CHIR99021 (CHIR). This should lead to inhibition of any endogenous WNT signaling in the cells while specifically activating the canonical WNT signaling axis via GSK3- $\beta$ . CHIR is an inhibitor of GSK3- $\beta$  which leads to  $\beta$ -catenin signaling, therefore activating canonical WNT signaling. The low concentration of CHIR was chosen to achieve a slight dorsalization of the cell identity without reaching neural crest formation (Chambers et al., 2012). Higher

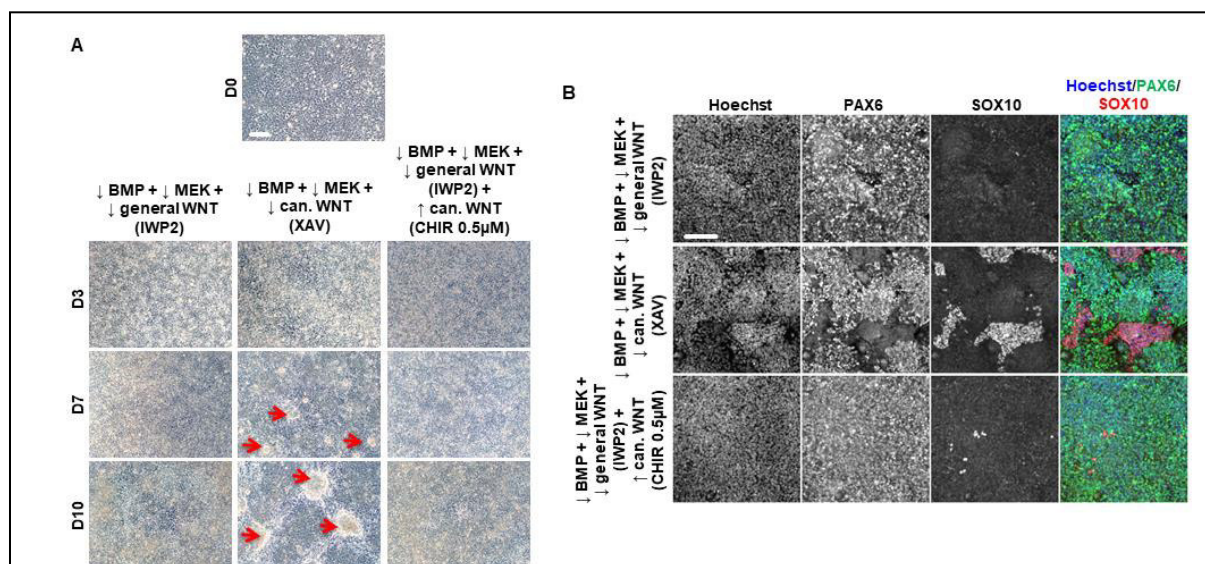


**Figure 32: Non-canonical WNT signaling is responsible for neural crest formation.**

hiPSC line1 was treated with inhibitors of BMP and MEK pathways and either with a general WNT inhibitor (IWP2), a canonical WNT inhibitor (XAV) or a general WNT inhibitor (IWP2) with slight simultaneous canonical WNT activation (0.5 $\mu$ M CHIR).

A: Phase contrast images of the cells at D0, D7 and D10 of induction. Sphere formation can be seen when canonical WNT is inhibited alone without any other WNT inhibition. Red arrows indicate sphere formation.

B: Immunofluorescence staining of cells at D6 of induction. Cells were stained for the neuroectodermal marker PAX6 and the neural crest marker SOX10. SOX10+ patches can be seen when canonical WNT is inhibited alone without any other WNT inhibition. Some single SOX10+ cells can also be found when general WNT is inhibited and cells are treated with the canonical WNT activator CHIR. The images indicate that non-canonical WNT signaling has a greater influence on neural crest formation compared to canonical WNT signaling. Scale bar: 100 $\mu$ M.



concentrations, such as 3 $\mu$ M, might lead, besides to the formation of neural crest, to caudalization of the culture towards mid- and hindbrain (Li et al., 2011).

After one week of induction, the condition with canonical WNT inhibition showed sphere formation and by immunofluorescence staining the spheres were positive for SOX10 (Figure 18A and B), indicating formation of neural crest. Inhibition of general WNT signaling did neither induce sphere formation in the culture nor formation of SOX10+ cells (Figure 18A and B). Inhibition of general WNT with simultaneous activation of slight canonical WNT by 0.5 $\mu$ M CHIR led to similar results, except that in immunofluorescence stainings, single SOX10+ cells formed (Figure 18A and B).

When analyzing gene expression on mRNA level, inhibition of BMP, MEK and canonical WNT signaling by XAV led to the highest fold increase (72-fold) for the neural crest marker *SOX10* (Figure 19). This confirmed the findings on morphological level as well as on protein level by immunofluorescence staining (Figure 8A and B). Further, this condition led to the highest upregulation of *OTX2*, which is a dorsal fore- and midbrain marker and initially to an upregulation of *FOXP1*, but then to a downregulation

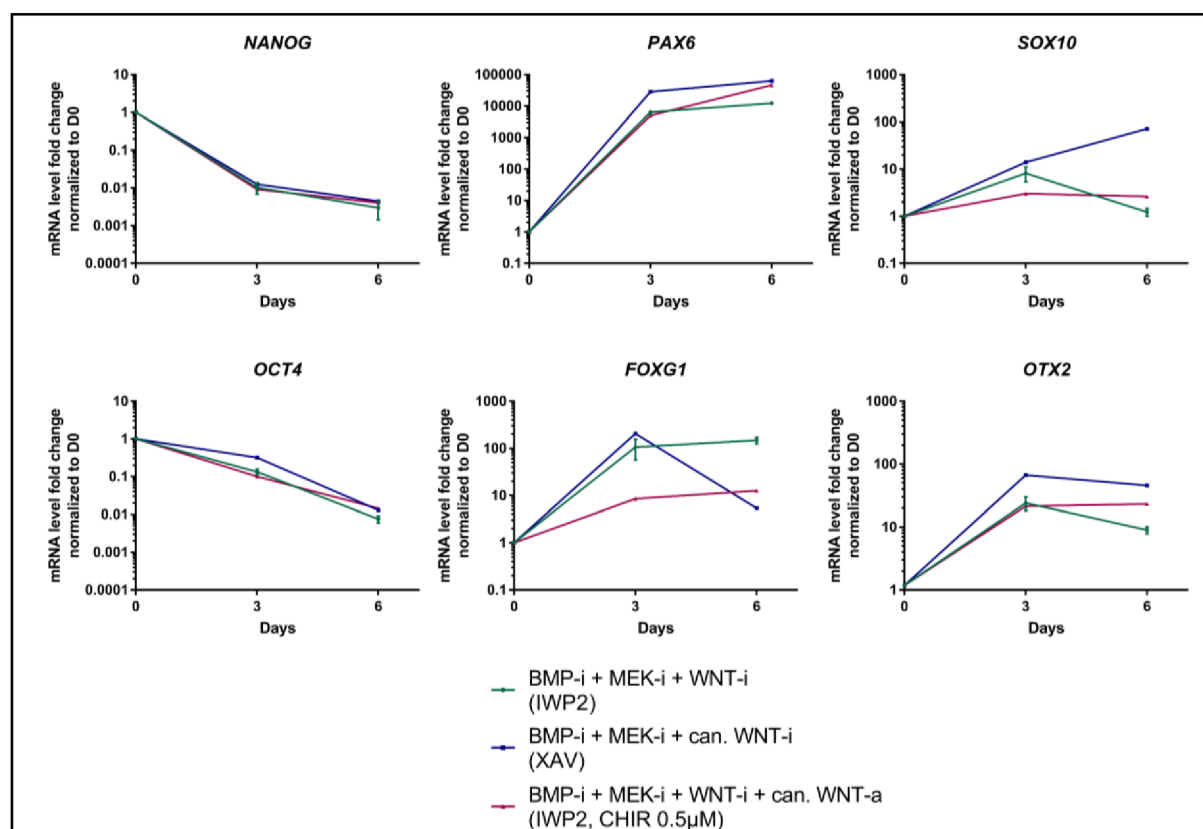


**Figure 34: Different inhibition and activation of WNT signaling leads to different outcomes on mRNA level.**

qPCR analysis for the genes *NANOG*, *OCT4*, *PAX6*, *FOXG1*, *SOX10* and *OTX2*. Samples were normalized to the three housekeeping genes *ACTB*, *B2M* and *GAPDH*. Further, cells were normalized to the average of D0 and set to 1. Canonical WNT inhibition leads to highest fold increase in *PAX6* and *SOX10*. and to a rapid downregulation of *FOXG1* from D3 onwards. General WNT inhibition leads to highest fold increase for *FOXG1*. Data were normalized to the housekeeping genes *ACTB*, *GAPDH* and *B2M* and then to D0. For inhibition of BMP, MEK and WNT pathways, n=3, other conditions n=1, error bars: SEM.

of *FOXC1* from D3 onwards, indicating a caudalization of the cells in the later days of the differentiation process (Figure 19).

Contrary to the expectations that WNT signaling leads to dorsalization of forebrain progenitors or even neural crest formation, canonical WNT activation led only to a slight upregulation of *FOXC1* and *SOX10* compared to the other conditions (Figure 19).

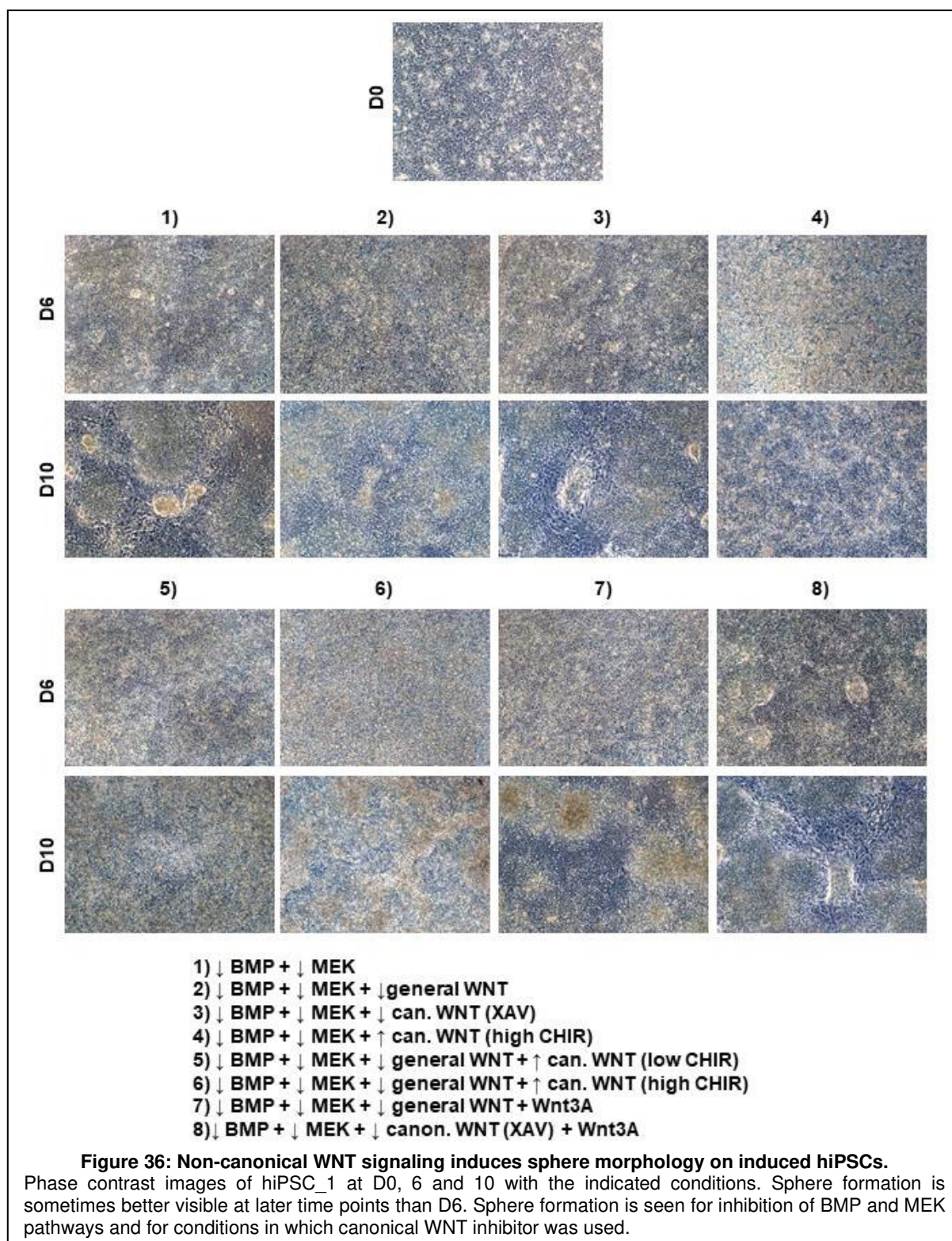
This experiment indicated that neural crest formation was potentially induced by endogenous non-canonical WNT signaling pathway components of the cells which was not inhibited by XAV treatment. Canonical WNT signaling only seemed to be a minor activator of neural crest in the used conditions as seen on the immunofluorescence stainings (Figure 18B). Further, non-canonical WNT signaling seemed to have a caudalizing effect as *OTX2* was upregulated whereas *FOXC1* was being downregulated (Figure 19).

To further clarify the role of WNT signaling, additional conditions were tested in hiPSC\_1:

- 1) Inhibition of BMP and MEK pathways as control for neural crest prone lines
- 2) Inhibition of BMP, MEK and general WNT pathways by IWP2
- 3) Inhibition of BMP, MEK and canonical WNT inhibition by XAV to see the effect of non-canonical endogenous WNT signaling if present
- 4) Inhibition of BMP and MEK pathways plus canonical WNT activation by high (3 $\mu$ M) CHIR concentrations
- 5) Inhibition of BMP, MEK and general WNT pathways plus slight canonical WNT activation by IWP2 and 0.5 $\mu$ M CHIR respectively to see the effect of slight canonical WNT activity with other WNT signaling blocked
- 6) Inhibition of BMP, MEK and general WNT pathways plus strong canonical WNT activation by IWP2 and CHIR respectively to see the effect of strong canonical WNT activity without any other WNT signaling
- 7) Inhibition of BMP, MEK and general WNT pathways by IWP2 plus WNT3A signaling to see the effect of canonical WNT signaling as WNT3A is known to activate canonical WNT signaling in cells.

8) Inhibition of BMP, MEK and canonical WNT pathways by XAV plus WNT3A signaling to see if canonical WNT activation by WNT3A are inhibited by the canonical WNT inhibitor XAV.

On phase contrast images, for some conditions sphere formation was observed (Figure 20). Sphere formation was seen for conditions 1), 3) and 8) when inhibiting BMP and MEK pathways only or when inhibiting additionally canonical WNT pathways

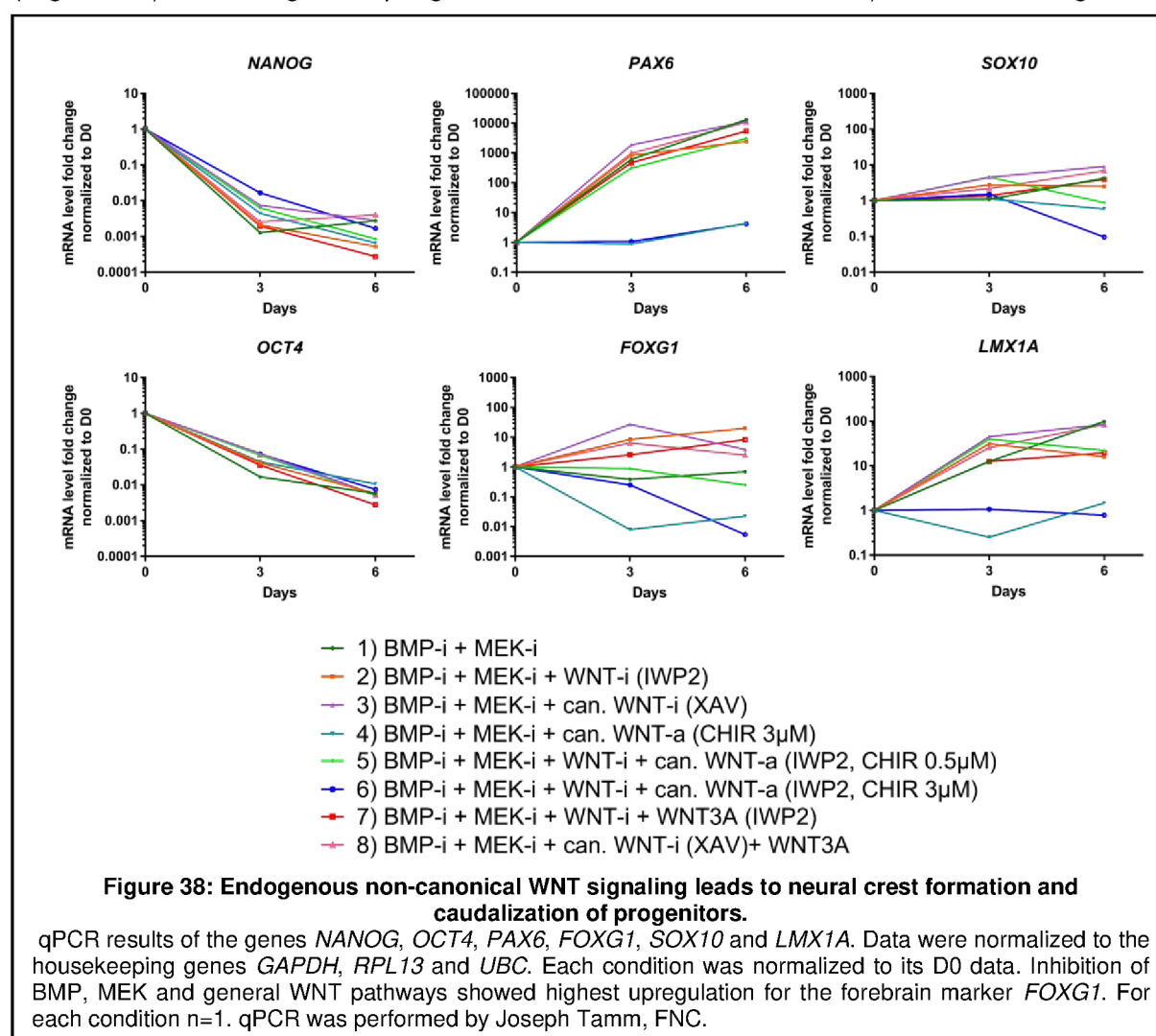


by XAV respectively (Figure 20). These findings indicated that canonical WNT signaling either prevents sphere formation or that non-canonical WNT signaling has an influence on sphere formation.

In previous experiments, the spheres were SOX10<sup>+</sup>. Also, on mRNA level these three conditions led to the highest upregulation of *SOX10* mRNA by 4 to 9-fold compared to the other conditions (Figure 21).

Further, RNA data showed that the conditions with strong canonical WNT activation by CHIR, means conditions 4) and 6), led to no fold increase for *PAX6* and even a downregulation of *FOXG1* mRNA (Figure 21). Contrary to the expectations, also no upregulation of *LMX1A* was seen which would indicate a caudalization of the cultures (Figure 21). The rest of the conditions led to a fold increase for *LMX1A* (Figure 21): Highest increase with 80 to 100-fold upregulation at D6 was seen for condition 1), 3) and 8) (Figure 21).

When looking at *FOXG1* fold changes, the conditions showed strong differences (Figure 21): Here, highest upregulation was seen for condition 2) when inhibiting BMP,



MEK and general WNT pathway at D6 with an upregulation of 20-fold (Figure 21). Therefore, this condition was considered as the most promising one when aiming for forebrain neurons.

All the conditions led to downregulation of the pluripotency markers *OCT4* and *NANOG* (Figure 21).

Highest *FOXP1* upregulation was observed for condition 2) by inhibition of BMP, MEK and general WNT pathways. Therefore, this condition was considered as the minimal essential condition needed for forebrain induction.

### 3.2.4 Induction conditions are reproducible in various hiPSC lines

As the minimal induction condition was identified, namely inhibition of BMP, MEK and general WNT pathways, in a next attempt, this condition was tested in several different hiPSC lines: It was tested in the three control lines hiPSC\_1 - 5, and in two hiPSC lines carrying either an AD mutation in the PSEN1 gene (hiPSC\_PSEN1) or a mutation found in frontotemporal dementia in the MAPT gene (hiPSC\_MAPT).

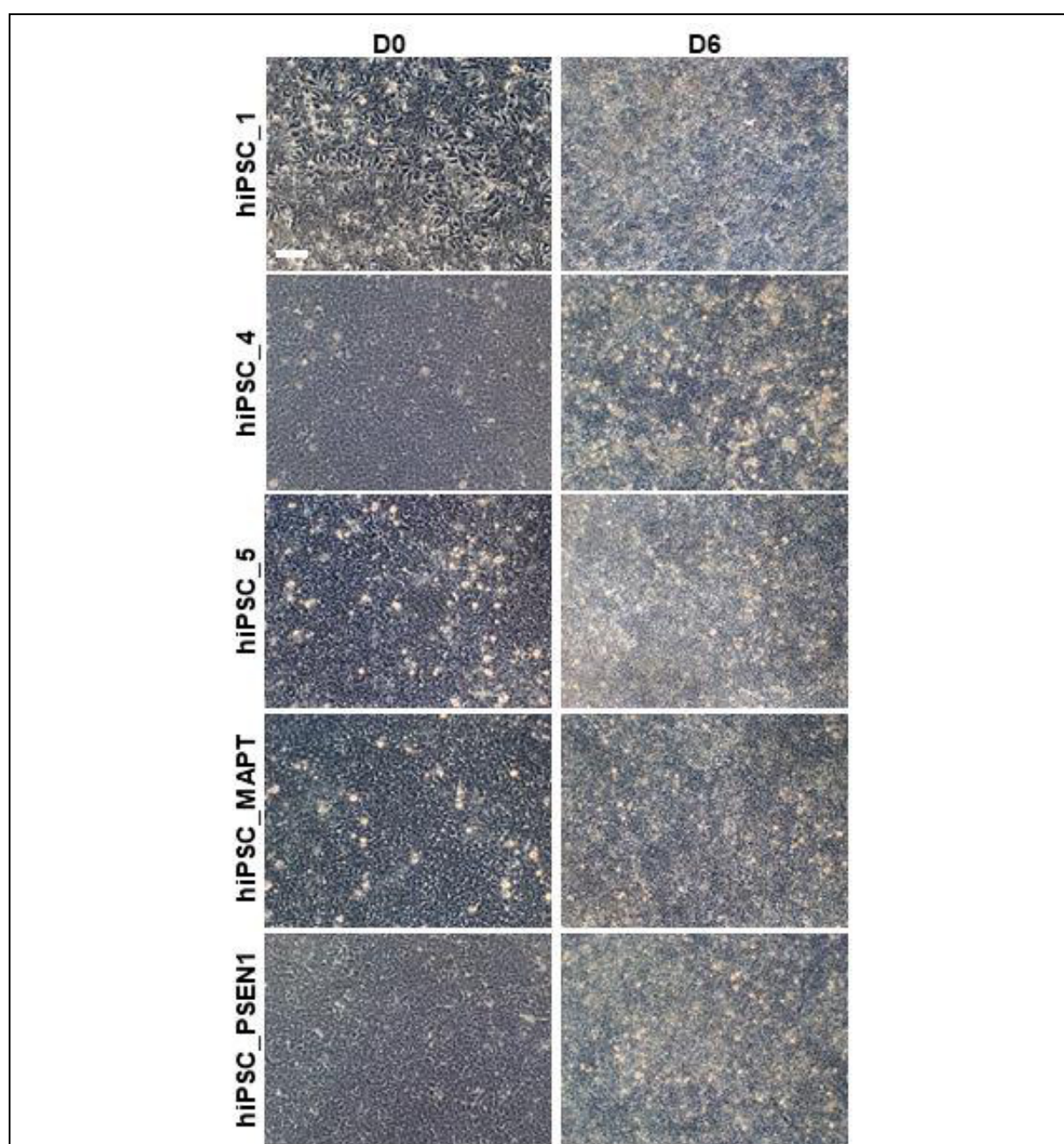
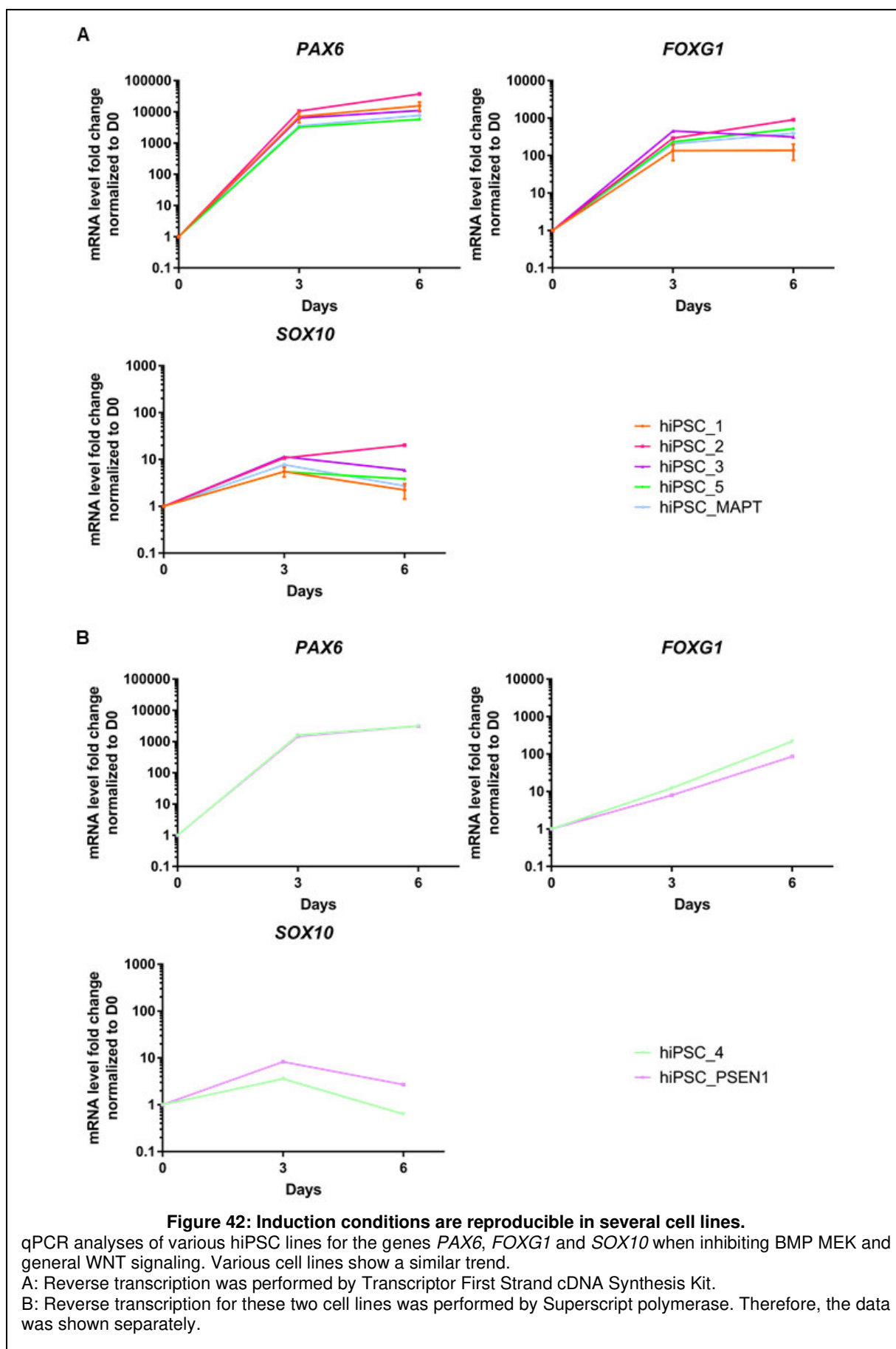


**Figure 40: Inhibition of BMP, MEK and general WNT is reproducible in various hiPSC lines.**

The five different lines hiPSC\_1, hiPSC\_4, hiPSC\_5 and the two disease lines hiPSC\_MAPT and hiPSC\_PSEN were induced by inhibiting either BMP, MEK and general WNT or by inhibiting BMP, MEK, general WNT and SHH. Phase contrast images indicate comparable behavior among hiPSC lines and between induction conditions. Scale bar: 100 $\mu$ m.

All tested cell lines showed similar behavior on morphological level during neural



induction (Figure 22). Further, the different lines showed similar tendency on RNA levels during neural induction (Figure 23): Inhibition of BMP, MEK and general WNT pathways led to an upregulation of *PAX6* between 5800-fold and 37 000-fold at D6 (Figure 23).

For *FOXG1*, an upregulation between 140 and 900-fold was seen when BMP, MEK and WNT pathways were inhibited (Figure 23). For *SOX10*, an upregulation between 2 and 20-fold was seen when BMP, MEK and WNT pathways were inhibited (Figure 23).

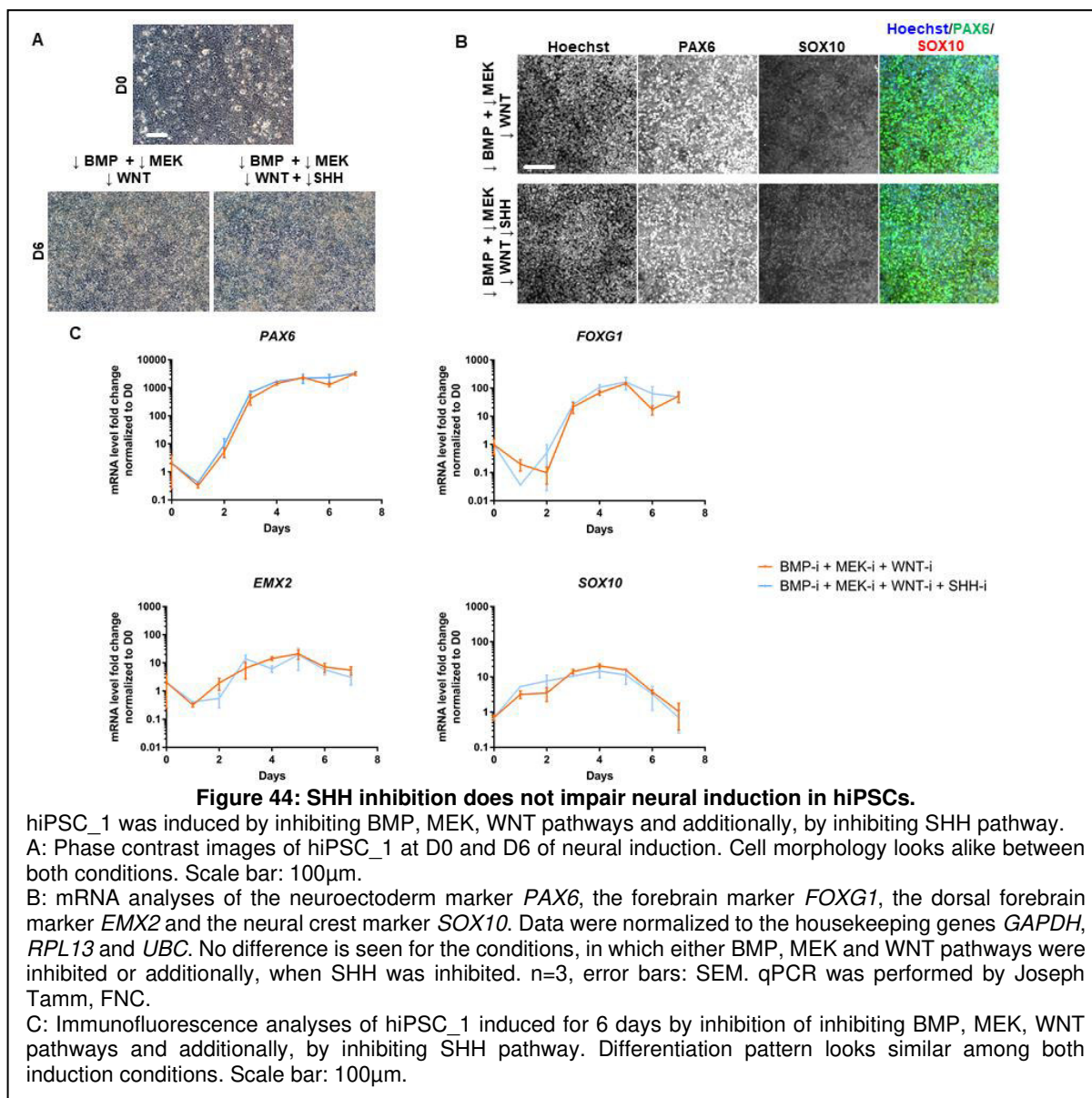
In conclusion, the minimal induction condition by inhibition of BMP, MEK and WNT pathways was reproducible in 7 individual hiPSC lines from which 2 were lines bearing mutations for AD or tauopathy.



### 3.2.5 SHH inhibition does not affect neural induction and could be used in case of ventralization of the culture

In a next attempt, the SHH inhibitor Cyclopamine was included during induction to determine a possible dorsalizing effect.

On cell morphology, SHH did not have an adverse effect and after 6 days of induction with inhibitors of BMP, MEK, WNT and SHH, the cell layer shows rosette formation (Figure 24A). Further, immunofluorescence staining analyses also did not show any difference between both conditions. When looking on mRNA fold change no difference can be observed between the condition of inhibiting BMP, MEK and general WNT and the condition with additional SHH inhibitor (Figure 24B). An interesting marker in that regard is *EMX2*, which is a dorsal forebrain marker. A reason why no difference is



observed between both conditions might be that no SHH is being expressed and therefore, inhibition might not show any difference.

Therefore, it was concluded that inhibition of SHH is not affecting neural induction, but is not yet needed in the differentiation process and that SHH inhibition might have beneficial effects later during the expansion phase of NPCs.

### 3.2.6 Various expansion conditions after neural induction lead to neuronal outcome in cells

Once minimal induction conditions were identified, which were a combination of BMP, MEK and general WNT inhibition for 6 days, the next step towards neuronal differentiation is the expansion phase of the neural progenitor cells.

Usually, expansion and at the same time consolidation of the CNS identity is performed by basic fibroblast growth factor (bFGF), also known as FGF2, exposure (Elkabetz et al., 2008; Falk et al., 2012; Shi et al., 2012a; Yao et al., 2006; Zhang et al., 2001).

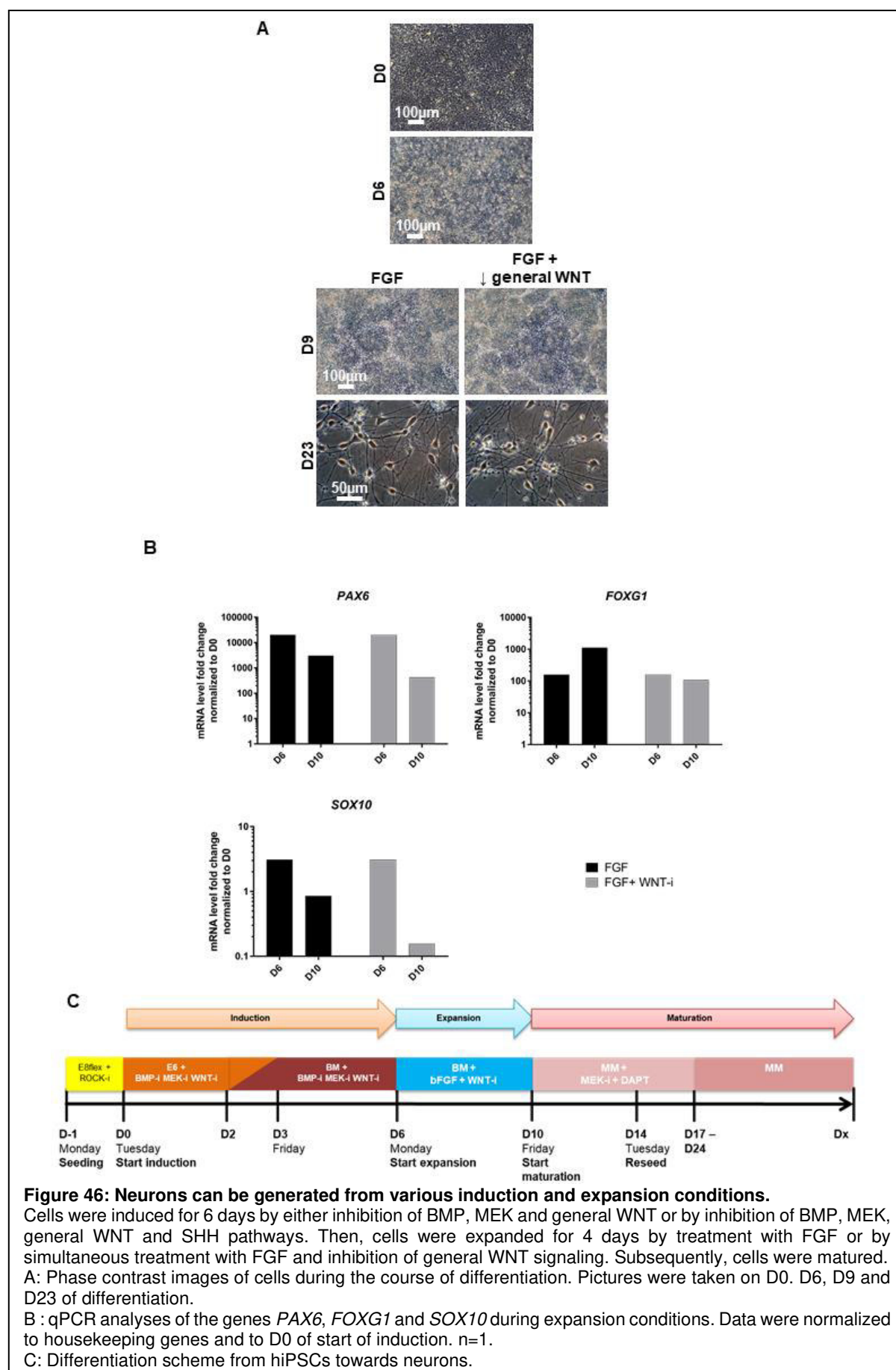
Therefore, bFGF (FGF) was used as an expansion condition, but also FGF and general WNT inhibition were evaluated to prevent influence of endogenous WNT signaling during that period. As cells are supposedly still very early in development when expansion starts, namely after 6 days of induction, general WNT inhibition could still help in this stage to avoid neural crest formation.

In both expansion conditions the neural progenitors formed a distinct rosette layer, indicative of CNS identity (Figure 25A at D9). In both expansion conditions used neurons were differentiating in later stages (Figure 25A). In brief, after 4 days of expansion, cells were matured in maturation medium (MM). MM consists of basal medium with several ingredients that support neuronal survival, such as BDNF and GDNF, but also cAMP, vitamin C and LN521 to promote adhesion during the course of final differentiation (Lepski et al., 2013; May, 2012). In the beginning, MM was supplemented with DAPT, a  $\gamma$ -secretase inhibitor and a MEK inhibitor which supports the final maturation of neurons (Borghese et al., 2010). After 4 days, cells were replated into fresh dishes coated with PLO and LN521. As soon as the culture contained cells with neuronal morphology only, this was usually the case after 1-2 weeks of maturation, DAPT and the MEK inhibitors were excluded from the medium (Figure 25C).

Neurons could also be generated when using not only hiPSC\_1 but also in other hiPSC lines, for instance in hiPSC\_4 and in the Alzheimer's Disease line PSEN1 (Figure 35A).

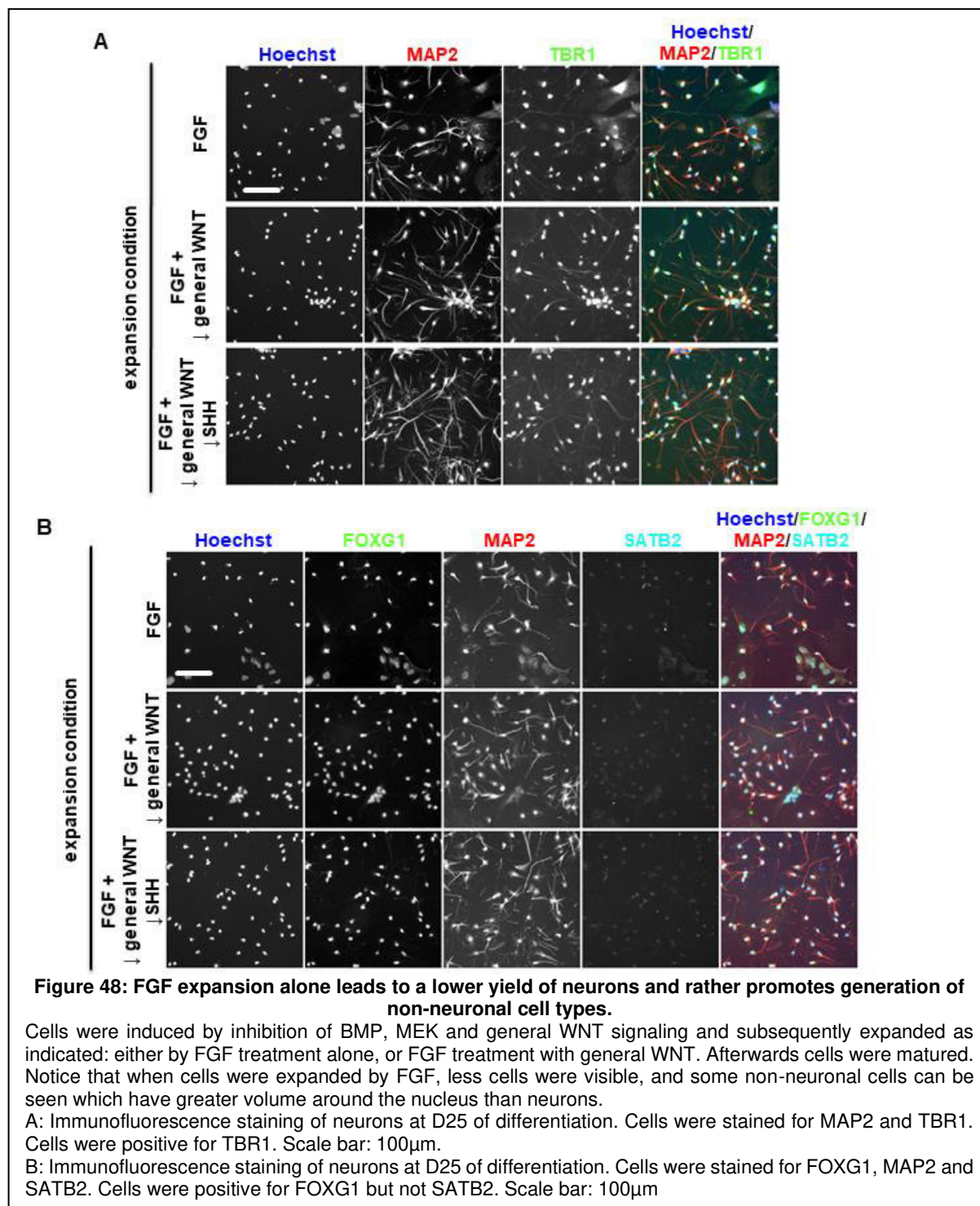
On RNA level, fold decreases were observed for *PAX6* and *SOX10* over expansion time (Figure 25B). Fold decrease for *PAX6* was moderate as a decrease of only 10 to 50-fold was observed and *PAX6* was still strongly expressed, indicating that cells present were of neural progenitor identity (Figure 25B). The decrease of *SOX10* was best when WNT inhibitor is included and probably indicates that the cells lose their ability of neural crest formation over time which was of benefit in this regard

(Figure 25B). *FOXP1* expression was not strongly influenced by the tested conditions,



indicating that the cells maintained a CNS forebrain identity. When maintained with additional WNT inhibition, neural crest propensity was potentially even decreased stronger (Figure 25B). This would be in line with the known roles of WNT signaling in development.

In a next experiment, cells were induced by inhibition of the BMP, MEK and general WNT pathways for 6 days, and then expanded with either one of the three expansion



conditions: FGF treatment only, FGF treatment with simultaneous general WNT inhibition or by FGF treatment with simultaneous inhibition of general WNT and SHH signaling. After 4 days of expansion, cells were matured as described (Figure 25C). The resulting neurons were used for characterization by immunofluorescence staining (Figure 26 and 27). Staining for cortical layer markers indicated that the majority of cells was of early cortical layer identity as the cells were positive for TBR1 (TBR1<sup>+</sup>,

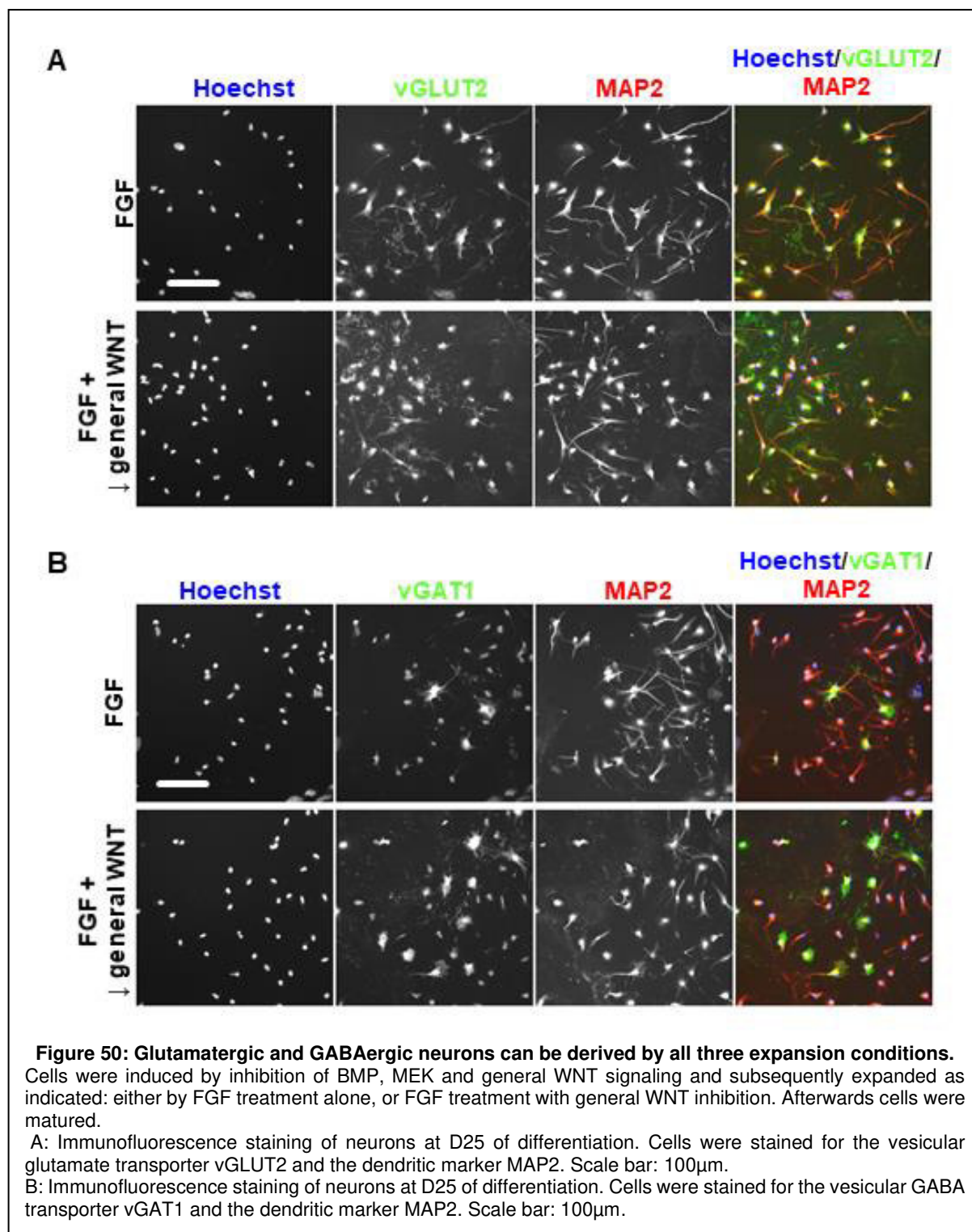
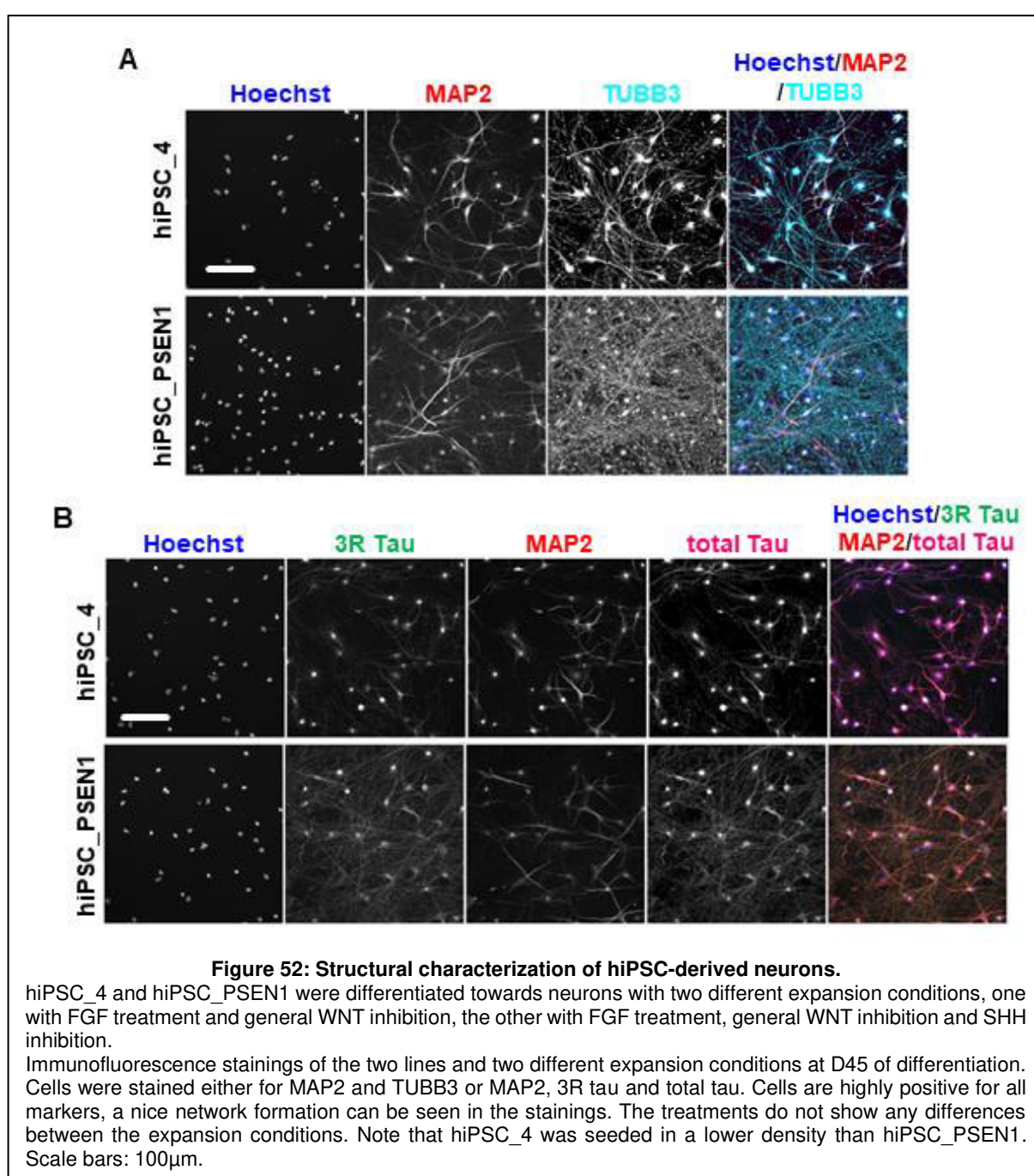


Figure 27). Further, on immunofluorescence staining level, no difference was observed between expansion condition FGF with inhibitor of WNT pathways and with additional inhibition of SHH pathway (Figure 27).

The resulting neurons from FGF expansions did not look as promising as the ones of the two other expansion conditions (Figures 26 and 27). In all immunofluorescence stainings it looked like the cells derived by the FGF treatment alone also generated a non-neuronal cell type as less cells were generated, some of which had a bigger cell volume around the nucleus compared to neurons (Figure 26 and 27). Therefore, the



assumption arised that some additional inhibitors might be necessary in the expansion conditions to prevent the differentiation of an unwanted cell type.

Further, derived neurons were stained for glutamatergic and GABAergic markers (Figure 27). Both expansion conditions generated glutamatergic and GABAergic neurons (Figure 27).

The differentiation protocol was also tested in the hiPSC lines hiPSC\_4 and PSEN1. Characterization by immunofluorescence stainings indicated similar results as the stainings in hiPSC\_1. These cells were characterized structurally by staining of cytoskeletal markers tubulin  $\beta$ 3 (TUBB3) and tau (Figure 28). The cells showed network formation visible by TUBB3 staining and tau staining (Figure 28). The culture

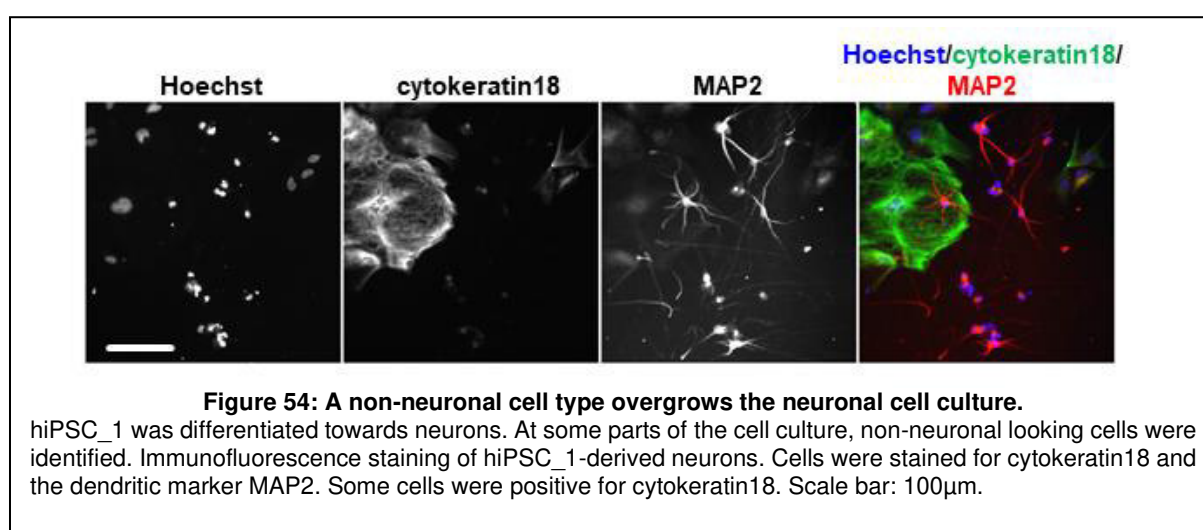
To summarize the findings from these experiments, the minimal induction condition, namely inhibition of BMP, MEK and general WNT pathways, was sufficient to generate neuronal outcome in the end. Conditions for the expansion and solidification of cortical NPC identity were evaluated: FGF only, FGF with simultaneous inhibition of general WNT pathways and FGF simultaneous inhibition of general WNT and SHH pathways. All expansion conditions were also suitable for deriving neurons. When evaluating mRNA data, expansion conditions with WNT inhibition had advantages in downregulation of neural crest marker *SOX10*.

Therefore, it can be concluded to use further pathway inhibitors during expansion simultaneous to FGF treatment to avoid formation of any other cell types. WNT inhibition can further decrease neural crest formation.



### 3.2.7 A non-neuronal cell type overgrows the neuronal culture

During individual differentiation attempts of the neuronal culture some non-neuronal cell types were visible also when expansion conditions were used, in which pathway inhibitors, such as WNT inhibition, were present. The longer the culture was grown, the more this cell type was overgrowing the neuronal culture (Figure 29), due to their proliferative nature compared to the postmitotic neurons. The cobblestone-like morphology was reminiscent of an epithelial cell type, such as keratinocytes. Indeed, upon immunofluorescence analysis, these cells could be identified as positive for cytokeratin18, further indicating such an identity.

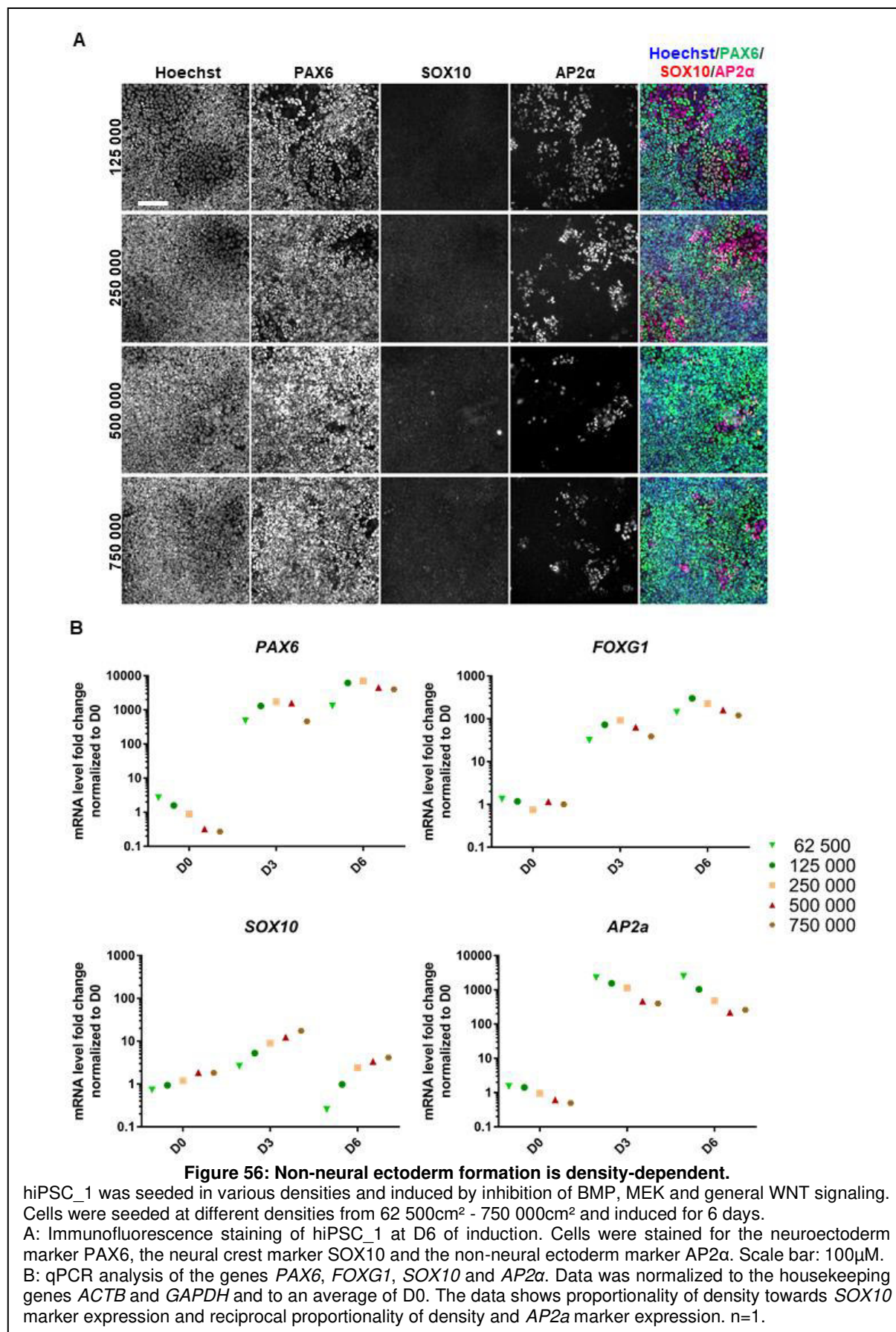


One possibility, how cytokeratin18<sup>+</sup> cells might arise from this culture, was that differentiating hiPSCs developed into the wrong lineage. During neural induction, which is part of the ectodermal lineage, some cells might become for instance cells from neural crest, non-neural ectoderm, ect. (Tchieu et al., 2017). In this regard, besides SOX10 as neural crest marker, AP2 $\alpha$ , which is a non-neural ectoderm marker, was an additional marker that appeared to be of interest.

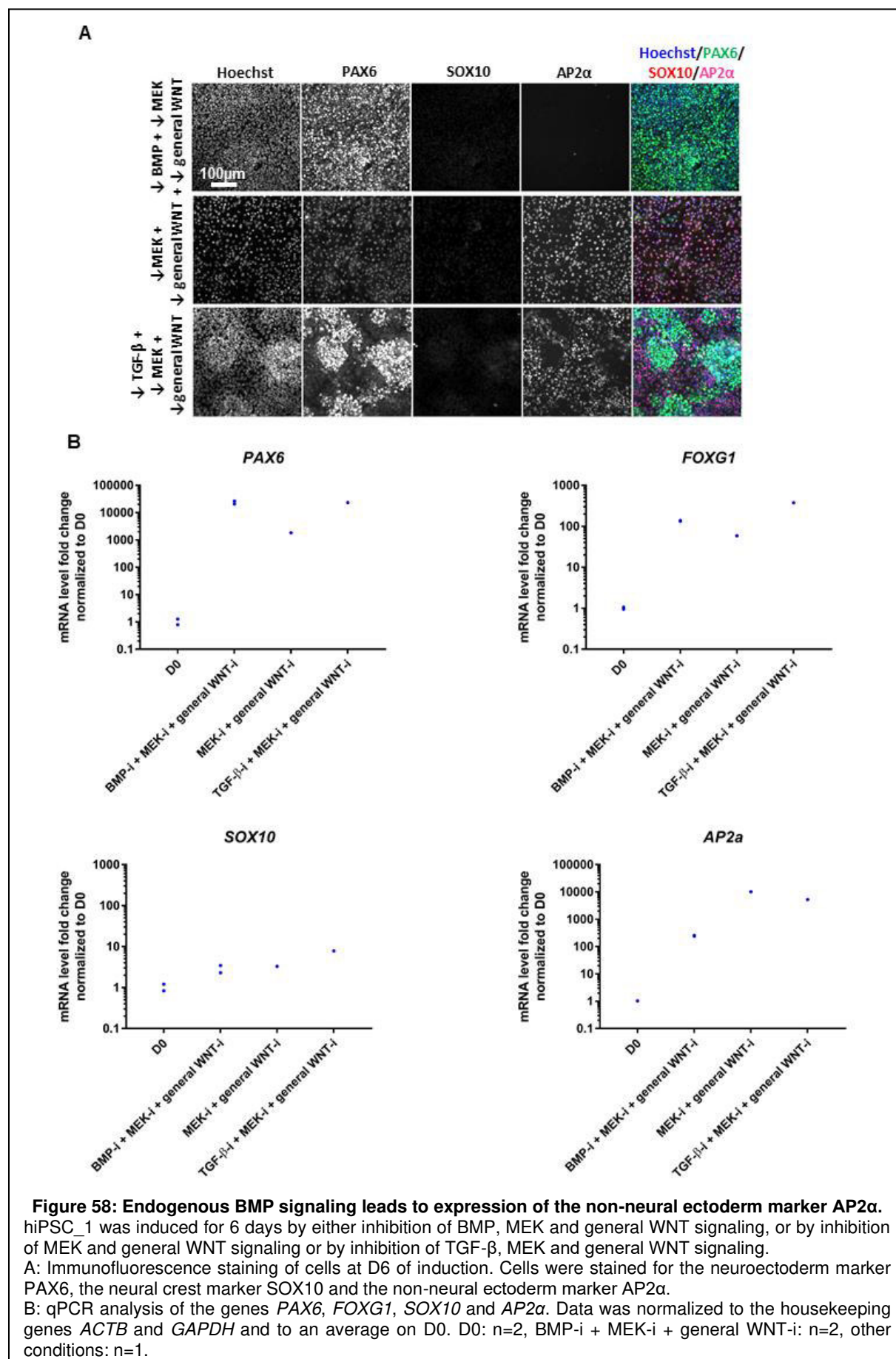
Further, effects that might influence neural crest formation or non-neural ectoderm formation were taken into consideration, such as cell density during neural induction (Chambers et al., 2009).

Therefore, in an experiment, cells were seeded in the densities 62 500, 125 000, 250 000, 500 000 and 750 000 cells/cm<sup>2</sup> and the next day, neural induction was started as outlined before. At the end of induction, cells were stained for cell lineage markers and RNA samples were collected for qPCR.

Immunofluorescence staining analyses indicated greater AP2 $\alpha$  expression in less



dense cultures compared to denser cultures (Figure 30A). RNA analyses indicated that



*PAX6* and *SOX10* expression was proportional to seeded cell density (Figure 30B). This was contradictory in the case of *SOX10*, which was described by Chambers to be reciprocally proportional to cell density (Chambers et al., 2009).

Interestingly, *AP2α* seems to be reciprocally proportional to seeded cell density on immunofluorescence staining images as well as on RNA level (Figure 19A and B).

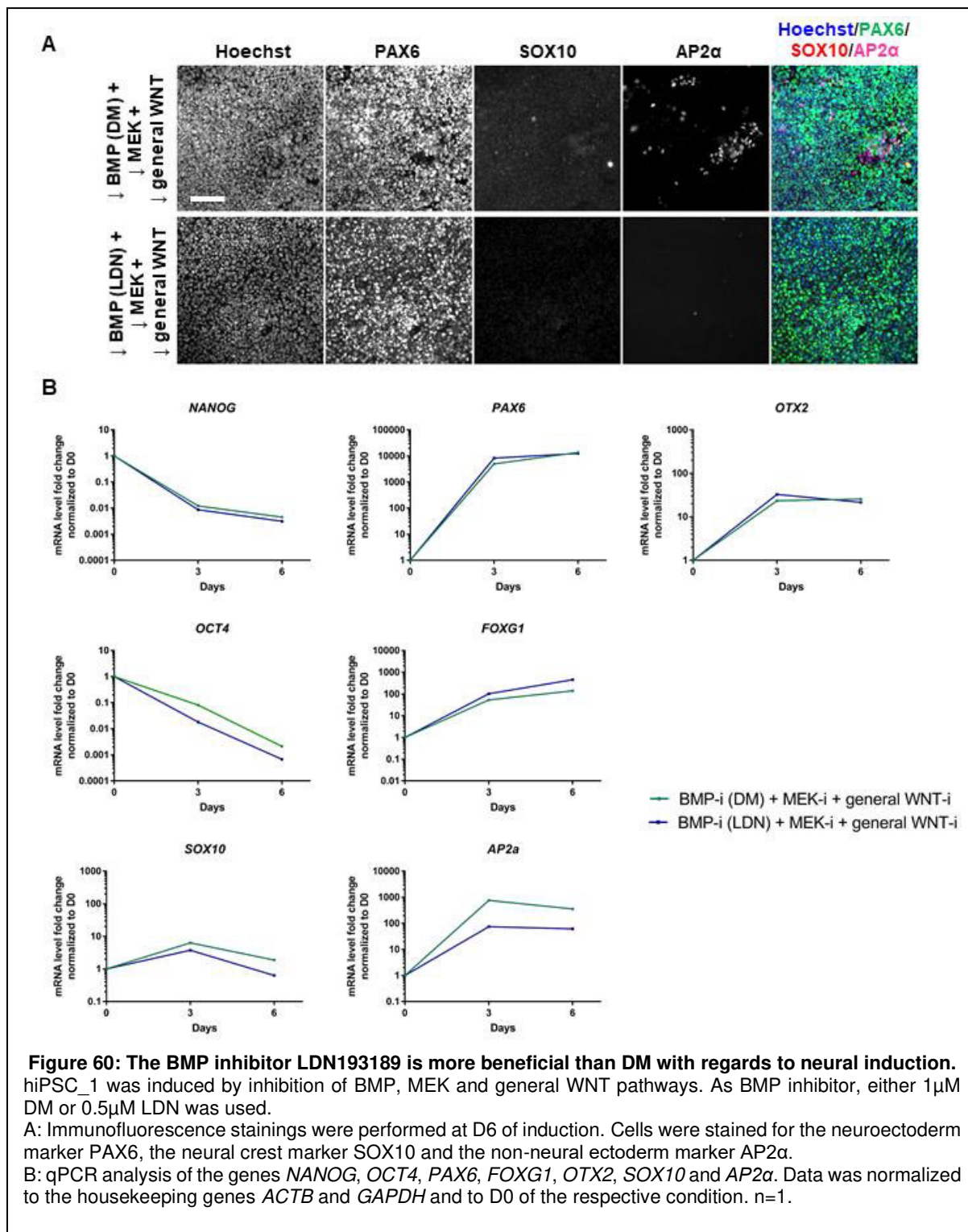
Further, some cells appeared to be positive for *PAX6* as well as *AP2α*.

According to development (Tchieu et al., 2017; Wilson and Hemmati-Brivanlou, 1995), formation of non-neural ectoderm is dependent on BMP signaling. This is particularly interesting, as BMP inhibition is often used in neural induction (dSMADi, our conditions), but various BMP signaling inhibitors exist. To evaluate whether endogenous BMP signaling could still be responsible for *AP2α*<sup>+</sup> cells, hiPSC\_1 was induced by three different induction conditions: Inhibition of BMP, MEK and general WNT inhibitors, inhibition of BMP and MEK inhibitors only and inhibition of TGF-β, MEK and general WNT inhibitors. Indeed, cells that were not induced by using a BMP inhibitor formed *AP2α*<sup>+</sup> cells (Figure 31A), indicating the definite need for such an inhibitor. This finding was also recapitulated on mRNA level: The conditions without BMP inhibitor showed a higher fold increase for *AP2α/TFAP2* compared to the condition containing a BMP inhibitor (Figure 31B).

In a subsequent experiment, the two BMP inhibitors Dorsomorphin (DM) and LDN193189 (LDN), which are structurally similar and are both ALK inhibitors, were compared with each other. In various publications, either one of both inhibitors was used (Chambers et al., 2012; Greber et al., 2011; Maroof et al., 2013; Qi et al., 2017; Shi et al., 2012b). Briefly, cells were induced as previously described by inhibiting BMP pathway either by 1μM of DM or 0.5μM of LDN, with additional inhibition of MEK and WNT pathways. Concentration of LDN was lower as potency is greater for this compound. BMP inhibition by DM could not completely prevent formation of *AP2α*<sup>+</sup> cells on immunofluorescence stainings, whereas LDN could completely prevent expression of *AP2α* in cells (Figure 32A).

On RNA level, LDN showed some advantages compared to DM: Induction by LDN led to a quicker downregulation of *OCT4*, a higher fold increase for *FOXP1*, but a lower increase for *SOX10* and *AP2α* compared to the induction with DM (Figure 32B).

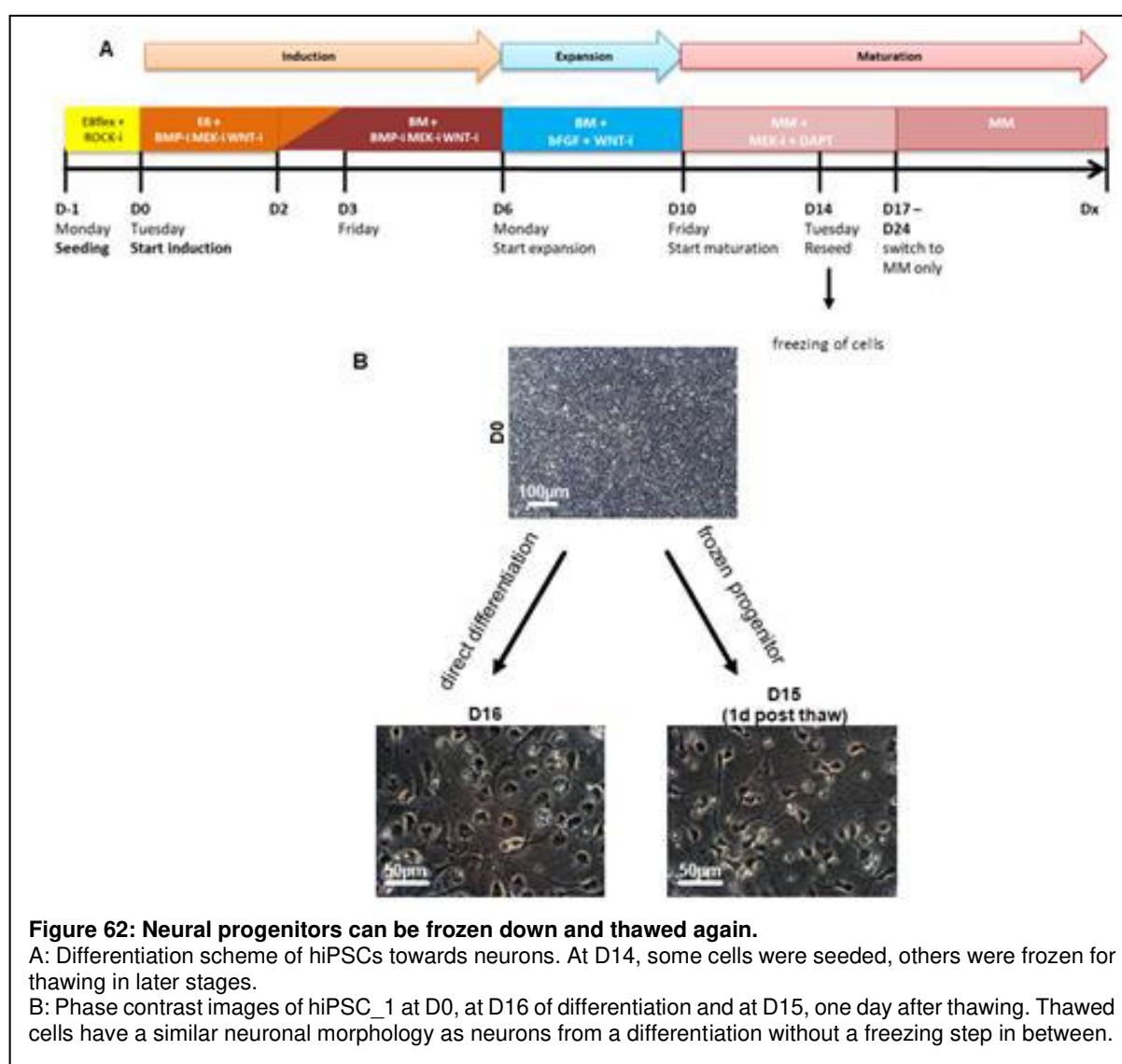
The data led to the conclusion that LDN had greater efficiency in inhibiting BMP signaling compared to DM and should be preferred.



### 3.2.8 A freezable neural progenitor cell type is acquired in the established differentiation protocol

A great benefit of a differentiation protocol is the possibility of deriving a freezable progenitor cell type. Getting hold of such a progenitor allows the generation of large, frozen cell banks which, once successfully characterized, can be used in less time for more reproducible results.

Therefore, hiPSC\_1 was differentiated as described until day 14 of differentiation (Figure 33A). At this time point, cells were being replated. A part of the cells was replated, whereas the other portion was frozen using a controlled rate freezing container and stored in liquid nitrogen temperatures. The frozen progenitors were thawed at a later time point. Cell viability during replating was at 95% for cells that were directly replated, compared to the thawed cells, in which viability of cells was only 74%. Nevertheless, one day after thawing, the progenitors already had a neuronal



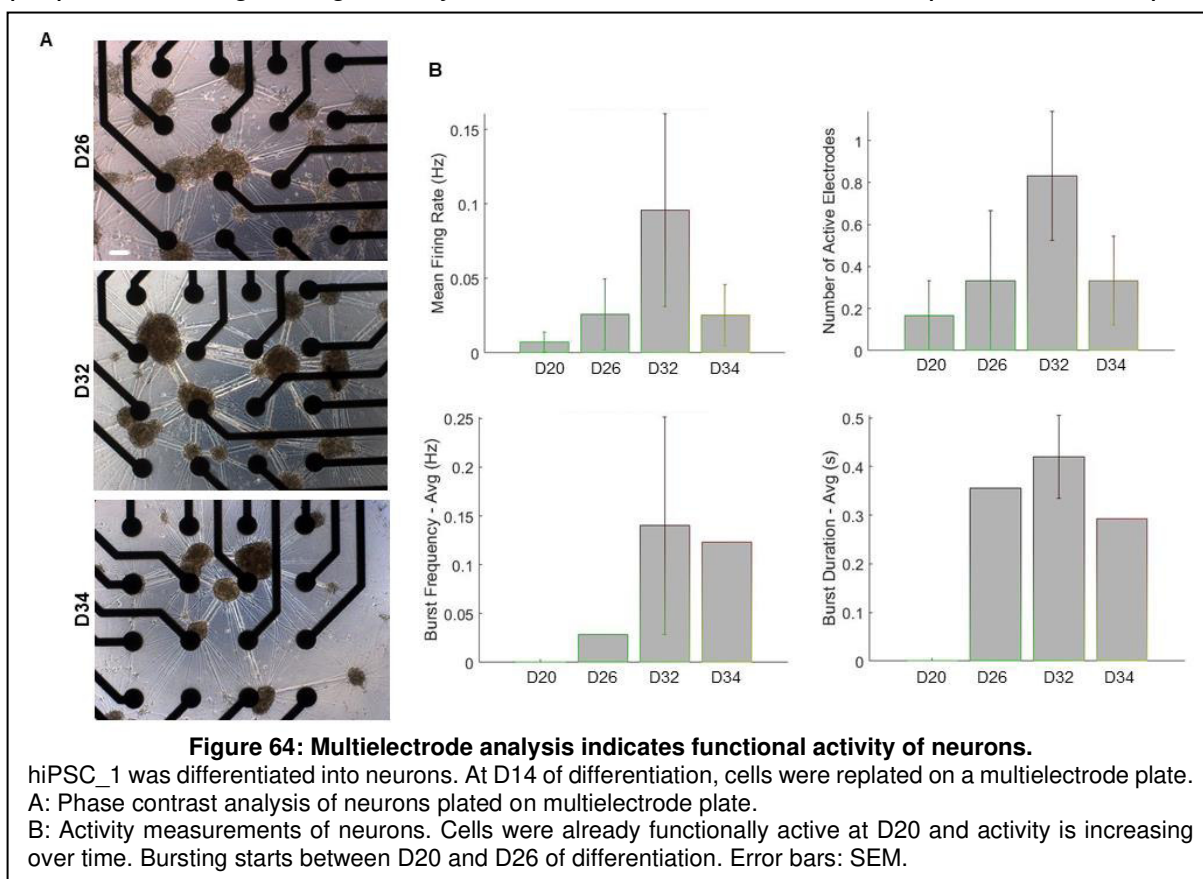
morphology, comparable to the progenitors that were replated directly without any freezing step.

This experiment indicated that a freezable progenitor can be derived from this differentiation protocol. This would also allow to perform the generation of this progenitor in large batches, skipping the first 14 days of the protocol for repetitive experiments.

### 3.2.9 hiPSC-derived neurons become electrophysiologically active in a time-dependent manner

To determine whether the forming neurons are functionally active, neuronal progenitors were replated onto coated multielectrode array (MEA) dishes at D14 of differentiation. The cells were regularly measured on the Axion Maestro Pro MEA device. Cells attached to the multielectrode plate and showed functional activity already at D20 of differentiation starting from the hiPSC stage (Figure 34A and B). The mean firing rate at D20 was at approximately 0.01Hz and increasing up to 0.95Hz at D32. Afterwards, mean firing rate seemed to decrease until 0.025Hz. Same trend could be observed for the number of active electrodes, burst frequency and burst duration. Bursting of cells started between D20 and D26 of differentiation.

The high variability of the measurements could be attributed to the fact that coating of the plates could be optimized: On one hand coating might vary as the bottom of multielectrode plates is made of glass whereas the other plates used to culture cells were made of plastic, for which the coating protocol was initially optimized for. On multielectrode plates cells formed patches and neurites looked like connecting fibers, it is possible that they were not attached tightly to the well, which is highly needed for proper recording of signals by the electrodes, which are incorporated in the plate





bottom (Figure 34B). Therefore, cells might detach after a certain amount of time, indicating the decrease of activity after D32 of differentiation, but not necessarily a decrease in neural activity (Figure 34).

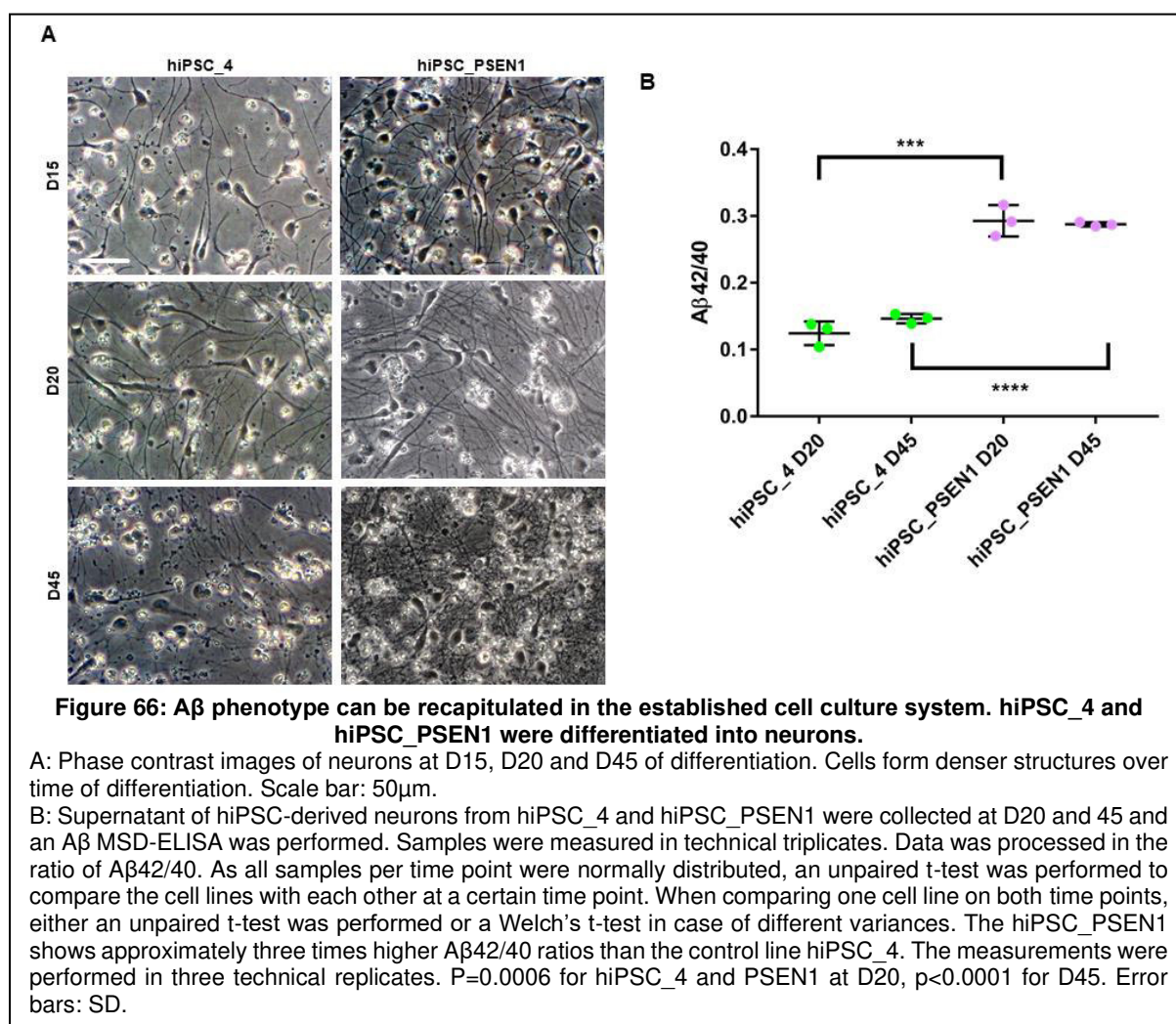
In general, the cells were already active from D20 of differentiation with a trend of growing mean firing rate over time, which could be optimized using better attachment conditions.

### 3.2.10 A $\beta$ phenotype can be recapitulated *in vitro* by the use of the established differentiation protocol

The next question was: Is the differentiation protocol suitable for deriving neurons capable of modeling disease-relevant features in AD?

For the following experiment, a healthy control line hiPSC\_4, and the AD line PSEN1 were differentiated into neurons with the aforementioned protocol. Already from D15 onwards, morphologically mature neurons were visible (Figure 35A). Medium supernatants were collected at D20 and D45 of differentiation to perform A $\beta$  ELISA using the MSD ELISA platform.

The ratio of A $\beta$ 42/40 was calculated for the two time points and a significant difference was seen between hiPSC\_4 and the PSEN1 line for each of the time points (Figure 35B). The A $\beta$ 42/40 was approximately three-fold higher for the PSEN1-diseased line compared to the healthy control line hiPSC\_4, which is expected from a mutation that is known to shift the ratio of 42/40 to a higher value, thus causing AD



(Kondo et al., 2013). Further, the ratio did not show any difference between day 20 and 45 when considered each line alone (Figure 35B). However, standard deviation was greater at day 20 compared to day 50 for both cell lines. An explanation might be, that cells are more variable when they are younger compared to an older time point when they have matured and equalized for a longer time.

The findings indicated that the A $\beta$ 42/40 ratio did not change much over time in a cell line and therefore, disease modeling for the A $\beta$  phenotype was already possible at early differentiation stages, and also indicating that the protocol can be used to model key AD pathology *in vitro*.

## 4 DISCUSSION

In this work an hiPSC-derived neuronal cell culture system was established which is xeno-free, chemically defined, quick and robust. Understanding of the biology underlying the different behavior of different hiPSC lines was crucial for optimization of the protocol. It was shown that it bears the potential for studying cortical diseases, such as Alzheimer's Disease and other tauopathies.

### 4.1 Implementation of xeno-free and chemically-defined cell culture conditions

An ethical concern in research and development is the use of animals or animal-derived components, such as sera and serum-derived proteins. In the context of the "3R-concept", the use of animals should be reduced, replaced and refined (Russel and Burch, 1992). In this context, a goal was to develop a cell culture system that is xeno-free, which means free of ingredients of foreign species. Thus, when working with hiPSCs, the components in the media should derive from human or from recombinant proteins manufactured in an animal-free manner. Here, chemically-defined media were used with recombinant human proteins that were manufactured in an animal-free procedure. Supplements which contained animal proteins, for instance the B27 supplement needed for differentiation, was switched to a xeno-free version.

Further, instead of using Matrigel as a coating agent for hiPSCs, NPCs and neurons, two different coating agents were assessed, namely human recombinant vitronectin (VTN-N) and laminin-521 (LN521). VTN-N is widely used as coating agent in combination with the E8flex medium. Nevertheless, advantages were found when using LN521: It seems to be component in the extracellular matrix of an embryo as well as in the cortex (Hyysalo et al., 2017; Laperle et al., 2015). Therefore, this coating appeared attractive as it can be used throughout the differentiation process without switching to another matrix protein. An additional advantage of replacing Matrigel by LN521 is that the variability in cell culture can also be reduced as Matrigel might contain various growth factors as contaminants that might affect culture, which is not the case for recombinant proteins. LN521 was already tested in hiPSCs with beneficial effects: Cells adhere, grow and maintain their pluripotency (Laperle et al., 2015; Rodin et al., 2014).

When switching hiPSCs from Matrigel to LN521, a higher attachment rate of hiPSCs compared to Matrigel was observed. This has the advantage of not losing that many

cells during the passaging process. Additionally, the maintenance of hiPSCs on LN521 showed a persistent OCT4 expression of the cells, indicating the maintenance of their pluripotency state, as expected from their growth pattern.

Nevertheless, other animal-derived ingredients had to be switched to recombinant solutions: This was the case for BSA towards HSA. As BSA is one ingredient of the B27 supplement, the need to switch to its xeno-free counterpart, mainly CTS-B27, was mandatory. Cell morphology and differentiation ability were unaffected by all aspects observed and measured.

The CTS-B27 belongs to a product line that is cell therapy competent: That means that the established cell culture system is a step closer to be of quality of cell replacement therapies. But to achieve this high-quality standard, other ingredients also need to be certified in that direction. This is not the case as in this work, the main focus was to develop a chemically-defined and above all a xeno-free system for research use. Further, the costs of ingredients rise with higher quality standards, which makes the system less affordable for use in research only. This has to be taken into consideration, but the steps towards cell replacement quality seem feasible.

A last step into the direction of a chemically defined and xeno-free culture system was the exchange of the proteins FGF, BDNF and GDNF towards recombinant proteins manufactured in an animal-free manner as well as replacing the carrier protein, that again is BSA, into HSA. This also has to be applied during the process of reconstitution of the recombinant proteins and generating working stock solutions. When using these xeno-free proteins, functional cortical neurons could be derived out of the protocol.

All in all, it can be concluded that the switch towards xeno-free and chemically-defined ingredients in the cell culture system worked well as the goal of differentiation, meaning guiding hiPSCs towards cortical neurons, was achieved.

#### 4.2 Development of a robust differentiation protocol to generate hiPSC-derived cortical neurons

In the course of establishing an hiPSC-derived neuronal cell culture system, the goal was to define a differentiation protocol that is very robust and applicable on a lot of different hiPSC lines, ideally all hiPSC lines tested.

Several factors might influence variability in culture and therefore, the robustness of a protocol: One factor already addressed is the use of animal-derived ingredients which

might vary from batch to batch due to being natural compounds or components. By developing a more chemically-defined protocol, this factor could already be minimized. As a next step, variability was eliminated by choosing an adherent cell culture system. The use of a 3D culture system might be indeed more physiological than an adherent 2D culture system. But it bears several variability potentials: The forming 3D embryoid bodies vary greatly in size and therefore, the system is not very scalable and reproducible. Further, when applying for instance small molecules and other pathway modulators such as growth factors, penetration into the embryoid body might be hindered, especially for growth factors that are larger than small molecules. Further, a gradient of small molecules and growth factors will form from the outside of the embryoid body to the inside, differently affecting differentiation of the cells in the embryoid body (Van Winkle et al., 2012).

Further, it is impossible to derive only a single cell type when using a 3D approach: Other cell types will arise that will “contaminate” the wanted cell type and a cell segregation step might be necessary (Lancaster and Knoblich, 2014). Therefore, it is much easier to derive a single cell type when using an adherent cell culture.

The robustness of a differentiation protocol further underlies the beneficial manipulation of pathways in the system. Such pathways in this regard were identified to be the WNT and BMP pathways.

WNT signaling is an important factor to consider during differentiation: Endogenous WNT signaling activity might vary among lines and also can change dynamically over time (Blauwkamp et al., 2012; Moya et al., 2014; Ortmann and Vallier, 2017). This in turn might affect differentiation capabilities of cells. This was also observed, when differentiating the cells without WNT inhibitor: hiPSC\_1 showed neural crest formation, which could be prevented when the general WNT inhibitor IWP2 was applied. In that regard the aim was to clarify the effect of WNT signaling in our cell culture system. We found out that endogenous non-canonical WNT signaling might lead to unwanted neural crest differentiation. When applying the canonical WNT inhibitor XAV939 (XAV), sphere formation and therefore neural crest cannot be prevented, contradictory to findings of Qi and colleagues (Qi et al., 2017)

In their differentiation condition they use the canonical WNT inhibitor XAV to reduce neural crest formation, whereas in our cell culture system this inhibition is not enough

to prevent neural crest formation. Instead, when they use CHIR99021, which activates canonical WNT signaling, their cells express the neural crest marker SOX10 (Qi et al., 2017). A possible explanation to the contradictory findings might be that Qi and colleagues use dSMADi as main induction condition, whereas in this protocol here only BMP and MEK inhibitors are applied for induction. Also, it cannot be ruled out that if less WNT signaling-prone lines are used, XAV as a WNT inhibitor is sufficient to prevent neural crest formation. Therefore, the difference might underly the different induction paradigms. Pathway crosstalk cannot be completely excluded, but for the presented differentiation paradigm, complete block of endogenous WNT signaling, independent of canonical or non-canonical, by the use of IWP2 is recommended and worked in even difficult to differentiate hiPSC lines.

Another factor contributing to variability in cell culture during neural induction was found to be BMP signaling: It became clear that in case BMP signaling is inefficiently blocked in the culture, the risk of non-neural ectoderm formation appears (Tchieu et al., 2017; Wilson and Hemmati-Brivanlou, 1995). In this regard we found out that the BMP inhibitor LDN 193189 (LDN) better inhibits BMP signaling than Dorsomorphin (DM): LDN is a second generation BMP inhibitor and therefore, its efficacy is expected to be better than the one of DM. Many protocols use DM to block BMP signaling in the dSMADi paradigm, without reporting too much formation of non-neural ectoderm. The most likely explanation why complete BMP inhibition was crucial in the protocol which was developed here is that additionally, blockage of FGF signaling was used. As discussed above, this was greatly accelerating differentiation, but if FGF is blocked and BMP signaling is present, ectodermally determined cells efficiently form non-neural ectoderm (Tchieu et al., 2017). This allowed the identification of LDN as the superior BMP inhibitor for this and future applications in differentiating hiPSCs.

Further, density-dependent effects on differentiation were found: Contrary to findings of Chambers and colleagues, it was found out that neural crest formation is reciprocally proportional to initial cell density during induction (Chambers et al., 2009). Further, a density dependence was found towards non-neural ectoderm formation. Here again, the contradictory differences might be attributed to the different differentiation paradigms used: Chambers uses dSMADi, contrary to the work here, in which inhibitors of BMP, MEK and WNT were used. Still, in the end, the developed differentiation protocol here can be applied efficiently to hiPSCs to derive cortical

neurons. Further, several factors were identified that might affect robustness of the differentiation, such as BMP and WNT signaling, that was examined here in more detail. We found out differences between canonical and non-canonical WNT signaling and that non-canonical WNT signaling contributes to neural crest formation, when canonical signaling is inhibited.

Also, other signaling pathways can be influenced in the established differentiation protocol: SHH was described as a signaling pathway that is important in patterning of the ventral region of the neural tube. In case a GABAergic culture is derived out of the differentiation protocol, a way to dorsalize the culture might be the inhibition of SHH by Cyclopamine (Cao et al., 2017; Li et al., 2009). Application of Cyclopamine during neural induction in this cell culture setting does not influence neuroectoderm formation in a negative way. Further, Cyclopamine could also be applied during expansion of NPCs to avoid ventral cultures to manifest.

All these findings indicate that it is important to know the cells in use and their pathway activity: The more is known about the pathways and their degree of activity, the better can the pathways be identified that need modulation to derive the cell type of interest. A universally applicable differentiation protocol should therefore take all possible pathway deviations into account and block/activate these as needed. That would allow the highest number of lines to be differentiated, independently of whether each pathway inhibitor is needed for each individual line to the same extent. It should be further noted that the strategy to specifically focus on hard-to-differentiate hiPSC lines, such as hiPSC\_1, turned out to be crucial for successfully developing such a robust differentiation system.

#### 4.3 Establishment of a quick differentiation protocol from hiPSC towards cortical neurons

Differentiation protocols from hPSCs towards cortical neurons already existed (Kirwan et al., 2015; Shi et al., 2012a). A big challenge is to accelerate the differentiation so that the length of usually several months could be reduced to only several weeks. Here, an alternative towards cortical neuron differentiation was presented: A different paradigm was used to the generally applied dSMADi, which inhibits BMP and TGF- $\beta$  pathways to derive neuroectodermal cells. It was found out that inhibition of TGF- $\beta$  pathways is not necessary for neural induction. By the help of MEK inhibition the



induction phase could be accelerated so that only 6 days of induction are need instead of 12 days (Kirwan et al., 2015; Shi et al., 2012a).

The established cell culture system has a freezable neural progenitor cell (NPC) type. By this advantage larger batches of NPCs can be generated and in later stages, 10 days of induction and expansion can be saved. Also, it has to be taken into consideration that in routine application of the protocol, time saving is even higher, as the need for taking or keeping hiPSC lines in culture prior to neural induction is also non-existent if frozen batches of NPCs are used. The frozen batches also allow generation of large stocks, which can be used for repetitive experiments more robustly, as also hiPSC lines from different passages are not induced each time. Further, neurons can be derived from D15 of differentiation on, which are already showing electrophysiological activity from D20 of differentiation. This is comparable to a recent publication by Qi et al: They describe in their differentiation protocol that their neurons are functionally active from D16 onwards of differentiation (Qi et al., 2017). On the other hand, they lack a freezable progenitor.

#### 4.4 Alzheimer's Disease modeling with hiPSC-derived neurons

When using the differentiation protocol with an Alzheimer patient-derived hiPSC line, namely hiPSC\_PSEN1, the A $\beta$  phenotype typical for AD could be recapitulated *in vitro*, proving, that the developed protocol and thus the developed cell culture system is suitable for AD modeling. Further, the disease phenotype could already be identified within 20 days of differentiation compared to already published A $\beta$  disease modeling from Kondo and colleagues, which performed A $\beta$  phenotyping at D72 of differentiation (Kondo et al., 2013).

For a more physiological disease modeling approach or to check how other cell types are involved in the AD phenotype a co-culture system of neurons with, for instance astrocytes, microglia or all three of them would be an option (Oksanen et al., 2017; Sirkis et al., 2016). Still, it should be noted that this would make cultures more complex and individual cellular contributions more difficult to elaborate.

The differentiation protocol makes our developed cell culture system very suitable for A $\beta$  disease modeling already at an early differentiation stage, which is a key feature of AD pathology.

#### 4.5 General conclusion

It can be concluded that the established differentiation protocol from hiPSCs towards cortical neurons is successful with regards to several aspects:

The culturing environment of hiPSCs as well as the differentiation protocol itself were established in a xeno-free manner which makes it consistent with the “3R-concept” which aims to replace, refine and reduce the use of animals and animal-derived components in research (Russel and Burch, 1992).

An advantage of the established differentiation protocol is the accelerated induction phase leading to a greatly accelerated differentiation: By the use of the MEK inhibitor PD0325901, the induction phase of the protocol could be reduced by 50% compared to other differentiation protocols (Kirwan et al., 2015; Shi et al., 2012a).

An additional advantage of this protocol is that a neural progenitor is generated which is suitable for freezing: The progenitor that is formed after the induction and expansion phase can be frozen down in large batches and thawed for final maturation.

Further, the differentiation protocol can be used for all hiPSC lines so far tested and also for lines that seem to be more prone for neural crest formation: By the use of the WNT inhibitor IWP2 present during neural induction as well as during expansion the established differentiation protocol prevents the formation of neural crest in culture.

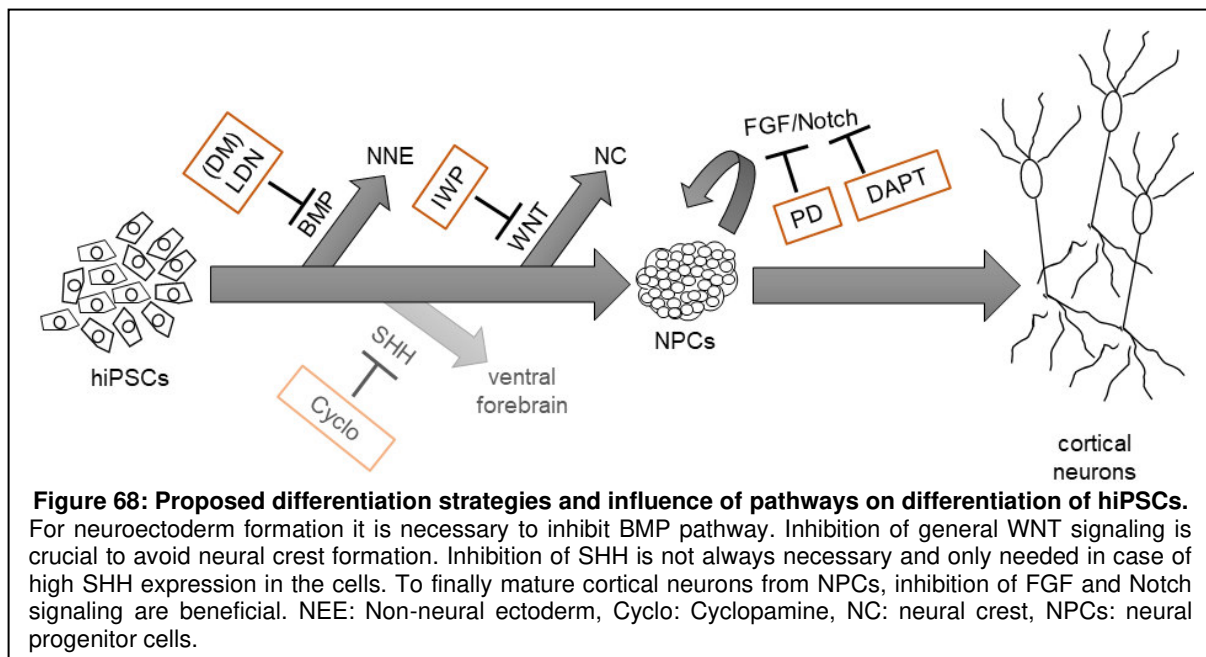
In case hiPSC lines need to be used with this differentiation protocol in the future that do not behave like all the lines tested, other signaling pathways can be modulated at any time, such as it was tested for SHH signaling by adding the SHH inhibitor Cyclopamine (Cao et al., 2017). This makes the differentiation protocol adjustable to any hiPSC line if needed, although it was not observed that this treatment was necessary or had any additional beneficial effect in all lines tested so far. This could be an intrinsic feature of the paradigm used, or just no SHH signaling present in these cell lines. Observation of SHH expression in the cells in future experiments could be used to mitigate that risk and act accordingly, if needed.

Further, the hiPSC-derived neurons are positive for early layer cortical marker TBR1 and for several structural markers, such as MAP2,  $\beta$ 3-tubulin and tau. The expression of the more early (lower cortical layer) marker TBR1 is also expected for a fast protocol, as it was shown that the formation of later (upper) cortical layers *in vitro* is recapitulating fetal development, where these layers are also formed later in CNS formation (Shi et al., 2012b). This derived neuronal culture is suitable for AD modeling: The A $\beta$

phenotype, which is a key pathology for modeling AD *in vitro*, was already detectable within 20 days of differentiation.

With all these findings it was able to develop a quick and robust differentiation protocol towards cortical neurons which could be used in several healthy control hiPSC lines but also in diseased lines such as the AD hiPSC\_PSEN1 line and the tauopathy hiPSC\_MAPT line.

Here, the minimal differentiation conditions were identified to derive cortical neurons without the risk of obtaining a foreign cell type, such as neural crest or non-neural ectoderm: Inhibition of BMP, MEK and WNT. In case other pathways influence the



differentiation in a negative way, these might also be addressed. Figure 36 summarizes the signaling pathways that might lead to an unwanted cell type outcome (Figure 36).

The established protocol bears a great potential with regards to study the molecular mechanisms of AD and some tauopathies, for target identification and drug discovery, but without the need for animal-derived components.

## 5 SUMMARY

In an aging world, neurodegenerative diseases, such as Alzheimer's Diseases start to appear more and more in society. Unfortunately, only drugs ameliorating the symptoms, but no preventive or curative medications are available. One underlying reason is that only animal models exist that do not fully reflect the human pathophysiology, leading to the difficulty of translating findings into humans. Therefore, it is of great importance to access an authentic *in vitro* cell culture system to study disease. Such a cell culture system would also have the potential to be used in later stages of drug discovery and drug development.

Here, a quick, robust and chemically-defined xeno-free differentiation protocol was developed to obtain a human induced pluripotent stem cell (hiPSC)-derived cortical neuron cell culture system. Several factors influencing variability of differentiation were addressed and identified, leading to faster generation of cells, greater robustness and wide applicability among different hiPSC lines. Further, it was shown that the derived culture system is suitable for disease modeling in Alzheimer's Disease as the A $\beta$ -pathology could be recapitulated in the cells, already at a very early time point of differentiation.

The established differentiation protocol is a promising tool in disease modeling of Alzheimer's Disease and other tauopathies, without the need of animal-derived cell culture supplements and reagents.

## 6 ZUSAMMENFASSUNG

Wir leben in einer immer älter werdenden Gesellschaft. In einer solchen Welt kommen neurodegenerative Erkrankungen, wie die Alzheimer-Erkrankung, immer öfter vor. Leider gibt es keine Medikamente, welche die Krankheit aufhalten, oder die Ursachen ursächlich bekämpfen. Lediglich welche, die die Symptome dämpfen. Ein Grund hierfür ist, dass nur Tiermodelle existieren, die die menschliche Pathophysiologie nicht komplett widerspiegeln. Dies führt zu einer erschwerten Übertragung von Erkenntnissen auf den Menschen. Daher ist es von großer Wichtigkeit, ein authentisches *in vitro* Zellkultursystem zu erschaffen, um die Erkrankung zu untersuchen. Solch ein Zellkultursystem hätte auch das Potential in späteren Phasen, wie der Wirkstoffentdeckung und Medikamentenentwicklung, genutzt zu werden.

In dieser Arbeit wurde ein schnelles, robustes und chemisch definiertes Differenzierungsprotokoll entwickelt, um ein von humanen, induzierten, pluripotenten Stammzellen (hiPSC) abgeleitetes kortikales Zellkultursystem für Nervenzellen zu erhalten. Zahlreiche Faktoren, die die Variabilität der Differenzierung betreffen, wurden untersucht und identifiziert, was zu einer schnelleren Generierung der Zellen, größerer Robustheit und Anwendbarkeit des Protokolls unter hiPSC-Linien führte. Des Weiteren wurde gezeigt, dass sich das abgeleitete Zellkultursystem als Krankheitsmodell für die Alzheimer-Erkrankung eignet, da die A $\beta$ -Pathologie mit den Zellen nachgestellt werden konnte, und zwar bereits zu einem frühen Zeitpunkt der Differenzierung.

Das etablierte Differenzierungsprotokoll ist ein vielversprechendes Werkzeug zur Modellierung der Alzheimer-Erkrankung und anderen Tauopathien, ohne den Bedarf von tierischen Zellkulturzusätzen oder von Tieren abstammenden Reagenzien.

## 7 REFERENCES

Alonso, A.D.C., Zaidi, T., Grundke-Iqbal, I., and Iqbal, K. (1994). Role of abnormally phosphorylated tau in the breakdown of microtubules in Alzheimer disease. *Proc Natl Acad Sci USA* *91*, 5562-5566.

Alzforum (2018). Online: <https://www.alzforum.org/mutations>, Stand: 27.04.2018.

Alzheimer's Association (2019). Online: <https://www.alz.org/>, Stand: n.a.

Alzheimer, A. (1907). Über eine eigenartige Erkrankung der Hirnrinde. *Zentralbl Nervenheilk Psych* *18*, 177-179.

Arriagada, P.V., Growdon, J.H., Hedley-Whyte, E.T., and Hyman, B.T. (1992). Neurofibrillary tangles but not senile plaques parallel duration and severity of Alzheimer's disease. *Neurology* *42*, 631-631.

Badenes, S.M., Fernandes, T.G., Cordeiro, C.S., Boucher, S., Kuning, D., Vemuri, M.C., Diogo, M.M., and Cabral, J.M. (2016). Defined Essential 8 Medium and Vitronectin Efficiently Support Scalable Xeno-Free Expansion of Human Induced Pluripotent Stem Cells in Stirred Microcarrier Culture Systems. *PLoS One* *11*, e0151264.

Bertram, L., Lill, C.M., and Tanzi, R.E. (2010). The genetics of Alzheimer disease: back to the future. *Neuron* *68*, 270-281.

Blauwkamp, T.A., Nigam, S., Ardehali, R., Weissman, I.L., and Nusse, R. (2012). Endogenous Wnt signalling in human embryonic stem cells generates an equilibrium of distinct lineage-specified progenitors. *Nat Commun* *3*, 1070.

Borghese, L., Dolezalova, D., Opitz, T., Haupt, S., Leinhaas, A., Steinfarz, B., Koch, P., Edenhofer, F., Hampl, A., and Brustle, O. (2010). Inhibition of notch signaling in human embryonic stem cell-derived neural stem cells delays G1/S phase transition and accelerates neuronal differentiation in vitro and in vivo. *Stem Cells* *28*, 955-964.

Braak, H., and Braak, E. (1991). Neuropathological staging of Alzheimer-related changes. *Acta Neuropathol* *82*, 239 - 259.

BrightFocusFoundation (2017). Online: <https://www.brightfocus.org/alzheimers-disease/infographic/amyloid-plaques-and-neurofibrillary-tangles>, Stand: 21.12.2017.

Brownjohn, P.W., Smith, J., Portelius, E., Serneels, L., Kvartsberg, H., De Strooper, B., Blennow, K., Zetterberg, H., and Livesey, F.J. (2017). Phenotypic Screening Identifies Modulators of Amyloid Precursor Protein Processing in Human Stem Cell Models of Alzheimer's Disease. *Stem Cell Reports* 8, 870-882.

Cao, S.Y., Hu, Y., Chen, C., Yuan, F., Xu, M., Li, Q., Fang, K.H., Chen, Y., and Liu, Y. (2017). Enhanced derivation of human pluripotent stem cell-derived cortical glutamatergic neurons by a small molecule. *Sci Rep* 7, 3282.

Chambers, S.M., Fasano, C.A., Papapetrou, E.P., Tomishima, M., Sadelain, M., and Studer, L. (2009). Highly efficient neural conversion of human ES and iPS cells by dual inhibition of SMAD signaling. *Nat Biotechnol* 27, 275-280.

Chambers, S.M., Qi, Y., Mica, Y., Lee, G., Zhang, X.J., Niu, L., Bilisland, J., Cao, L., Stevens, E., Whiting, P., *et al.* (2012). Combined small-molecule inhibition accelerates developmental timing and converts human pluripotent stem cells into nociceptors. *Nat Biotechnol* 30, 715-720.

Chen, B., Dodge, M.E., Tang, W., Lu, J., Ma, Z., Fan, C.W., Wei, S., Hao, W., Kilgore, J., Williams, N.S., *et al.* (2009). Small molecule-mediated disruption of Wnt-dependent signaling in tissue regeneration and cancer. *Nat Chem Biol* 5, 100-107.

Chen, G., Gulbranson, D.R., Hou, Z., Bolin, J.M., Ruotti, V., Probasco, M.D., Smuga-Otto, K., Howden, S.E., Diol, N.R., Propson, N.E., *et al.* (2011). Chemically defined conditions for human iPSC derivation and culture. *Nat Methods* 8, 424-429.

Choi, S.H., Kim, Y.H., Hebisch, M., Sliwinski, C., Lee, S., D'Avanzo, C., Chen, H., Hooli, B., Asselin, C., Muffat, J., *et al.* (2014). A three-dimensional human neural cell culture model of Alzheimer's disease. *Nature* 515, 274-278.

Corder, E.H., Saunders, A.M., Strittmatter, W.J., Schmechel, D.E., Gaskell, P.C., Small, G.W., Roses, A.D., Haines, J.L., and Pericak-Vance, M.A. (1993). Gene Dose of Apolipoprotein E Type 4 Allele and the Risk of Alzheimer's Disease in Late Onset Families. *261*, 261

- D'Amour, K.A., Agulnick, A.D., Eliazer, S., Kelly, O.G., Kroon, E., and Baetge, E.E. (2005). Efficient differentiation of human embryonic stem cells to definitive endoderm. *Nat Biotechnol* 23, 1534-1541.
- Drew, L., and Ashour, M. (2018). An age-old story. *Nature* 559.
- Duan, L., Bhattacharyya, B.J., Belmadani, A., Pan, L., Miller, R.J., and Kessler, J.A. (2014). Stem cell derived basal forebrain cholinergic neurons from Alzheimer's disease patients are more susceptible to cell death. *Molecular Neurodegeneration* 9.
- Ebert, A.D., Yu, J., Rose, F.F., Jr., Mattis, V.B., Lorson, C.L., Thomson, J.A., and Svendsen, C.N. (2009). Induced pluripotent stem cells from a spinal muscular atrophy patient. *Nature* 457, 277-280.
- Elkabetz, Y., Panagiotakos, G., Al Shamy, G., Socci, N.D., Tabar, V., and Studer, L. (2008). Human ES cell-derived neural rosettes reveal a functionally distinct early neural stem cell stage. *Genes Dev* 22, 152-165.
- Espuny-Camacho, I., Michelsen, K.A., Gall, D., Linaro, D., Hasche, A., Bonnefont, J., Bali, C., Orduz, D., Bilheu, A., Herpoel, A., *et al.* (2013). Pyramidal neurons derived from human pluripotent stem cells integrate efficiently into mouse brain circuits in vivo. *Neuron* 77, 440-456.
- Falk, A., Koch, P., Kesavan, J., Takashima, Y., Ladewig, J., Alexander, M., Wiskow, O., Taylor, J., Trotter, M., Pollard, S., *et al.* (2012). Capture of neuroepithelial-like stem cells from pluripotent stem cells provides a versatile system for in vitro production of human neurons. *PLoS One* 7, e29597.
- Franco, R., and Cedazo-Minguez, A. (2014). Successful therapies for Alzheimer's disease: why so many in animal models and none in humans? *Front Pharmacol* 5, 146.
- Goedert, M., and Jakes, R. (2005). Mutations causing neurodegenerative tauopathies. *Biochim Biophys Acta* 1739, 240-250.
- Greber, B., Coulon, P., Zhang, M., Moritz, S., Frank, S., Muller-Molina, A.J., Arauzo-Bravo, M.J., Han, D.W., Pape, H.C., and Scholer, H.R. (2011). FGF signalling inhibits neural induction in human embryonic stem cells. *EMBO J* 30, 4874-4884.



- Grskovic, M., Javaherian, A., Strulovici, B., and Daley, G.Q. (2011). Induced pluripotent stem cells--opportunities for disease modelling and drug discovery. *Nat Rev Drug Discov* 10, 915-929.
- Haass, C., Kaether, C., Thinakaran, G., and Sisodia, S. (2012). Trafficking and proteolytic processing of APP. *Cold Spring Harb Perspect Med* 2, a006270.
- Hemmati-Brivanlou, A., and Melton, D.A. (1994). Inhibition of Activin Receptor Signaling Promotes Neuralization in *Xenopus*. *Cell* 77, 273-281.
- Ho, R., Sances, S., Gowing, G., Amoroso, M.W., O'Rourke, J.G., Sahabian, A., Wichterle, H., Baloh, R.H., Sareen, D., and Svendsen, C.N. (2016). ALS disrupts spinal motor neuron maturation and aging pathways within gene co-expression networks. *Nat Neurosci* 19, 1256-1267.
- Huang, Y.A., Zhou, B., Wernig, M., and Sudhof, T.C. (2017). ApoE2, ApoE3, and ApoE4 Differentially Stimulate APP Transcription and Abeta Secretion. *Cell* 168, 427-441 e421.
- Hyysalo, A., Ristola, M., Makinen, M.E., Hayrynen, S., Nykter, M., and Narkilahti, S. (2017). Laminin alpha5 substrates promote survival, network formation and functional development of human pluripotent stem cell-derived neurons in vitro. *Stem Cell Res* 24, 118-127.
- Iqbal, K., Alonso Adel, C., Chen, S., Chohan, M.O., El-Akkad, E., Gong, C.X., Khatoon, S., Li, B., Liu, F., Rahman, A., *et al.* (2005). Tau pathology in Alzheimer disease and other tauopathies. *Biochim Biophys Acta* 1739, 198-210.
- Jack, C.R., Knopman, D.S., Jagust, W.J., Shaw, L.M., Aisen, P.S., Weiner, M.W., Petersen, R.C., and Trojanowski, J.Q. (2010). Hypothetical model of dynamic biomarkers of the Alzheimer's pathological cascade. *Lancet Neurol* 9, 119-128.
- Janelidze, S., Zetterberg, H., Mattsson, N., Palmqvist, S., Vanderstichele, H., Lindberg, O., van Westen, D., Stomrud, E., Minthon, L., Blennow, K., *et al.* (2016). CSF Abeta42/Abeta40 and Abeta42/Abeta38 ratios: better diagnostic markers of Alzheimer disease. *Ann Clin Transl Neurol* 3, 154-165.

Jucker, M., and Walker, L.C. (2013). Self-propagation of pathogenic protein aggregates in neurodegenerative diseases. *Nature* 501, 45-51.

Kibbey, M.C. (1994). Maintenance of the EHS sarcoma and Matrigel preparation. *Journal of Tissue Culture Methods* 16, 227-230.

Kimberly, W.T., Xia, W., Rahmati, T., Wolfe, M.S., and Selkoe, D.J. (2000). The Transmembrane Aspartates in Presenilin 1 and 2 Are Obligatory for  $\gamma$ -Secretase Activity and Amyloid  $\beta$ -Protein Generation. *The Journal of Biological Chemistry* 275, 3173–3178.

Kirkeby, A., Grealish, S., Wolf, D.A., Nelander, J., Wood, J., Lundblad, M., Lindvall, O., and Parmar, M. (2012). Generation of regionally specified neural progenitors and functional neurons from human embryonic stem cells under defined conditions. *Cell Rep* 1, 703-714.

Kirwan, P., Turner-Bridger, B., Peter, M., Momoh, A., Arambepola, D., Robinson, H.P., and Livesey, F.J. (2015). Development and function of human cerebral cortex neural networks from pluripotent stem cells in vitro. *Development* 142, 3178-3187.

Kondo, T., Asai, M., Tsukita, K., Kutoku, Y., Ohsawa, Y., Sunada, Y., Imamura, K., Egawa, N., Yahata, N., Okita, K., *et al.* (2013). Modeling Alzheimer's disease with iPSCs reveals stress phenotypes associated with intracellular Abeta and differential drug responsiveness. *Cell Stem Cell* 12, 487-496.

Kondo, T., Imamura, K., Funayama, M., Tsukita, K., Miyake, M., Ohta, A., Woltjen, K., Nakagawa, M., Asada, T., Arai, T., *et al.* (2017). iPSC-Based Compound Screening and In Vitro Trials Identify a Synergistic Anti-amyloid beta Combination for Alzheimer's Disease. *Cell Rep* 21, 2304-2312.

Kosik, K.S., Joachim, C.L., and Selkoe, D.J. (1986). Microtubule-associated protein tau ( $\tau$ ) is a major antigenic component of paired helical filaments in Alzheimer disease. *Proc Natl Acad Sci USA* 83, 4044-4048.

Lam, M.T., and Longaker, M.T. (2012). Comparison of several attachment methods for human iPS, embryonic and adipose-derived stem cells for tissue engineering. *J Tissue Eng Regen Med* 6 Suppl 3, s80-86.

- Lamb, T.M., Knecht, A.K., W. C. Smith, S. E. Stachel, A. N. Economides, N. Stahl, G. D. Yancopolous, and Harland, R.M. (1993). Neural Induction by the Secreted Polypeptide Noggin. *Science* 262, 713-718.
- Lancaster, M.A., and Knoblich, J.A. (2014). Generation of cerebral organoids from human pluripotent stem cells. *Nat Protoc* 9, 2329-2340.
- Laperle, A., Hsiao, C., Lampe, M., Mortier, J., Saha, K., Palecek, S.P., and Masters, K.S. (2015). alpha-5 Laminin Synthesized by Human Pluripotent Stem Cells Promotes Self-Renewal. *Stem Cell Reports* 5, 195-206.
- LaVaute, T.M., Yoo, Y.D., Pankratz, M.T., Weick, J.P., Gerstner, J.R., and Zhang, S.C. (2009). Regulation of neural specification from human embryonic stem cells by BMP and FGF. *Stem Cells* 27, 1741-1749.
- Lepski, G., Jannes, C.E., Nikkhah, G., and Bischofberger, J. (2013). cAMP promotes the differentiation of neural progenitor cells in vitro via modulation of voltage-gated calcium channels. *Front Cell Neurosci* 7, 155.
- Li, W., Sun, W., Zhang, Y., Wei, W., Ambasudhan, R., Xia, P., Talantova, M., Lin, T., Kim, J., Wang, X., *et al.* (2011). Rapid induction and long-term self-renewal of primitive neural precursors from human embryonic stem cells by small molecule inhibitors. *Proc Natl Acad Sci U S A* 108, 8299-8304.
- Li, X.J., Zhang, X., Johnson, M.A., Wang, Z.B., Lavaute, T., and Zhang, S.C. (2009). Coordination of sonic hedgehog and Wnt signaling determines ventral and dorsal telencephalic neuron types from human embryonic stem cells. *Development* 136, 4055-4063.
- Lin, Y.T., Seo, J., Gao, F., Feldman, H.M., Wen, H.L., Penney, J., Cam, H.P., Gjoneska, E., Raja, W.K., Cheng, J., *et al.* (2018). APOE4 Causes Widespread Molecular and Cellular Alterations Associated with Alzheimer's Disease Phenotypes in Human iPSC-Derived Brain Cell Types. *Neuron* 98, 1141-1154 e1147.
- Lo, B., and Parham, L. (2009). Ethical issues in stem cell research. *Endocr Rev* 30, 204-213.

- Love, S., Plaha, P., Patel, N.K., Hotton, G.R., Brooks, D.J., and Gill, S.S. (2005). Glial cell line–derived neurotrophic factor induces neuronal sprouting in human brain. *Nature Medicine* *11*, 703 - 704.
- Ludwig, T.E., Levenstein, M.E., Jones, J.M., Berggren, W.T., Mitchen, E.R., Frane, J.L., Crandall, L.J., Daigh, C.A., Conard, K.R., Piekarczyk, M.S., *et al.* (2006). Derivation of human embryonic stem cells in defined conditions. *Nat Biotechnol* *24*, 185-187.
- Maroof, Asif M., Keros, S., Tyson, Jennifer A., Ying, S.-W., Ganat, Yosif M., Merkle, Florian T., Liu, B., Goulburn, A., Stanley, Edouard G., Elefanty, Andrew G., *et al.* (2013). Directed Differentiation and Functional Maturation of Cortical Interneurons from Human Embryonic Stem Cells. *Cell Stem Cell* *12*, 559-572.
- May, J.M. (2012). Vitamin C transport and its role in the central nervous system. *Subcell Biochem* *56*, 85-103.
- Mertens, J., Marchetto, M.C., Bardy, C., and Gage, F.H. (2016). Evaluating cell reprogramming, differentiation and conversion technologies in neuroscience. *Nat Rev Neurosci* *17*, 424-437.
- Mica, Y., Lee, G., Chambers, S.M., Tomishima, M.J., and Studer, L. (2013). Modeling neural crest induction, melanocyte specification, and disease-related pigmentation defects in hESCs and patient-specific iPSCs. *Cell Rep* *3*, 1140-1152.
- Moretti, A., Bellin, M., Welling, A., Jung, C.B., Lam, J.T., Bott-Flügel, L., Dorn, T., Goedel, A., Höhnke, C., Hofmann, F., *et al.* (2010). Patient-Specific Induced Pluripotent Stem-Cell Models for Long-QT Syndrome. *N Engl J Med* *363*, 1397-1409.
- Moya, N., Cutts, J., Gaasterland, T., Willert, K., and Brafman, D.A. (2014). Endogenous WNT signaling regulates hPSC-derived neural progenitor cell heterogeneity and specifies their regional identity. *Stem Cell Reports* *3*, 1015-1028.
- Munst, S., Koch, P., Kesavan, J., Alexander-Mays, M., Munst, B., Blaess, S., and Brustle, O. (2018). In vitro segregation and isolation of human pluripotent stem cell-derived neural crest cells. *Methods* *133*, 65-80.

- Oksanen, M., Petersen, A.J., Naumenko, N., Puttonen, K., Lehtonen, S., Gubert Olive, M., Shakirzyanova, A., Leskela, S., Sarajarvi, T., Viitanen, M., *et al.* (2017). PSEN1 Mutant iPSC-Derived Model Reveals Severe Astrocyte Pathology in Alzheimer's Disease. *Stem Cell Reports* 9, 1885-1897.
- Orr, M.E., Sullivan, A.C., and Frost, B. (2017). A Brief Overview of Tauopathy: Causes, Consequences, and Therapeutic Strategies. *Trends Pharmacol Sci* 38, 637-648.
- Ortmann, D., and Vallier, L. (2017). Variability of human pluripotent stem cell lines. *Curr Opin Genet Dev* 46, 179-185.
- Qi, Y., Zhang, X.J., Renier, N., Wu, Z., Atkin, T., Sun, Z., Ozair, M.Z., Tchieu, J., Zimmer, B., Fattahi, F., *et al.* (2017). Combined small-molecule inhibition accelerates the derivation of functional cortical neurons from human pluripotent stem cells. *Nat Biotechnol* 35, 154-163.
- Raber, J., Huang, Y., and Ashford, J.W. (2004). ApoE genotype accounts for the vast majority of AD risk and AD pathology. *Neurobiol Aging* 25, 641-650.
- Reinhardt, P., Schmid, B., Burbulla, L.F., Schondorf, D.C., Wagner, L., Glatza, M., Hoing, S., Hargus, G., Heck, S.A., Dhingra, A., *et al.* (2013). Genetic correction of a LRRK2 mutation in human iPSCs links parkinsonian neurodegeneration to ERK-dependent changes in gene expression. *Cell Stem Cell* 12, 354-367.
- Ren, Y., Jiang, H., Hu, Z., Fan, K., Wang, J., Janoschka, S., Wang, X., Ge, S., and Feng, J. (2015). Parkin mutations reduce the complexity of neuronal processes in iPSC-derived human neurons. *Stem Cells* 33, 68-78.
- Rodin, S., Antonsson, L., Hovatta, O., and Tryggvason, K. (2014). Monolayer culturing and cloning of human pluripotent stem cells on laminin-521-based matrices under xeno-free and chemically defined conditions. *Nat Protoc* 9, 2354-2368.
- Russel, W., and Burch, R. (1992). *The principles of human experimental technique* (1959). Universities Federation for Animal Welfare (UFAW) Herts, UK: Potters Bar 238.
- Serrano-Pozo, A., Frosch, M.P., Masliah, E., and Hyman, B.T. (2011). Neuropathological alterations in Alzheimer disease. *Cold Spring Harb Perspect Med* 1, a006189.

Shi, Y., Kirwan, P., and Livesey, F.J. (2012a). Directed differentiation of human pluripotent stem cells to cerebral cortex neurons and neural networks. *Nat Protoc* 7, 1836-1846.

Shi, Y., Kirwan, P., Smith, J., Robinson, H.P., and Livesey, F.J. (2012b). Human cerebral cortex development from pluripotent stem cells to functional excitatory synapses. *Nat Neurosci* 15, 477-486, S471.

Sirkis, D.W., Bonham, L.W., Aparicio, R.E., Geier, E.G., Ramos, E.M., Wang, Q., Karydas, A., Miller, Z.A., Miller, B.L., Coppola, G., *et al.* (2016). Rare TREM2 variants associated with Alzheimer's disease display reduced cell surface expression. *Acta Neuropathol Commun* 4, 98.

Smith, J.R., Vallier, L., Lupo, G., Alexander, M., Harris, W.A., and Pedersen, R.A. (2008). Inhibition of Activin/Nodal signaling promotes specification of human embryonic stem cells into neuroectoderm. *Dev Biol* 313, 107-117.

Sternecker, J.L., Reinhardt, P., and Scholer, H.R. (2014). Investigating human disease using stem cell models. *Nat Rev Genet* 15, 625-639.

Takahashi, K., Tanabe, K., Ohnuki, M., Narita, M., Ichisaka, T., Tomoda, K., and Yamanaka, S. (2007). Induction of pluripotent stem cells from adult human fibroblasts by defined factors. *Cell* 131, 861-872.

Tchieu, J., Zimmer, B., Fattahi, F., Amin, S., Zeltner, N., Chen, S., and Studer, L. (2017). A Modular Platform for Differentiation of Human PSCs into All Major Ectodermal Lineages. *Cell Stem Cell* 21, 399-410 e397.

The\_World\_Bank\_Group (2017). Online: <https://data.worldbank.org/indicator/SP.DYN.LE00.IN>, Stand:

Thomson, J.A., Itskovitz-Eldor, J., Shapiro, S.S., Waknitz, M.A., Swiergiel, J.J., Marshall, V.S., and Jones, J.M. (1998). Embryonic Stem Cell Lines Derived from Human Blastocysts. *Science* 282, 1145-1147.

Vallier, L., Alexander, M., and Pedersen, R.A. (2005). Activin/Nodal and FGF pathways cooperate to maintain pluripotency of human embryonic stem cells. *J Cell Sci* 118, 4495-4509.

- Van Winkle, A.P., Gates, I.D., and Kallos, M.S. (2012). Mass Transfer Limitations in Embryoid Bodies during Human Embryonic Stem Cell Differentiation. *Cells Tissues Organs* 196, 34-47.
- Vicario-Abejon, C., Collin, C., McKay, R.D.G., and Segal, M. (1998). Neurotrophins Induce Formation of Functional Excitatory and Inhibitory Synapses between Cultured Hippocampal Neurons. *The Journal of Neuroscience* 18, 7256–7271.
- WHO (2019). Online: <https://www.who.int/news-room/fact-sheets/detail/dementia>, Stand: 14.05.2019.
- Wilson, P.A., and Hemmati-Brivanlou, A. (1995). Induction of epidermis and inhibition of neural fate by Bmp-4. *Nature* 376, 331-333.
- Woodruff, G., Reyna, S.M., Dunlap, M., Van Der Kant, R., Callender, J.A., Young, J.E., Roberts, E.A., and Goldstein, L.S. (2016). Defective Transcytosis of APP and Lipoproteins in Human iPSC-Derived Neurons with Familial Alzheimer's Disease Mutations. *Cell Rep* 17, 759-773.
- Xu, C., M. S. Inokuma, J. Denham, K. Golds, P. Kundu, Gold, J.D., and Carpenter, M.K. (2001). Feeder-free growth of undifferentiated human embryonic stem cells. *Nature Biotechnology* 19, 971-974.
- Xu, R.H., Chen, X., Li, D.S., Li, R., Addicks, G.C., Glennon, C., Zwaka, T.P., and Thomson, J.A. (2002). BMP4 initiates human embryonic stem cell differentiation to trophoblast. *Nat Biotechnol* 20, 1261-1264.
- Yao, S., Chen, S., Clark, J., Hao, E., Beattie, G.M., Hayek, A., and Ding, S. (2006). Long-term self-renewal and directed differentiation of human embryonic stem cells in chemically defined conditions. *PNAS* 103, 6907–6912.
- Yasuda, S.-y., Ikeda, T., Shahsavarani, H., Yoshida, N., Nayer, B., Hino, M., Vartak-Sharma, N., Suemori, H., and Hasegawa, K. (2018). Chemically defined and growth-factor-free culture system for the expansion and derivation of human pluripotent stem cells. *Nature Biomedical Engineering* 2, 173-182.

Zhang, S.-C., Wernig, M., Duncan, I.D., Brüstle, O., and Thomson, J. (2001). In vitro differentiation of transplantable neural precursors from human embryonic stem cells. *Nature* 409, 1129-1133.



## 8 APPENDIX

### 8.1 Publications

Ercan, E., Eid, S., Weber, C., **Kowalski, A.**, Bichmann, M., Behrendt, A., Matthes, F., Krauss, S., Reinhardt, P., Fulle, S., Ehrnhoefer, D. E. (2017). A validated antibody panel for the characterization of tau post-translational modifications. *Molecular Neurodegeneration* (2017) 12:87 DOI 10.1186/s13024-017-0229-1.

### 8.2 Presentations and poster contributions

**Alexandra Kowalski**, Justine Miller, Jürgen Korffmann, Joseph Tamm, Miroslav Cik and Peter Reinhardt: A chemically defined differentiation protocol independent from dual SMAD inhibition generates cortical neurons from hiPSCs by avoiding endogenous propensity towards neural crest Poster at AbbVie Celebration of Science, 15<sup>th</sup> November 2018.

**Alexandra Kowalski**: FGF and WNT modulation for robust induction of telencephalic neurons from hiPSCs. Poster at AbbVie Science Days, 13<sup>th</sup>/14<sup>th</sup> November 2018.

**Alexandra Kowalski**: Development of a differentiation protocol from hiPSCs to cortical neurons to phenotype Alzheimer's Disease. Presentation at German Stem Cell Network Conference, Non-PI-Meeting, 18<sup>th</sup> September 2018.

**Alexandra Kowalski**: FGF and WNT modulation for robust induction of telencephalic neurons from hiPSCs. Presentation at AbbVie Science Days, 19<sup>th</sup> April 2018.

## 9 LEBENS LAUF

### PERSONALIEN

Name und Vorname: Kowalski Alexandra  
Geburtsdatum: 30.07.1991  
Geburtsort: Saarbrücken  
Familienstand: ledig  
Vater: Kowalski Artur  
Mutter: Kowalski Agathe (geb. Snela)

### SCHULISCHER WERDEGANG

2002 – 2010 Otto-Hahn-Gymnasium, Saarbrücken  
15.06.2010 Abitur

### UNIVERSITÄRER WERDEGANG

WS2010 – WS2014 Bachelor Biotechnologie  
Hochschule Mannheim  
Bachelorarbeit: Level of Secondary Metabolites from *in vitro*  
Cultures of *Kalanchoe pinnata* after Transformation by  
*Agrobacterium rhizogenes*  
12.03.2014 Bachelorabschluss, Note: 1,5  
SS2014 – SS2015 Master Biomedical Science and Technology  
Hochschule Mannheim  
Masterarbeit: Puumala Nucleocapsid Protein Colocalizes  
with the Actin Cytoskeleton and Infection Induces Functional  
Consequences in Human Podocytes  
22.09.2015 Masterabschluss, Note: 1,1

## 10 ACKNOWLEDGEMENTS

First of all, I want to thank three people without whom this project wouldn't have been possible: I thank Mathias Hafner, Peter Reinhardt and Georg Teerstappen for the topic of my doctoral thesis and the opportunity of a cooperation between Hochschule Mannheim and AbbVie in which I could take part in.

Further, I thank professor Mathias Hafner for supervising me as my doctoral father, and for advising me with regards to my thesis and scholarships.

Most of all, I want to thank Peter Reinhardt for being my direct supervisor at AbbVie: I could not imagine a supervisor, that is more dedicated to his work and who is so smart in his scientific field. You really know everything! Thank you for your input and your positive energy which always motivated me. I could always count on you. Especially during difficult times, you always supported me and my decisions. Further, thank you for thoroughly reading my thesis manuscript and for your great input. I am very happy that you were my supervisor. Thank you!

I thank Mathias Hafner, Rüdiger Rudolf and Peter Reinhardt for regularly meeting with me for progress reports and discussions on the topic of my doctoral thesis. Thanks for your time, advise and input.

I thank all my direct colleagues from the "hiPSC-lab", Peter, Daniela, Gabriele, Lamiaa, Nathalie, Cecilia, Jürgen, Madeleine and Claudia, for great scientific and non-scientific conversations. Thanks for the great time in the lab, during lunch breaks and lab outings. It was a great pleasure to work with all of you, it was a great time that I will always remember.

Special thanks go to Jürgen Korffmann to whom I could mostly outsource the preparations of my RNA samples for qPCR.

Further, I thank my colleague in the US, Joseph Tamm, who performed qPCR of certain RNA samples on his fluidigm platform. Thanks for your practical work and also

for the quick communication and providing all the info needed for the materials and methods section. It was a great collaboration.

I thank Bettina Liebel on training and advise on the use of the ArrayScan and on subsequent analysis of images.

I want to thank my friends for their interest and support during my thesis. Thank you for nice conversations, sharing your experience and being there for me.

I want to thank especially my beloved partner, Matthias Weiß. Thank you for your support, patience and care during this intense time.